

**MODELING MULTIDIMENSIONAL LARGE STRAIN
CONSOLIDATION OF TAILINGS**

by

Daniel Priestley

B.A.Sc., The University of British Columbia, 2011

A THESIS SUBMITTED IN PARTIAL FULFILLMENT OF
THE REQUIREMENTS FOR THE DEGREE OF

MASTER OF APPLIED SCIENCE

in

THE FACULTY OF GRADUATE STUDIES
(Mining Engineering)

THE UNIVERSITY OF BRITISH COLUMBIA
(Vancouver)

December 2011

© Daniel Priestley, 2011

Abstract

Mine sites generate large volumes of tailings materials, requiring storage in tailings impoundments. Large strain consolidation of tailings materials represents a major factor in determining how a tailings impoundment will behave over time. Being able to accurately model these phenomena ensures that the effects of long term consolidation may be considered in the design of future tailings impoundments. SoilVision Systems has created an internal version of the SVOFFICE 2009 finite element modeling software capable of evaluating these scenarios. Prior to this research, preliminary benchmarks have been established, but the software had not yet been applied to multi-dimensional scenarios to benchmark the results. The goal of this research was to first benchmark the software against literature case studies. Following this, the software could then be applied to multi-dimensional tailings impoundments to study how the modeling could be performed and what factors require further consideration. Benchmarking of the software showed that the software is capable of recreating a wide variety of case studies from the literature. Further test were used to determine the effects of various material parameters on the material. Applications to multidimensional scenarios show that the software is capable of analyzing a wide variety of scenarios and considering numerous factors not found in other software packages. While the software does require additional functionality, it has been found to be a viable tool for examining multidimensional consolidation effects in tailings impoundments.

Preface

This project was completed under the supervision of University of British Columbia (UBC) Professor Dirk van Zyl PhD, and in participation with SoilVision Systems founder, Murray Fredlund PhD as part of an NSERC Industrial Post-Graduate Scholarship.

All of the benchmarks mentioned in Chapters 4 and 5 have been or are likely to be published by SoilVision Systems in their verification and validation manual for the large strain consolidation functionality. The author of this document performed all of the research, calculations and modeling involved in completing these benchmarks and wrote the initial draft of the verification manual. A preliminary version of the Large Strain Consolidation Verification Manual, covering the contributions the author has made to this subject, has been reprinted with permission in Appendix A.

A version of Chapter 2, as well as Appendix B, was completed in partnership with Lawrence Charlebois, EIT and submitted for assessment in the course CIVL 570: Advanced Soil Mechanics. My work focused on the theoretical material, including the explanation of the coordinate systems and the derivation of the large strain theory based upon small strain theory.

Section 5.1, as well as the Townsend B and CONDES0 comparisons made in the verification manual have been published. Priestley, D., Fredlund, M., & van Zyl, D. (2010). Benchmarking Multi-dimensional Large Strain Consolidation Analyses. *Uranium 2010 Proceedings* (pp. 271-288). Saskatoon: Met Soc. I conducted all of the modelling and drafted the original paper. I also compiled all of the edits made by the co-authors.

A version of section 4.2.1 and 5.2, as well as the Caldwell et al. Case Study 1 on sulphide tailings will be published in the Tailings and Mine Waste 2011 conference

proceedings. Again, I was responsible for all of the modeling, as well as drafting the original manuscript and making the subsequent edits.

Table of Contents

| | |
|---|-------------|
| Abstract..... | ii |
| Preface..... | iii |
| Table of Contents | v |
| List of Tables | x |
| List of Figures..... | xi |
| List of Symbols | xv |
| Acknowledgements | xvi |
| Dedication | xvii |
| Chapter 1: Introduction | 1 |
| 1.1 The Role of Large Strain Consolidation | 1 |
| 1.2 Project Objectives | 2 |
| Chapter 2: Theory and Literature Review..... | 4 |
| 2.1 Limitations of Conventional Consolidation Theory | 5 |
| 2.2 Large Strain Consolidation Theory | 6 |
| 2.2.1 Lagrangian Coordinate System..... | 6 |
| 2.2.2 One Dimensional Large Strain Derivation (Lee, 1979)..... | 7 |
| 2.2.3 Constitutive Equations | 10 |
| 2.3 Significant Additions to Large Strain Theory | 11 |
| 2.4 Multidimensional Large Strain Consolidation..... | 13 |
| 2.4.1 Geometrical Discretization | 13 |
| 2.4.2 Multi-Dimensional Large Strain Formulation (Jeeravipoolvarn, 2010) | 14 |
| 2.5 Methods of Analysis | 15 |

| | | |
|--|--|----|
| 2.5.1 | CONDES0..... | 15 |
| 2.5.1.1 | Original Formulation (Yao and Znidarcic, 1997) | 15 |
| 2.5.1.2 | Coffin's (2010) Expanded Quasi-Multidimensional Version | 16 |
| 2.5.2 | FSConsol..... | 16 |
| 2.5.3 | Plaxis..... | 16 |
| 2.6 | Testing for Large Strain Consolidation | 17 |
| 2.6.1 | Limitations of Conventional Consolidation Testing and Analysis Methods | 17 |
| 2.6.2 | Variations of the Finite-Strain Consolidation Test | 18 |
| Chapter 3: SVOFFICE Consolidation Modeling | 19 | |
| 3.1 | Model Geometry | 20 |
| 3.1.1 | Coordinate System | 20 |
| 3.1.2 | Staged Filling | 20 |
| 3.2 | Material Parameters | 21 |
| 3.2.1 | Poisson's Ratio..... | 21 |
| 3.2.2 | Initial Stress Limit..... | 22 |
| 3.3 | Boundary Conditions | 22 |
| 3.3.1 | SVSolid | 23 |
| 3.3.2 | SVFlux | 23 |
| 3.4 | Initial Conditions | 23 |
| 3.4.1 | SVSolid | 24 |
| 3.4.2 | SVFlux | 24 |
| 3.5 | Preliminary Benchmarking..... | 24 |
| Chapter 4: One Dimensional Verification and Validation..... | 26 | |

| | | |
|--|--|-----------|
| 4.1 | Benchmark Examples | 26 |
| 4.2 | One Dimensional Modeling Considerations..... | 31 |
| 4.2.1 | Poisson's Ratio..... | 31 |
| 4.2.2 | Pond Height..... | 33 |
| 4.3 | Results of Benchmarking..... | 35 |
| Chapter 5: Modeling Multi-Dimensional Tailings Deposits | | 37 |
| 5.1 | Effects of Multidimensionality – Column Analysis | 37 |
| 5.1.1 | Material Properties | 38 |
| 5.1.2 | Geometry/Boundary Conditions | 39 |
| 5.1.3 | Results | 40 |
| 5.1.4 | Discussion | 43 |
| 5.2 | 2D Tailings Impoundment | 43 |
| 5.2.1 | Geometry and Boundary Conditions..... | 44 |
| 5.2.2 | Material Parameters | 44 |
| 5.2.3 | Sloping Boundary Conditions..... | 46 |
| 5.2.4 | Effect of an Underdrain..... | 48 |
| 5.2.5 | Spatial Variability | 50 |
| 5.3 | 2D Tailings Pit..... | 51 |
| 5.3.1 | Geometry..... | 53 |
| 5.3.2 | Extrapolation of Material Parameters | 53 |
| 5.3.3 | Boundary Conditions | 55 |
| 5.3.4 | Results | 56 |
| 5.3.4.1 | Settlement..... | 57 |

| | |
|--|-----------|
| 5.3.4.2 Pore-water Pressure Dissipation..... | 62 |
| 5.3.4.3 Impact of Lateral Drainage | 67 |
| 5.3.5 Discussion | 72 |
| 5.4 3D Modeling Considerations | 74 |
| 5.5 3D Tailings Impoundment Model | 76 |
| 5.5.1 Geometry..... | 76 |
| 5.5.2 Material Parameters | 79 |
| 5.5.3 Boundary Conditions | 79 |
| 5.5.4 Results and Discussion..... | 79 |
| 5.5.5 Conclusions..... | 90 |
| 5.6 Summary | 90 |
| Chapter 6: Discussion of Multidimensional Modeling using SVOOffice..... | 92 |
| 6.1 Geometry and Material Parameters | 92 |
| 6.1.1 Poisson Ratio..... | 92 |
| 6.2 Boundary Conditions | 94 |
| 6.2.1 Sloping Deformation Boundary Conditions | 94 |
| 6.2.2 Lateral Flux | 95 |
| 6.3 Spatial Variability | 96 |
| 6.4 Advantages of Multidimensional Modeling | 96 |
| 6.5 Areas of Further Refinement | 97 |
| Chapter 7: Conclusion..... | 99 |
| 7.1 Practical Applications | 99 |
| 7.2 Potential for Future Research | 100 |

| | | |
|--|--|-----|
| 7.3 | Closing Remarks..... | 101 |
| Bibliography | 103 | |
| Appendices..... | 107 | |
| Appendix A SVOOffice Large Strain Consolidation Verification Manual - Draft..... | 108 | |
| Appendix B Large Strain Consolidation Testing Methods..... | 166 | |
| B.1 | Oedometer Step-Loading Test | 166 |
| B.2 | Constant Rate of Deformation (CRD) Test..... | 166 |
| B.3 | Controlled Gradient Test..... | 167 |
| B.4 | Constant Rate of Loading Test..... | 167 |
| B.5 | Continuous Loading Test | 167 |
| B.6 | Seepage-Induced Consolidation Test..... | 168 |

List of Tables

| | |
|--|----|
| Table 4-1: Overview of benchmarked models and key findings. | 28 |
| Table 5-1: Comparison of literature and calculated material parameters for the gold tailings compressibility function at the minimum and maximum void ratios. | 54 |
| Table 6-1: Comparison of Poisson's Ratio for different case studies. | 93 |
| Table 6-2: Values of assumed and measured Poisson`s Ratio taken from literature..... | 94 |

List of Figures

| | |
|--|----|
| Figure 2-1: Comparison of Eulerian and Lagrangian coordinate systems [after (Schiffman, Vick, & Gibson, 1988)]. | 7 |
| Figure 4-1: Comparison of filling curve and Caldwell et al.'s predictions against SVOffice. | 32 |
| Figure 4-2: Changes in the final surface height with Poisson's Ratio..... | 33 |
| Figure 4-3: Variation in interface height with time due to the application of various head boundaries. Note: the lines fall immediately above one another, therefore, there is only one line observed. | 34 |
| Figure 4-4: Variation in excess pore-water pressure with time due to the application of various head boundaries. Note: the lines fall immediately above one another, therefore, there is only one line observed..... | 35 |
| Figure 5-1: Compressibility curve of oil sands column 1 (Jeeravipoolvarn et al. 2008)..... | 38 |
| Figure 5-2: Oil sands column 1 void ratio-hydraulic conductivity curve (Jeeravipoolvarn et al. 2008). | 38 |
| Figure 5-3: Oil sands column 1 model geometry in 1D, 2D and 3D. Note: only 25% of nodes are shown for the 1D analysis for the sake of clarity..... | 40 |
| Figure 5-4: Oil sands column comparison of 1D, 2D and 3D column test results. | 41 |
| Figure 5-5: SVOffice, experimental and literature prediction effective stress profiles at various times | 41 |
| Figure 5-6: SVOffice, experimental and literature prediction excess pore-water pressure profiles at various times | 42 |
| Figure 5-7: SVOffice, experimental and literature prediction void ratio profiles at various times | 42 |

| | |
|---|----|
| Figure 5-8: Compressibility and permeability relationships of sulfide and gossan tailings ... | 45 |
| Figure 5-9: Geometry of 2-D tailings impoundment model | 46 |
| Figure 5-10: Fixed geometry deformation after 20 years with void ratio profile..... | 47 |
| Figure 5-11: Sliding geometry deformation after 20 years with void ratio profile. | 48 |
| Figure 5-12: Comparison of 2D impoundment heights at center of deposit for fixed and sliding boundary conditions against the filling curve and Caldwell et al. (1984) prediction. | 48 |
| Figure 5-13: Flux vectors in the fixed boundary condition scenario..... | 49 |
| Figure 5-14: 2D deformation with under drain after 20 years with void ratio profile..... | 50 |
| Figure 5-15: Two material disposal scenario after 20 years with void ratio profile..... | 51 |
| Figure 5-16: Filling height comparison of the effect of the under drain and the 2 material disposal scenario..... | 51 |
| Figure 5-17: Gold tailings impoundment geometry (Anstey and Williams, 2007). | 53 |
| Figure 5-18: Compressibility function fitted to gold tailings parameters..... | 55 |
| Figure 5-19: Hydraulic conductivity function fitted to gold tailings..... | 55 |
| Figure 5-20: Deformed mesh of the gold tailings impoundment after 30 years of consolidation | 56 |
| Figure 5-21: Tailings surface elevation through filling to a final time of 30 years | 57 |
| Figure 5-22: Cumulative tailings settlement over 30 years | 57 |
| Figure 5-23: Time series of displacement distribution for times a) 5 years b) 10 years c) 15 years and d) 20 years..... | 59 |
| Figure 5-24: Void ratio distribution for times a) 5 years b) 10 years c) 15 years and d) 20 years | 61 |

| | |
|---|----|
| Figure 5-25: Pore-water pressure variation over time at the base of the gold tailings and slightly above, where the maximum pwp is observed | 63 |
| Figure 5-26: Excess pore-water pressure variation over time at the base of the gold tailings and slightly above, where the maximum pwp is observed. | 63 |
| Figure 5-27: Excess pore-water pressure distributions for times a) 5 years, b) 10 years, and c) 15 years (excess pore-water pressure has almost completely dissipated)..... | 65 |
| Figure 5-28: Groundwater flux vectors at times a) 9 years and b) 15 years..... | 66 |
| Figure 5-29: Tailings surface elevation through filling to a final time of 30 years | 68 |
| Figure 5-30: Cumulative tailings settlement over 30 years | 68 |
| Figure 5-31: Pore-water pressure variation with time when the bedrock hydraulic conductivity is and is not considered by the model | 69 |
| Figure 5-32: Excess pore-water pressure variation with time when the bedrock hydraulic conductivity is and is not considered by the model | 69 |
| Figure 5-33: Excess pore-water pressure distribution when the hydraulic conductivity of the surrounding bedrock is not considered for times a) 6 year b) 9 years and c) 12 years..... | 71 |
| Figure 5-34: Groundwater flux vectors after 9 years when bedrock is not considered. | 71 |
| Figure 5-35: Cross-section illustrating the effect of layering deposits in three dimensions. Note: model is exaggerated 10 times in the vertical direction..... | 75 |
| Figure 5-36: Caldwell et al. (1984) 3D tailings impoundment interpolated geometry. Note: model is exaggerated 10 times in the vertical direction..... | 77 |
| Figure 5-37: 3D Caldwell et al. (1984) impoundment showing the 4 layers used to simulate staged filling. Note: model is exaggerated 10 times in the vertical direction..... | 78 |

| | |
|---|----|
| Figure 5-38: Cross-section of mesh generated for the 3D Caldwell et al. (1984) tailings impoundment. Note: model is exaggerated 10 times in the vertical direction..... | 78 |
| Figure 5-39: Interface height at the lowest point for 3D impoundment geometry as compared to the fill height and the predictions made by Caldwell et al..... | 80 |
| Figure 5-40: 3D time series of impoundment filling and settlement for times a) 0 years, b) 5 years, c) 10 years, d) 15 years and e) 20 years. Note: model is exaggerated 10 times in the vertical direction. | 83 |
| Figure 5-41: Top surface displacement at the end of filling (20 years)..... | 84 |
| Figure 5-42: Location within the impoundment of the cross-sectional view point. | 84 |
| Figure 5-43: Cross section of surface displacement for X=1300 meters at the end of filling (20 years). | 85 |
| Figure 5-44: Void ratio profile of impoundment cross-section at times a) 2 years b) 5 years c) 10 years d) 15 years e) 20 years..... | 87 |
| Figure 5-45: Pore-water pressure profile of impoundment cross-section at times a) 2 years b) 5 years c) 10 years d) 15 years e) 20 years..... | 88 |
| Figure 5-46: Excess pore-water pressure profile of impoundment cross-section at time a) 2 years b) 5 years and c) 15 years (excess pore-water pressure has almost completely dissipated). | 89 |

List of Symbols

| | |
|----------------------------|---|
| A, B, C, D, Z | Coefficients for the hydraulic conductivity and compressibility functions |
| a | Vertical Eulerian Coordinate |
| a_v | Compressibility |
| c_v | Coefficient of Consolidation |
| c_s | Coefficient of Swelling |
| e | Void Ratio |
| e_o | Initial Void Ratio |
| k | Hydraulic Conductivity of Soil |
| n | Porosity |
| q | Flow velocity |
| r | Radial Coordinate (horizontal) |
| t | Time |
| v_f | Velocity of Fluid |
| v_s | Velocity of Solids |
| z | Vertical Lagrangian Coordinate |
| μ | Pore Water Pressure |
| μ_{excess} | Excess Pore Water Pressure |
| $\mu_{\text{hydrostatic}}$ | Hydrostatic Pore Water Pressure |
| γ_w | Unit weight of Water (9810 kN/m^3) |
| γ_s | Unit weight of Soil |
| σ | Total Stress |
| σ' | Effective Stress |
| ν | Poisson's Ratio |

Acknowledgements

I would like to take this opportunity to thank the people who contributed to this research and without whom this would not have been possible. I would like to particularly thank my supervisor, Professor Dirk van Zyl. His in depth practical knowledge and attention to detail taught me many valuable lessons and furthered my understanding of engineering greatly.

Thanks also goes to Dr Murray Fredlund and the rest of the staff at SoilVision Systems Ltd for their financial and practical support in completing the aspects of this research related to the application of their software. I greatly enjoyed my time at their office in Saskatoon, where their assistance greatly improved my understanding of the software, as well as my table hockey skills.

I would also like to thank the other members of my committee, Doctors John Howie and Bern Klein, for their assistance in editing and analyzing the research performed. I have benefitted greatly from their insights and assistance. The National Science and Engineering Research Council (NSERC) also deserves acknowledgement for the financial support provided for this project through a two year industry partnership scholarship (IPS).

My enduring gratitude goes to my family; my parents and my brother who supported and encouraged me throughout my education. Finally, I would like to thank my wife, Maria, whose love and support enabled me to pursue my interest in mining and reclamation.

Dedication

To my wife, Maria

Chapter 1: Introduction

Large tailings impoundments are required to safely store the vast amounts of finely ground materials produced during mining operations and to prevent them from affecting the surrounding environment. The design of these impoundments is both expensive and challenging. Of critical importance is determining how much capacity is required to store the volume of tailings required through the life of the mine. Reclamation of the tailings impoundment must also be performed before final closure of the mine can be completed. Both of these questions require an understanding of consolidation characteristics, which can determine the amount of settlement during the life of the mine, and thus the impoundment capacity, as well as how much post-closure settlement, pore-water pressure dissipation and seepage will occur and over what time scale.

The study and design of tailings impoundments requires a set of modeling tools that incorporates all of the significant factors affecting consolidation. Where previous software tools have been limited to one dimensional analyses, or quasi-multidimensional analyses, SoilVision Systems Inc. has developed a finite element software package capable of analyzing consolidation as a fully three dimensional system. This thesis investigates the application of large strain consolidation using SVOOffice 2009 to tailings impoundments.

1.1 The Role of Large Strain Consolidation

Large strain consolidation refers to an advanced method of modeling the consolidation behavior of high deformation soils. Mine tailings are generally deposited at high void ratios and can consolidate significantly thereafter. The conventional consolidation analysis used in the design of building foundations, road embankments and other large earth

projects, is unsuitable when considering very large deformations. Therefore in 1967, Gibson, English and Hussey, developed a more robust formulation, which eliminated many of the assumptions made by conventional theories. With the advent of more powerful computers and finite element software, it is now feasible to solve large deformation consolidation problems using these theories. Chapter 2 discusses how large strain analyses differ from conventional consolidation used in soil mechanics.

1.2 Project Objectives

This research builds upon the work of Dr. Murray Fredlund (Fredlund, Donaldson, & Gitirana, 2009), in which the necessity of establishing multi-dimensional software capable of accurately modeling large strain consolidation was illustrated. Further application of the software to literature scenarios and other finite element solutions is required to show the software can be applied with a degree of confidence to large strain consolidation problems.

The greatest feature of SVOFFICE is its ability to consider large strain consolidation occurring in multiple dimensions. While previous papers (Jeeravipoolvarn, 2010; Coffin, 2010) have investigated quasi-multidimensional theories, SVOFFICE is the first software where 3D seepage, stresses and deformations are all considered. The effects of this multidimensionality will be investigated, as well as the assumptions regarding boundary conditions and model construction which are required.

The first objective of this research is to apply SVOFFICE to literature case studies of one dimensional large strain consolidation to verify that the software is capable of reproducing the results of these case studies. In doing so, greater confidence can be gained in applying the model to large strain consolidation scenarios. A second objective is to apply SVOFFICE to two and three dimensional scenarios, to investigate the effects associated with

multi-dimensionality and provide further insight as to how large strain consolidation can be modeled using the software.

Chapter 2: Theory and Literature Review

The conventional theory of consolidation is still widely used today, as the calculations do not require numerical modeling and the majority of correlations have been developed using these parameters. The c_v coefficient used can be considered constant for many soils (Gibson, English, & Hussey, 1967). However, for extremely soft soils, such as fatty clays (Terzaghi, 1943), and particularly where large changes in void ratio occur, the assumptions made by Terzaghi become less applicable and large strain calculations are required. The large changes that occur in the void ratio can significantly change the saturated hydraulic conductivity of the tailings. Also, the tailings compressibility will tend to change with void ratio.

Large strain consolidation is generally applied for calculating the consolidation of mine tailings, river sediments and dredged materials. These materials require this type of analysis as they can experience very large deformations and changes in void ratio. For example, dredged material studied in a column test experiences deformations of 23% of initial height in a period of eight days (Bartholomeeusen, et al. 2002).

Large strain consolidation has been linked to the process of sedimentation when material is deposited below water (Monte & Krizek, 1976; Koppula & Morgenstern, 1982; Oliveira-Filho & van Zyl, 2006). There is a specific void ratio where the material behavior changes from that of a fluid to that of a solid and this void ratio is generally treated as the initial void ratio used in large strain calculations. Furthermore, there is a noticeable trend in analysis that all soils are treated as monotonic consolidation problems, with no consideration

of secondary consolidation contributions. This has changed with the availability of numerical modeling techniques.

2.1 Limitations of Conventional Consolidation Theory

Karl Terzaghi wrote his Theory of Consolidation in 1925 (Coffin, 2010) and it has remained widely used in practice. In this paper it will be referred to as the conventional or small strain theory. In developing his theory, Terzaghi made several assumptions (Terzaghi, 1943):

- The voids of the soil are completely filled with water
- The water and soil components are incompressible
- Darcy's law is valid
- The hydraulic conductivity, k , does not change
- The system is laterally confined
- The relationship between void ratio and effective stress is given by

$$a_v(e) = \frac{de}{d\sigma'} = \frac{e_0 - e}{\sigma' - \sigma'_0} \quad 2-1$$

Where a_v is referred to as the coefficient of compressibility and is treated as a constant value.

- Infinitesimal strain (referred to here as small strain)
- Self-weight of soils is ignored
- Free of time dependent effects (i.e. secondary consolidation)

It has been found that these assumptions do not reflect the actual material behavior observed in the field. The analysis of soft materials such as sediments or soft clays makes the assumption of infinitesimal strain inconsistent with the material behavior. Also, the hydraulic conductivity and compressibility of the soils are considered by the conventional

theory to be constant values. Hydraulic conductivity has in fact been found to be highly sensitive to changes in void ratio (Schiffman, 1982), while it has been shown that linear approximations of the slope of the effective stress-void ratio line are inappropriate (Davies & Raymond, 1965; Liu & Znidarcic, 1991). Finally, ignoring the self-weight effects of the soil is considered to be an incorrect assumption, as in many cases this is the dominant driver of consolidation (Schiffman 1982). Terzaghi acknowledged that the aforementioned relationship is not valid in cases where secondary consolidation exceeds 20% of total settlement (Znidarcic, Croce, Pane, Ko, Olsen, & Schiffman, 1984).

2.2 Large Strain Consolidation Theory

In 1967, Gibson, England, and Hussey set out to create a formulation of the consolidation equation in which the limitations of small strain had been removed and variations in hydraulic conductivity and compressibility were allowed. They examined a method by which their formulation could be made linear, as well as a more robust non-linear formulation. Their 1D formulation that was developed is presented below. (Gibson, English, & Hussey, 1967)

$$\pm \left(\frac{\gamma_s}{\gamma_w} - 1 \right) \frac{d}{de} \left[\frac{k(e)}{1+e} \right] \frac{\delta e}{\delta a} + \frac{\delta}{\delta a} \left[\frac{k(e)}{\gamma_w(1+e)} \frac{d\sigma'}{de} \frac{\delta e}{\delta a} \right] + \frac{\delta e}{\delta t} = 0 \quad 2-2$$

2.2.1 Lagrangian Coordinate System

The Gibson formulation is based on the Lagrangian coordinate system (Schiffman, Vick, & Gibson, 1988) which is rooted in continuum mechanics where a strict definition of deformation is observed. Most soil mechanics analyses uses the Eulerian method whereby the plane of reference is fixed and the rate of flux and soil movement are measured (Gibson,

Schiffman, & Cargill, 1981). With regards to consolidation, this becomes difficult as the volume of the slurry will change over time as water leaves the system, decreasing the void ratio and thus the overall volume.

Large strain consolidation employs the Lagrangian system whereby a fixed volume of dry soils is used as a basis of measurement. The soil within the volume remains constant, while the volume of water and the height of the column vary over time. The z term is used to indicate the unit volume of the dry soil fraction of the slurry. Figure 1 shows how z remains constant while the slurry height, a , varies with void ratio.

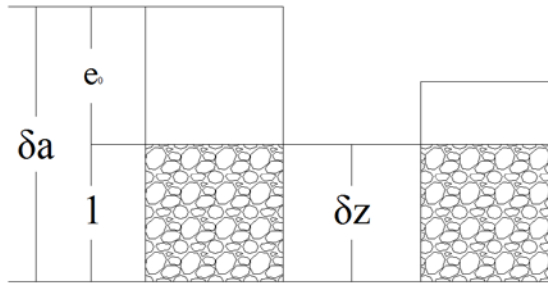


Figure 2-1: Comparison of Eulerian and Lagrangian coordinate systems [after (Schiffman, Vick, & Gibson, 1988)].

To convert from the Eulerian coordinates to Lagrangian coordinates, the convention is given by (Gibson, Schiffman, & Cargill, 1981):

$$z = \int \frac{1}{(1 + e)} da \quad 2-3$$

Or

$$\frac{dz}{da} = \frac{1}{(1 + e)} \quad 2-4$$

2.2.2 One Dimensional Large Strain Derivation (Lee, 1979)

The flow velocity (q) through a soil of volume dz will be related to the velocity of the fluid through the soil pores in relation to the velocity of the soil:

$$q = n(v_f - v_s)$$

2-5

Where n is the porosity, v_f is the fluid velocity in the pores and v_s is the solids velocity.

The loss of fluid from the volume of soil will therefore result in a change in the ratio of void space to soil (void ratio). Therefore the void ratio can be written as:

$$\frac{\partial e}{\partial t} = -\frac{\partial n(v_f - v_s)}{\partial z} \quad \text{2-6}$$

Assuming that Darcy's Law (equation 2-7) holds true, the velocity of the fluid through the soil can be written in Eulerian and Lagrangian coordinates (equation 2-8).

$$q = -k \frac{\partial h}{\partial a} \quad \text{2-7}$$

$$n(v_f - v_s) = -\frac{k}{\gamma_w} \frac{\partial u_{excess}}{\partial a} = -\frac{k}{\gamma_w(1+e)} \frac{\partial u_{excess}}{\partial z} \quad \text{2-8}$$

Hydraulic conductivity $k(e)$ is no longer held constant and is considered a function of void ratio, as per the large strain assumptions. Thus the equation becomes:

$$\frac{\partial e}{\partial t} = \frac{\partial}{\partial z} \left(\frac{k(e)}{\gamma_w(1+e)} \frac{\partial u_{excess}}{\partial z} \right) \quad \text{2-9}$$

Rearranging and expanding upon the definition of effective stress profiles:

$$\frac{\partial u_{excess}}{\partial z} = \frac{\partial \sigma}{\partial z} - \frac{\partial \sigma'}{\partial z} - \frac{\partial u_{hydrostatic}}{\partial z} \quad \text{2-10}$$

The total stress is written in terms of the self weight of the soil (equation 2-10) using Eulerian coordinates. An external load can also be applied to the total stress, but is neglected herein. It can then be converted to Lagrangian (equation 2-11) using equation 2-4. Similarly the hydrostatic pore-water pressure gradient is equal to the unit weight of water and can also be written in Lagrangian coordinates (equation 2-12).

$$\frac{\partial \sigma}{\partial a} = -\frac{1}{(1+e)} (e \gamma_w + \gamma_s) \quad \text{2-11}$$

$$\frac{\partial \sigma}{\partial z} = \frac{\partial \sigma}{\partial a} \frac{\partial a}{\partial z} = -(e \gamma_w + \gamma_s) \quad 2-12$$

$$\frac{\partial u_h}{\partial z} = \frac{\partial u_h}{\partial a} \frac{\partial a}{\partial z} = -(1 + e) \gamma_w \quad 2-13$$

Therefore equation 2-9 can be rewritten as:

$$\frac{\partial u_{excess}}{\partial z} = -(e \gamma_w + \gamma_s) - \frac{\partial \sigma'}{\partial z} + (1 + e) \gamma_w \quad 2-14$$

Which can be rewritten as:

$$\frac{\partial u_{excess}}{\partial z} = (\gamma_w - \gamma_s) - \frac{\partial \sigma'}{\partial z} \quad 2-15$$

And the continuity equation becomes:

$$\frac{\partial e}{\partial t} = \frac{\partial}{\partial z} \left(\frac{k(e)}{\gamma_w(1 + e)} \left(-(\gamma_s - \gamma_w) - \frac{\partial \sigma'}{\partial z} \right) \right) \quad 2-16$$

This is rearranged to be:

$$\frac{\partial e}{\partial t} = - \left(\frac{\gamma_s}{\gamma_w} - 1 \right) \frac{\partial e}{\partial e} \frac{\partial}{\partial z} \left(\frac{k(e)}{(1 + e)} \right) - \frac{\partial}{\partial z} \left(\frac{k(e)}{\gamma_w(1 + e)} \left(\frac{\partial \sigma'}{\partial e} \frac{\partial e}{\partial z} \right) \right) \quad 2-17$$

This upon further rearrangement produces the same equation as Gibson, English and Hussey (1967):

$$\left(\frac{\gamma_s}{\gamma_w} - 1 \right) \frac{d}{de} \left[\frac{k(e)}{1 + e} \right] \frac{\delta e}{\delta z} + \frac{\delta}{\delta z} \left[\frac{k(e)}{\gamma_w(1 + e)} \frac{d \sigma'}{de} \frac{\delta e}{\delta z} \right] + \frac{\delta e}{\delta t} = 0 \quad 2-18$$

The formula is generally reduced using the following simplifications:

$$g(e) = - \frac{k(e)}{(1 + e) \gamma_w} \frac{d \sigma'}{de} \quad 2-19$$

$$f(e) = - \left(\frac{\gamma_s}{\gamma_w} - 1 \right) \frac{d}{de} \left[\frac{k(e)}{1 + e} \right] \frac{\delta e}{\delta z} \quad 2-20$$

Which renders the formula:

$$g(e) \frac{\partial^2 e}{\partial z^2} \pm f(e) = \frac{\partial e}{\partial t}$$

2-21

Which is convenient as $g(e)$ is closely related to the c_v property from Terzaghi. Similar to c_v , $g(e)$ is resistant to changes in void ratio, which when assumed to be constant can render the formula linear (Schiffman, 1982). This linearization allows it to be solved in a manner similar to that used by the conventional methods of calculation. However, this assumption requires that the self-weight term “ $f(e)$ ” be neglected.

2.2.3 Constitutive Equations

With the advent of large strain consolidation theory, it becomes necessary to generate functions for compressibility and hydraulic conductivity that will accurately model the soil behavior as the void ratio changes. Hydraulic conductivity is widely modeled using a power function as shown below (Townsend & McVay, 1990) (Jeeravipoolvarn, Scott, & Chalaturnyk, 2008) (Yao & Znidarcic, 1997).

$$k = Ce^D$$

2-22

C and D are dimensionless coefficients, which are determined experimentally and will be unique to each soil.

There is more debate surrounding how compressibility should be modeled. For ease of calculation, it is generally written as void ratio in terms of effective stress. Several suggested methods include a power function (Townsend & McVay, 1990), Weibull function (Jeeravipoolvarn, Scott, & Chalaturnyk, 2008) and extended power function (Liu & Znidarcic, 1991).

Arguably the most common compressibility model is the extended power function, as shown below. It was proposed by Liu and Znidarcic in 1991 (Liu & Znidarcic, 1991).

$$e = A(\sigma' + Z)^B$$

2-23

The A and B parameters are unitless and determined experimentally. The Z term has a value of effective stress and is used to prevent numerical difficulties arising from low effective stresses where the void ratio increases exponentially (Liu & Znidarcic, 1991). The modeling program *CONDESO* uses the extended power function and does not require an initial void ratio specification (Liu & Znidarcic, 1991). It is argued that the Z parameter represents the effective stress at which the ‘initial’ void ratio occurs.

2.3 Significant Additions to Large Strain Theory

Terzaghi’s conventional theory is considered to be a finite strain equation, where the variations in compressibility and hydraulic conductivity were not considered (Schiffman R. L., 1982). As is shown in section 2.2.2, the formulation created by Gibson, English and Hussey may be reduced to a linear formula very similar to Terzaghi’s.

When applied to “thin” clay layers, the Gibson, English and Hussey equation reduces to a formula which was equivalent to previous work performed in Japan by Mikasa in 1965 on the consolidation of rapidly deposited dredged fills (Schiffman, 1982). This paper was not consulted for the purposes of this thesis as it is only available in its native Japanese.

Monte and Krizek (1976) derived a fluid limit parameter where the behavior of the sediment transitioned from a fluid undergoing sedimentation to a slurry undergoing consolidation.

Robert Gibson returned to this field in 1981, when he published a paper along with Robert Schiffman and Kenneth Cargill which summarized the findings of the 1967 paper and then applied the theory to thick clay layers, where the self-weight effects are considered

(Gibson, Schiffman, & Cargill, 1981). Each of the authors of the 1981 report went on to add significant contributions to the study of large strain consolidation during their careers.

In 1982, Koppula and Morgenstern reformulated the Gibson equation in terms of excess pore water pressure to allow them to solve for problems where sedimentation is occurring (Koppula & Morgenstern, 1982).

Also in 1982, Robert Schiffman wrote an article to *Geo-Marine Letters*, outlining the breadth of large strain consolidation research as well as the significant changes that had been implemented to the formulation to solve certain formulae. One interesting point that was raised highlighted that all of the papers written to that date on this subject had only adapted the Gibson formulation for special circumstances, meaning that the general formulation remained uncontested. He also provided a list of numerical and analytical methods that had been applied to solve these problems. It is noted how these analysis methods only consider the monotonic consolidation of homogeneous normally consolidated clays. For the sake of brevity, these will not be investigated in detail. (Schiffman, 1982).

In the late 1970's and early 1980's there was a large amount of practical work completed in this field sponsored by the Florida Phosphate Institute. Studies were undertaken by Carrier, Bromwell, and Somogyi (1983) considering how this theory could be applied to the design of phosphate tailings storage facilities. While this research did not add significantly to the theory, it represents one of the first well published examinations of how these theories could be applied in practice.

Dobroslav Znidarcic from the University of Colorado has continued to work in this field developing new testing techniques for the study of tailings materials (Znidarcic, Croce, Pane, Ko, Olsen, & Schiffman, 1984). These are discussed in Section 2.7 and described in

detail in Appendix B. His research group also developed methods of modeling the compressibility relationship as was mentioned previously (Liu & Znidarcic, 1991). Znidarcic also co-developed the large strain consolidation modeling program, *CONDES0*, with Daniel Yao for the Florida Institute of Phosphate Research. (Yao & Znidarcic, 1997)

In Canada, there has been a significant body of research carried out at the University of Alberta on sedimentation and consolidation processes in oil sands tailings. The bitumen remaining in the tailings creates unique material parameters that require additional classification (Azam & Scott, 2005) and a special formulation for the compressibility curve has been proposed, consisting of a Weibull Function (Azam, Jeeravipoolvarn, & Scott, 2009). There has even been some investigation of secondary compression in oil sands tailings and how it relates to large strain calculations (Scott, Chalaturnyk, & Jeeravipoolvarn, 2004). SoilVision Systems Ltd. has been performing research in the area of consolidation since 2008. A paper on the multi-dimensional consolidation of uranium mine tailings was published previously (Fredlund et al., 2009).

2.4 Multidimensional Large Strain Consolidation

A brief summary of some of the multidimensional theories that have been developed is presented in the following sections, with particular emphasis placed on the material that has been referred to for this research.

2.4.1 Geometrical Discretization

One formulation which has been used to solve large strain consolidation of tailings impoundments is to use a geometrical discretization algorithm to allow 1D analysis methods to be applied to 3D tailings impoundment geometries. The methodologies vary from an upper bound solution where the 1D column, filled according to the general filling scheme, is

treated as the full settlement within the impoundment (an overestimate of consolidation) and a scheme where the pond is filled as a series of circular columns. The circular columns are developed by creating an inverted frustum cone out of the geometry, and using varying side slopes to make the cross-sectional area at given elevations equal to the physical impoundment. A filling scheme is introduced which fills the outermost column at a set elevation first. For a more detailed explanation of this approach refer to Coffin (2010). This underestimates impoundment capacity, as compression of the sloping sidewalls is not considered. The geometrical discretization methodology is used both by Coffin's (2010) expanded version of CONDES0, as well as FSConsol (Coffin, 2010). Gjerapic et al (2008), states that this methodology does not incorporate lateral deformations or horizontal fluxes. It is also stated that the assumptions made in creating the lower bound filling scheme do not allow for the full consolidation of the outermost columns.

2.4.2 Multi-Dimensional Large Strain Formulation (Jeeravipoolvarn, 2010)

In his 2010 PhD thesis, Silawat Jeeravipoolvarn presented a quasi-multidimensional theory of consolidation. This theory uses the assumption that the predominant deformation will be vertical and that horizontal consolidation can be neglected. The formulas he derived for two and three dimensions are shown in Equations 2-24 and 2-25 respectively, using the Lagrangian coordinates.

$$\frac{\delta}{\delta z} \left[\frac{-k_v(e)(1+e_0)}{\gamma_w(1+e)} \frac{\delta u}{\delta a} \right] + (1+e) \frac{\delta}{\delta x} \left[\frac{k_h(e)}{(1+e)} \frac{\delta u}{\delta x} \right] + \frac{\delta e}{\delta t} = 0 \quad 2-24$$

$$\begin{aligned}
& \frac{\delta}{\delta z} \left[\frac{-k_v(e)(1+e_0)}{\gamma_w(1+e)} \frac{\delta u}{\delta a} \right] \\
& + (1+e) \left\{ \frac{\delta}{\delta x} \left[\frac{k_h(e)}{(1+e)} \frac{\delta u}{\delta x} \right] + \frac{\delta}{\delta x} \left[\frac{k_h(e)}{(1+e)} \frac{\delta u}{\delta y} \right] \right\} \\
& + \frac{\delta e}{\delta t} = 0
\end{aligned} \tag{2-25}$$

These equations were benchmarked and compared to several different scenarios. Some of his findings include the effects of various impoundment geometries and drainage conditions. It is acknowledged that further work is required to simulate the deformation boundary conditions.

2.5 Methods of Analysis

Large strain consolidation equation has been previously solved in a variety of ways. Although Gibson, English and Hussey (1967) introduced several assumptions allowing for numerical solutions, the increase in capability and availability of personal computers has allowed for finite difference and finite element programs which are capable of solving the equation without assumptions. This section will present a brief summary of some of the programs available today. Of particular importance is the ability of the program to solve for multidimensionality. Therefore, most programs limited to 1D analyses are not discussed.

2.5.1 CONDES0

CONDES0 is a finite element program, developed at the University of Colorado. It was first developed in 1997 by Daniel Yao and Dobrslav Znidarcic. The program has been recently updated by Jeffrey Coffin (2010) to include a geometrical discretization scheme.

2.5.1.1 Original Formulation (Yao and Znidarcic, 1997)

The original, formulation of CONDES0 was limited to 1D analysis of large strain consolidation and desiccation. The implementation allows for the modeling of most common

1D factors, such as external loads and staged filling. However, it is unable to model scenarios using multiple sets of material properties.

2.5.1.2 Coffin's (2010) Expanded Quasi-Multidimensional Version

In 2010, Jeffrey Coffin published his PhD thesis, under the direction of Dobroslav Znidarcic, which updated CONDES0 to include a geometrical discretization scheme to investigate 3D geometries, as well as a Lagrangian filling scheme and graphical user interface. His work suggests a method of investigating tailings impoundments where the most consolidation observed (higher bound) is equal to a standalone 1D column test filled in increments according to the filling curve. This requires the assumption that the impoundment sides consolidate as much as the tailings. The lower bound methodology involves a more complex filling scheme where the impoundment is filled in stages of constant elevation. This removes the assumption that the impoundment sides compress equal to the settlement of the tailings.

2.5.2 FSConsol

FSConsol is a commercial software package capable of solving for one dimensional large strain consolidation (GWP, 2007). Coffin (2010) states that FSConsol uses a geometrical discretization algorithm similar to that employed by his own upper bound formulation.

2.5.3 Plaxis

Two case studies, (Anstey & Williams, 2007) (McDonald & Lane, 2010), use the generic finite element modeling program Plaxis, to model two dimensional in-pit deposition of Gold and Nickel tailings. While the McDonald and Lane (2010) models used the Modified Cam-Clay formulation, which is felt to represent only the small strain aspects of

consolidation, Anstey and Williams, (2007) did use a large strain consolidation formulation, although some assumptions were required to be made to work with the Plaxis formulation. Comparisons to the results presented by Anstey and Williams (2007) are made in Section 5.3.

2.6 Testing for Large Strain Consolidation

While the theory of large strain consolidation is generally accepted when considering the design of tailings impoundments, the results that are obtained from numerical solutions are still based upon the quality and applicability of laboratory data. While an in-depth discussion of the different testing methodologies is beyond the scope of this document, a brief discussion of some of the limitations of the conventional testing techniques and variations on these techniques is presented in this section. Appendix B contains a brief description of each of the techniques mentioned.

2.6.1 Limitations of Conventional Consolidation Testing and Analysis Methods

The first procedure for the analysis of oedometer (step-loading) consolidation testing was proposed by Terzaghi in 1925 and is discussed in detail in the writings of Znidarcic et al (1984). Znidarcic acknowledges how Terzaghi presents the equation for the change in pore water pressure over time in the finite strain framework.

Along with other analysis methods for oedometer testing - including the square root fitting, logarithm fitting, and linear finite strain methods – Terzaghi’s classical formulation is limited by the assumption of constant coefficients of compressibility and consolidation. Terzaghi also acknowledges that the aforementioned relationship is not valid in cases where secondary consolidation exceeds 20% of total settlement (Znidarcic, Croce, Pane, Ko, Olsen, & Schiffman, 1984).

For practical applications where large strains are observed over time, such as the consolidation of very high void ratio mine tailings, the assumption of constant hydraulic conductivity should be avoided. Large strains resulting from the compressibility of the material significantly lowers the hydraulic conductivity; hence the traditional assumptions lead to overestimations of hydraulic conductivity. It can be shown that without considering variable material characteristics, excess pore pressure dissipation, and hence strength-gain progress may be non-representative and potentially un-conservative in engineering practice.

2.6.2 Variations of the Finite-Strain Consolidation Test

There have been several methods developed to characterize the consolidation process using laboratory specimens. Most analyses are built on the foundation of Terzaghi's step-loading test; however, variations on this technique, such as the seepage induced consolidation test, have been proposed that do not rely on the consolidation theory framework, rather direct measurements of material parameters are undertaken. Furthermore, traditional testing methods have subsequently been updated to allow for better instrumentation and specimen characterization throughout testing. Analysis methods for test results also vary from test to test, each with limitations and advantages. All methods require some degree of general assumptions and adherence to boundary conditions for validity. A brief description of the different methods is presented in Appendix B.

Chapter 3: SVOFFICE Consolidation Modeling

The geotechnical software package SVOFFICETM has been supplemented with a large strain consolidation formulation. The large strain consolidation formulation is currently not available with the commercial packages. This chapter provides a basis for understanding how large strain models are defined using SVOFFICE, as well as some of the terminology used within this document. The SVOFFICE large strain consolidation formulation is a proprietary formulation, developed by SoilVision Systems Ltd. It uses a rigorous three dimensional stress-strain formulation that also couples three dimensional seepage. The same constitutive equations relating hydraulic conductivity and compressibility as the Gibson et al. (1967) formulation (Section 2.2.3) are used to relate the material behavior.

SVOFFICE uses a coupled deformation-flux analysis to solve for the large strain consolidation (Fredlund, Donaldson, & Gitirana, 2009). This couples the SVSolid stress deformation package with SVFlux for solving the groundwater seepage component. Although, the finite element equations consider both stress and seepage conditions simultaneously, the software is laid out, so that each is defined in a separate area of the software using the SVSolid and SVFlux interface respectively. Therefore in the subsequent sections, discussion of the stress and hydrologic conditions will be referred to under these headings.

As was discussed in Section 2.2, the original large strain formulation was written in terms of void ratio, which has the advantage of being directly related to both the effective stress and hydraulic conductivity. Fredlund et al. (2009) has stated that the SVOFFICE formulation is based on a rigorous general continuum solid mechanics approach. Furthermore

it is not subject to the assumption of zero horizontal deformation, as is seen in the Jeeravipoolvarn (2010) formulation (Fredlund M. , September 2011).

3.1 Model Geometry

Using both the SVSolid and SVFlux interfaces, the model geometry can be specified in 1, 2 or 3 dimensions. To allow for the specification of different shapes and spatially varying material parameters, the geometry is bounded by regions in 1 and 2D, while 3D uses regions to separate the horizontal extents and surfaces to separate the vertical. Material parameters can then be defined for each individual section of the model. Regions and surfaces can also be added over time to consider staged filling of tailings impoundments.

3.1.1 Coordinate System

In implementing the large strain formulation, SVOFFICE uses a Lagrangian coordinate system to define the material coordinates. The need for the Lagrangian coordinate system is discussed in Section 2.2.1. The Lagrangian formulation allows for movement of the mesh and thus changes in the stress state of the material over time. A small strain formulation is also available, which only uses the standard Eulerian system and does not consider the moving mesh.

3.1.2 Staged Filling

Staged filling is handled by adding regions or layers of meshed geometry to the impoundment to represent filling stages at certain times. Before they are phased-in, the new mesh does not have mass nor does it restrict flow from the system. The general practice that has been used in this report is to bring the new phase in at the mid-point time between the start and end of filling for that phase. To measure this mean height of tailings within a

column, the total displacement of the top surface is measured at all time points, and then added to the filling curve.

3.2 Material Parameters

To relate the material behavior to the mathematical model, SVOOffice requires a number of parameters. The most important parameters are the effective stress / void ratio / hydraulic conductivity relationships, discussed in Section 2.2.3. General soil parameters, such as specific gravity and initial void ratio are also required.

SVOOffice has currently implemented a number of ways to relate the void ratio to the effective stress including: power and extended power functions, as well as Weibull and logarithmic functions

It is common practice to use a power function to relate the hydraulic conductivity and void ratio (Liu & Znidarcic, 1991). SVOOffice supports this, as well as allows a dual power function to be specified, where different functions are applied over specific void ratio ranges. This has been seen when considering the different hydraulic conductivity relationships which apply over the sedimentation and consolidation regimes (Azam, Jeeravipoolvarn, & Scott, 2009).

3.2.1 Poisson's Ratio

The use of the stress-strain formulation SVOOffice requires that Poisson's Ratio values be given for all soils. Poisson's ratio is defined as the ratio of transverse strain (horizontal) to axial strain (vertical) as shown in equation 3-1 and is generally determined for soils by triaxial testing.

$$v = -\frac{\epsilon_x}{\epsilon_y} \quad 3-1$$

Poisson's ratio is found to play an interesting role when considering the stress based approach used by SVOFFICE to solve the large strain formulation. Gibson et al.'s (1967) original formulation was written in terms of void ratio and therefore did not consider Poisson's ratio. However, when a stress based approach is taken, Poisson's ratio determines the horizontal strain acting upon an element. While this would logically have some effect on two and three dimensional analyses, experimentation with the software found that varying values of Poisson's ratio lead to differing degrees of consolidation in one dimensional analysis as well. The effect of Poisson's ratio on one dimensional analysis is further investigated in Section 4.2.1.

3.2.2 Initial Stress Limit

The initial stress limit aids calculation by specifying the minimum stress that can be modeled. Using a power function to model compressibility, the void ratio increases to infinity as the effective stress approaches zero; therefore, it is necessary to limit how small a value of effective stress can be considered. Assuming that the initial stress limit is equal to the stress calculated for the initial void ratio has shown to produce good results. Other compressibility functions, such as the extended power function, do not increase exponentially at low effective stresses and therefore do not require this to be specified.

3.3 Boundary Conditions

Since consolidation is a coupled process, both deformation and groundwater flux boundary conditions are required. These are entered into the SVSolid and SVFlux portions of the software.

3.3.1 SVSolid

The boundary conditions in this section refer to the stress state due to external load and external factors limiting how the material will deform (i.e. immovable boundaries). The two main deformation boundary conditions consist of either fixed or free boundaries. These are meant to reflect the retaining structures used in the individual benchmarks, or the effects of surrounding parcels of slurry. In general, the bottom boundary is fixed horizontally and vertically, while the side boundaries are only held fixed in the horizontal. This allows the material to consolidate and for internal lateral motion, while still accounting for retaining structures. This is relatively simple for vertical sides, but becomes much more complicated when considering sloping side boundaries. This is discussed in Section 5.2.

To further define the stress regime affecting the system, external loads can be applied as either a point load or a distributed load across the consolidation surface. In some cases these can represent cover systems, although the flux conditions represented by these cover systems should also be considered.

3.3.2 SVFlux

SVFlux allows users to define two different types of boundaries: head and flux boundaries. Head boundaries (includes pressure head) allow the user to designate where the water table occurs and how it will vary over time. The flux boundaries are generally used to limit flow, using zero flux boundaries. They can also be used to imitate ground surfaces, where precipitation, evaporation and runoff are all considered.

3.4 Initial Conditions

Initial conditions refer to values that are placed on the system at the very beginning of the model run. These are generally consistent with the boundary conditions applied to the

system and help to reduce numerical instability. As consolidation involves flux and deformation calculations, initial conditions are required for both, as is explained below.

3.4.1 SVSolid

SVSolid requires the user to state the initial stress or deformation conditions affecting the model before the first time step is completed. The methodology which has resulted in the most success is to define the initial stress limit based upon the void ratio effective stress relationship. Generally an expression is entered where the effective stress is written based upon the initial void ratio. As models are solved considering the three dimensional stress-state, the horizontal stresses must also be defined in addition to the vertical.

3.4.2 SVFlux

The initial groundwater conditions are generally a statement of where the water table is at the beginning of consolidation. This can be defined based on the initial head or pressure head affecting the entire model for cases where the water table is level or by defining where the water table surface is. To avoid numerical errors, the initial head condition should generally be consistent with the applied boundary conditions.

3.5 Preliminary Benchmarking

Prior to the current study, preliminary benchmarking was performed by SoilVision Systems Ltd and published by Fredlund, Donaldson and Gitirana (2009). Their findings included the following benchmarks:

- Coupled vs. uncoupled analyses
- Analysis of the Mandel Cryer Effect in 2D from Cryer (1964)
- Townsend: A Scenario from Townsend and McVay (1987)

While these initial benchmarks assist in evaluating SVOFFICE as a suitable tool for large strain analyses, it is necessary to expand the benchmarking by considering other examples, using a wider variety of materials and boundary conditions.

Chapter 4: One Dimensional Verification and Validation

Applying large strain theory to multidimensional tailings deposits requires extensive benchmarking to develop confidence that the software results are reasonable and can be reliable. One of the goals of this thesis was to provide a degree of verification to the software. A number of one dimensional models were chosen to determine how the software could be applied to a number of different scenarios. SoilVision catalogs all of the models created that benchmark the company's software and releases a free software verification manual on their website. The benchmarks compiled as part of this research were formatted for and a draft verification manual submitted for SoilVision's use. The draft verification manual is presented in Appendix A, while a brief summary of the modeling methodology and results is presented in Section 4.1.

4.1 Benchmark Examples

Case studies were used to benchmark the software against published literature results. The case studies chosen as benchmarks are taken from published articles, where sufficient data was present to complete a reasonable approximation of the paper's own methodology. In some cases, where discrepancies were discovered or where data taken from the papers was found to be insufficient, additional data were gathered or estimations were made. These have been clearly indicated where they have occurred.

A total of 11 case studies were chosen for the purposes of the one-dimensional benchmarking. These case studies were intended to benchmark the SVOOffice consolidation software against a variety of theoretical and real world scenarios. Table 4-1 compares the

various benchmarks chosen for this report. The draft verification manual provided to SoilVision Systems ltd has been reprinted in Appendix A with their permission.

Table 4-1: Overview of benchmarked models and key findings.

| Case Study | Type of Tailings | Initial Void Ratio | Column Height | Compressibility Function | Time Period | Staged Filling | Poisson's Ratio | Original Prediction Method | Description |
|-------------------------------|-----------------------|--------------------|---------------|------------------------------------|-------------|----------------|-----------------|---|---|
| Bartholomeeusen et al. (2002) | Fluvial silt deposits | 2.47 | 0.565 meters | Power and Extended Power Functions | 8 Days | No | 0.35 | Modeling performed by multiple research groups and experimental results | This scenario compares the results of a small scale column consolidation experiment to numerical modeling estimates submitted by researchers. |
| CONDES0 | Phosphate tailings | 4.16 | 10 meters | Extended Power Function | 365 days | No | 0.49 | CONDES0 model results | This benchmark compares the results when CONDES0 and SVOffice are applied to the same 1D scenario. The effects of both staged and instantaneous filling are investigated. |
| | Phosphate tailings | 4.16 | 2 meters | Extended Power Function | 1000 days | Yes | 0.49 | | |

| Case Study | Type of Tailings | Initial Void Ratio | Column Height | Compressibility Function | Time Period | Staged Filling | Poisson's Ratio | Original Prediction Method | Description |
|--|--------------------|--------------------|---------------|--------------------------|-------------|----------------|-----------------|--|--|
| Townsend Scenario A (Townsend & McVay, 1990) | Phosphate tailings | 14.8 | 7.2 meters | Power Function | 8000 days | No | 0.49 | Modeling performed by multiple research groups | Townsend's Scenario A is intended to represent waste ponds that have recently received thickened clays. These clays are then allowed to consolidate under self weight conditions. |
| Townsend Scenario B (Townsend & McVay, 1990) | Phosphate tailings | 14.8, 22.8 | 7.2 meters | Power Function | 1200 days | Yes | 0.49 | Modeling performed by multiple research groups | Townsend's Scenario B predicts consolidation in a 7.2m pond filled in two 6 month stages (with a 6 month latency period between filling stages) and at different initial void ratios. This simulates mature tailings ponds that have been filled intermittently with thickened slurries. |
| Townsend Scenario C (Townsend & McVay, 1990) | Phosphate tailings | 14.8 | 7.2 meters | Power Function | 6000 days | No | 0.49 | Modeling performed by multiple research groups | Townsend's Scenario C predicts consolidation in a homogeneous waste pond with a surcharge load applied at the surface. This simulates a young tailings pond with a sand cap constructed on top of the tailings. |

| Case Study | Type of Tailings | Initial Void Ratio | Column Height | Compressibility Function | Time Period | Staged Filling | Poisson's Ratio | Original Prediction Method | Description |
|--|-------------------------|--------------------|---------------|--------------------------|-------------|----------------|-----------------|---|--|
| Townsend Scenario D (Townsend & McVay, 1990) | Phosphate tailings | 6.3-14.8 | 8.4 meters | Power Function | 8000 days | No | 0.49 | Modeling performed by multiple research groups | Townsend's Scenario D predicts consolidation in a mature waste pond with a sand/clay cap applied to the surface. This simulates a pond that has had time to develop layering with distinct void ratios. |
| Jeeravipoolvarn (2008) | Oil sands fine tailings | 5.17 | 10 meters | Weibull Function | 10000 days | No | 0.40 | Modeling performed by Jeeravipoolvarn et al. and experimental results | Two scenarios were taken from a comparison made by Jeeravipoolvarn (2008) based upon the results of a long term large strain consolidation experiment on oil sands tailings. The Weibull function is used here to compare the methodologies. |
| | Oil sands fine tailings | 0.87 | 10 meters | Weibull Function | 4380 days | No | 0.40 | | |
| Caldwell et al. (1984) | Sulfide tailings | 1.20 | 47.15 meters | Extended Power Function | 20 years | Yes | 0.30 | Numerical modeling results provided by Caldwell et al. | A number of real world case studies of large strain consolidation predictions for real tailings impoundments were presented by Caldwell et al (1984). These models were compiled based upon filling curves and two case studies were recreated in SVOOffice. |
| | Sulfide tailings | 2.40 | 119.3 ft | Extended Power Function | 27 years | Yes | 0.30 | | |

4.2 One Dimensional Modeling Considerations

Modeling 1D large strain consolidation in SVOffice requires several assumptions to be made. To better understand the impacts of these assumptions, literature and sensitivity studies were carried out.

4.2.1 Poisson's Ratio

Poisson's ratio is a required parameter within the SVOffice formulation (Section 3.2.1) that is not considered in most other large strain formulations. Therefore, values for different types of tailings are assumed in each model. To better understand how Poisson's ratio affects the results observed a sensitivity analysis was carried out where the Poisson's ratio was varied across the entire range of accepted values (0.01-0.49).

The first 1D Caldwell sulphide tailings case study was used to demonstrate the effect of varying the Poisson's ratio on consolidation. The surface height results, shown in Figure 4-1, illustrate that SVOffice agrees well with the 1D results obtained from Caldwell et al. (1984) when a Poisson's ratio of 0.3 is assumed. The largest variations occur early in the filling of impoundment, with the SVOffice results showing slightly less consolidation than those recorded in the literature. The Caldwell et al. (1984) values are plotted as points while SVOffice values are plotted as lines.

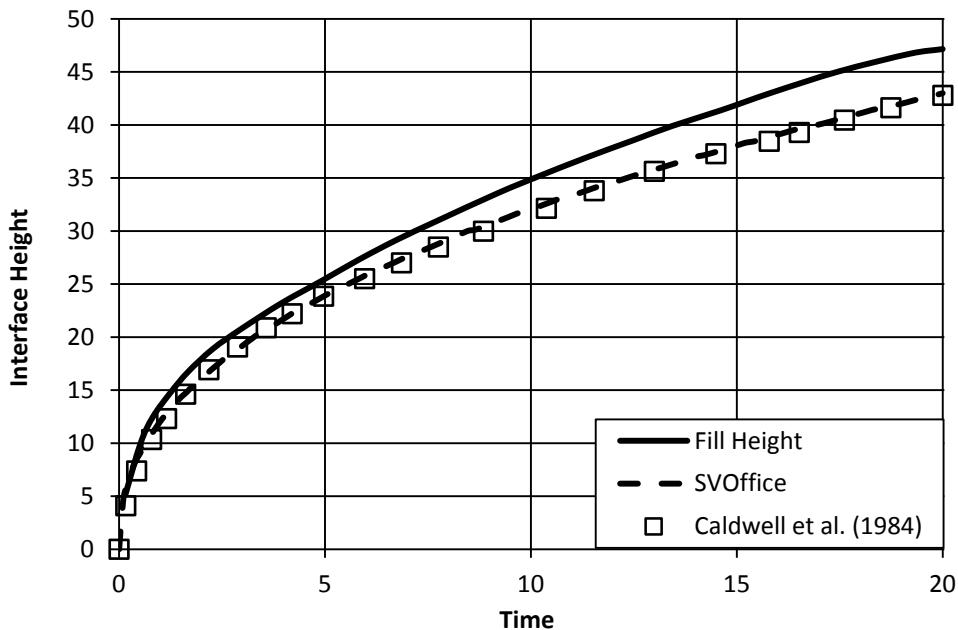


Figure 4-1: Comparison of filling curve and Caldwell et al.'s predictions against SVOFFICE.

A simple sensitivity analysis was created by varying the Poisson's ratio and comparing the predictions for the final height of the tailings deposit. Poisson's ratio has a significant effect on the results observed, as is presented in Figure 4-2. The lowest values of Poisson's Ratio produce the least amount of settlement, while the most settlement is observed at the highest Poisson's Ratio.

The Caldwell et al. (1984) results appear to correspond well with a Poisson's Ratio between 0.3 and 0.4. Consoli (1991) assumed a value of 0.30, which is stated to be a typical value for cohesion-less materials (Consoli & Sills, 2000). This value appears reasonable for loose sands, however, the sulphide tailings investigated here were finely ground (80% passing the number 400 sieve) (Caldwell et al., 1984), therefore higher values of Poisson's Ratio may be required.

4.2.2 Pond Height

A common assumption when modeling tailings consolidation is to assume that the entire system remains saturated. The simplest way to do this is to set the top flux boundary equal to the head value corresponding to the highest elevation of the tailings impoundment. However, in many cases, the water head above the tailings might vary significantly over the life of the impoundment, as the pond fills up. Therefore, a test was performed to determine what impact increasing the head would have on consolidation.

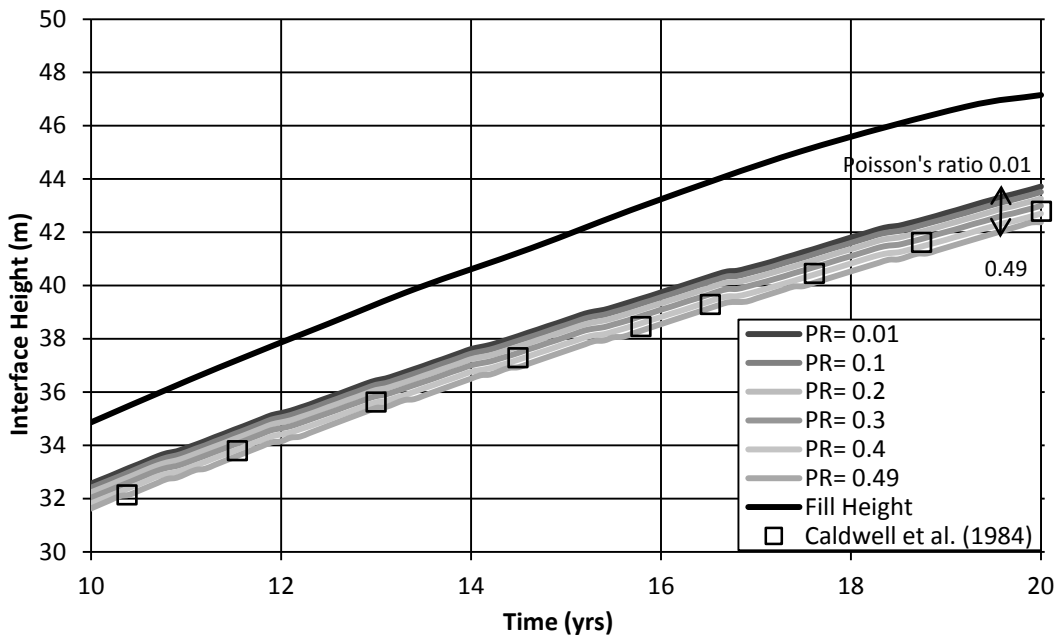


Figure 4-2: Changes in the final surface height with Poisson's Ratio.

The CONDES0 case study looking at instantaneous filling of a 10 meter column of tailings was chosen, and the scenario run for a variety of surface head values. Figure 4-3 and Figure 4-4 compare the column settlement and excess pore-water pressure of the benchmark case where a head equal to the column height (10m) is applied to much larger applied heads of 20, 50 and 100 meters. It was found that these increases in the head or in other terms, the

water level would have no impact upon the observed tailings consolidation. This is because the excess pore-water pressures do not change, along with the absolute pore-water pressures. The consolidation equation only considers changes in excess pore-water pressure, as this is what determines how the stress is transferred from the incompressible water to the soil matrix. The influence of unsaturated conditions will need to be considered, if the tailings are not completely saturated. However, if the tailings are saturated, a constant head equal to or greater than the maximum fill height of the tailings will lead to the same degree of consolidation being observed within the model.

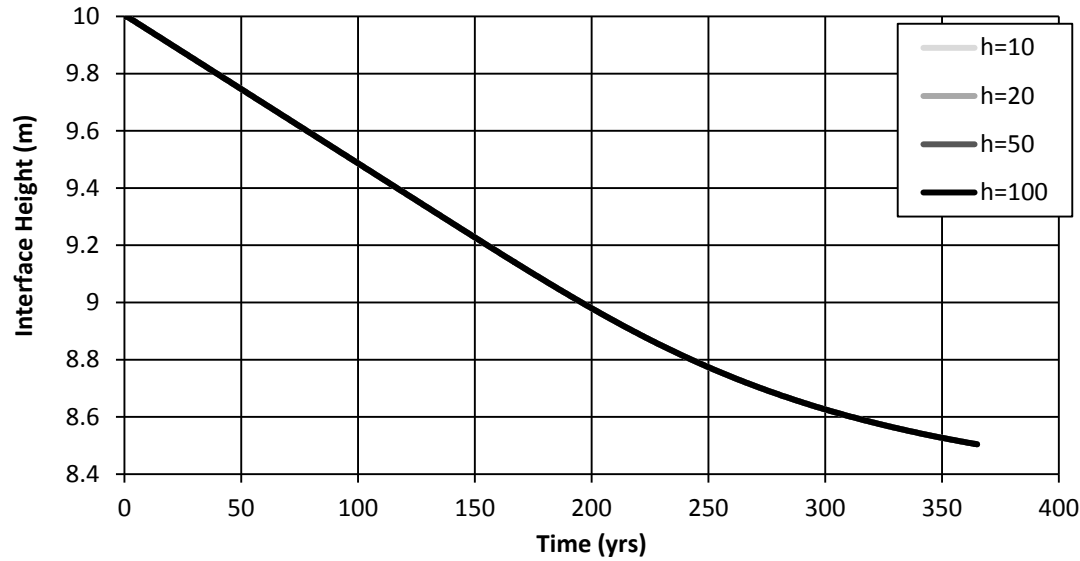


Figure 4-3: Variation in interface height with time due to the application of various head boundaries. Note: the lines fall immediately above one another, therefore, there is only one line observed.

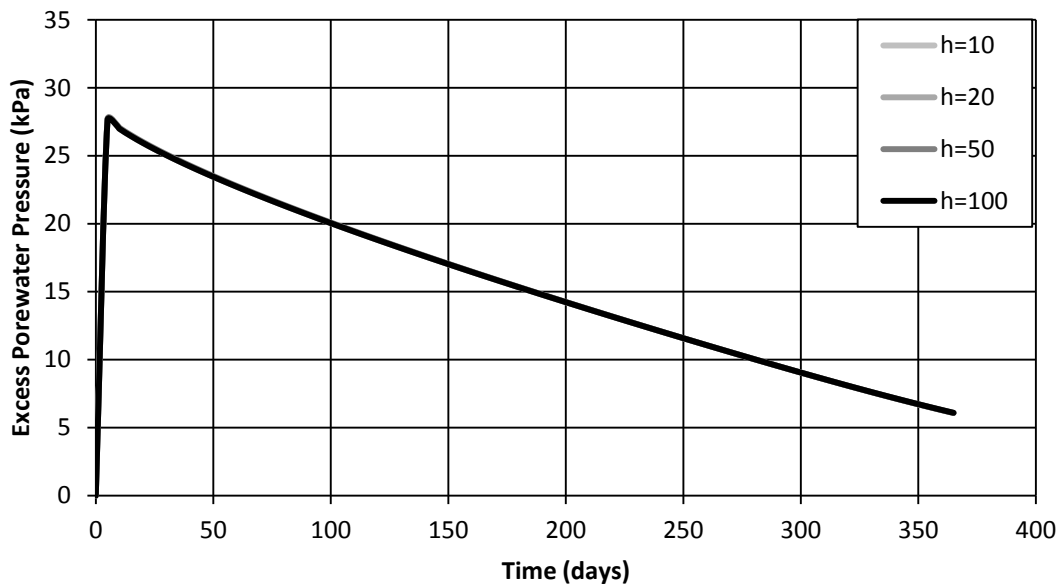


Figure 4-4: Variation in excess pore-water pressure with time due to the application of various head boundaries. Note: the lines fall immediately above one another, therefore, there is only one line observed.

4.3 Results of Benchmarking

When applied to the above case studies, a number of factors were benchmarked, to gain further insights. These benchmarks are presented in detail in Appendix A and include investigations of the following factors:

- 1D analyses
- Staged Filling Analyses
- Use of the Power, Extended Power and Weibull compressibility functions
- Standardized deformation boundary conditions
- Suggested flux boundary conditions
- External loading
- Gold Tailings (moderate material properties)
- Phosphate Tailings (high void ratios and large deformations)
- Oil Sands Tailings

The benchmarking shows that SVOffice is capable of duplicating many previous studies of large strain consolidation covering a wide variety of applications. The assumptions contained in the individual analyses and how these can be related in SVOffice are discussed in detail for each benchmark within Appendix A.

In addition the relative effects of pond height and Poisson's ratio were investigated to determine how they would affect the modeling procedure. It was determined that as long as the material remained saturated, there would be no impact of pond height upon consolidation. However, Poisson's ratio was found to have a significant effect upon the analyses and therefore requires further discussion.

Through the ongoing process of benchmarking, more confidence is gained in the applied methodology and results obtained when the program is applied to new scenarios. Although the current benchmarking provides a suitable basis for 1 dimensional analyses, further benchmarking to practical scenarios will be advantageous. The next chapter discusses applying the software to multidimensional scenarios and the results that can then be achieved.

Chapter 5: Modeling Multi-Dimensional Tailings Deposits

While one dimensional modeling is a valuable way to gain knowledge of tailings consolidation behavior, it becomes necessary to start considering multi-dimensional factors when designing large tailings impoundments. These factors can include lateral flow, side boundary influences and horizontal deformation. Chapter 5 presents several applications of the SVOffice large strain consolidation software to multi-dimensional scenarios. The initial scenario presents a comparison of two and three dimensional results to a simple column test. Idealized 2D geometry is then used to look at the impact of side slopes, under-drainage and variable depositional schemes. A comparison is also made to another literature study considering gold tailings deposited in a pit and the effect of lateral drainage on consolidation. Finally a 3D tailings impoundment is presented to show how topographic data can be used to create a 3D impoundment. As setting up the 3D models is somewhat challenging and currently requires some approximation, the manner in which the mesh is defined will be discussed.

5.1 Effects of Multidimensionality – Column Analysis

To compare the results of a 1 dimensional model with two and three dimensional results, the column test introduced by Jeeravipoolvarn et al. (2008) was evaluated as a multidimensional configuration. Two and three dimensional model results are compared to the one dimensional to examine any effects due to dimensionality.

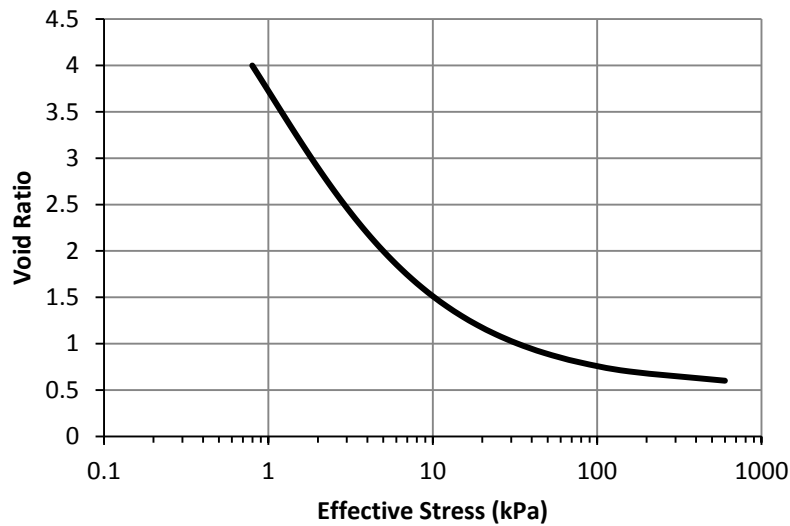


Figure 5-1: Compressibility curve of oil sands column 1 (Jeeravipoolvarn et al. 2008)

5.1.1 Material Properties

The material used consists of oil sands tailings taken from Syncrude's Mildred Lake Tailings Impoundment in 1982. It has a specific gravity of 2.28 and an initial void ratio of 5.17.

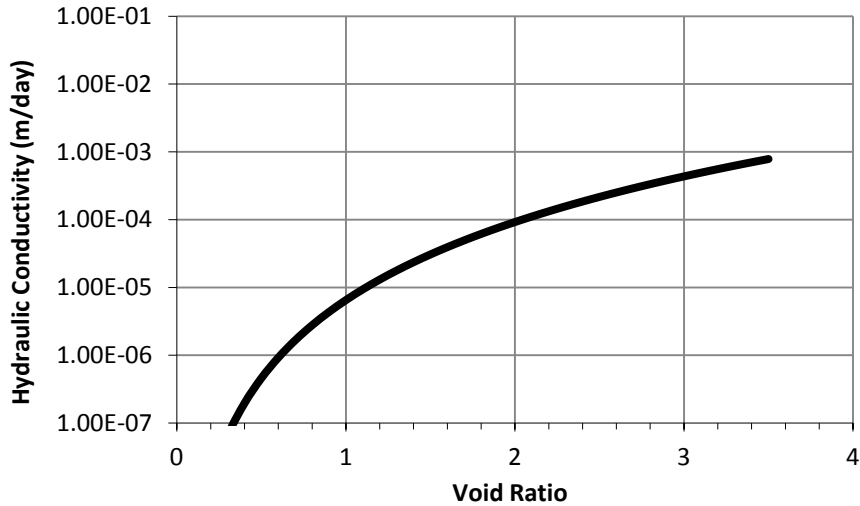


Figure 5-2: Oil sands column 1 void ratio-hydraulic conductivity curve (Jeeravipoolvarn et al. 2008).

Jeeravipoolvarn et al. (2008) uses a Weibull function to relate effective stress and void ratio, whereas the SVOFFICE software has implemented a number of different functions,

including Weibull. To compare the differences between the different functions both the Weibull and the Power Functions were tested. A suitable power series was found in Jeeravipoolvarn, 2010. The Weibull function is provided in equation 5-1 and the Power function in equation 5-2. Equation 5-3 shows the hydraulic conductivity – void ratio relationship. These are shown graphically in figures 5-1 and 5-2.

$$e = 5.50 - 4.97 * \exp(-1.03\sigma'^{-0.67}) \text{ (kPa)} \quad 5-1$$

$$e = 3.391\sigma'^{-0.308} \text{ (kPa)} \quad 5-2$$

$$k = 6.51 * 10^{-6} e^{3.824} \text{ (m/day)} \quad 5-3$$

The initial stress limit was set to be 0.254 kPa, as this is the minimum effective stress that should be observed based upon the initial void ratio. This is found by solving for the effective stress present at the initial void ratio using equation 5-1. A Poisson's ratio of 0.4 was assumed, since none was specified in the literature.

5.1.2 Geometry/Boundary Conditions

The model consists of a circular column, with a height of 10 m (Figure 5-3). It is assumed that the tailings are initially homogeneous and deposited instantaneously. The deformation boundary conditions consist of a lower boundary that is fixed in place, and an upper boundary that is free to deform. In the multi-dimensional models, the lateral boundaries are fixed in the horizontal, but are free to deform vertically. The flux conditions consist of a constant head of 10 m at the top boundary and a zero flux boundary at the bottom. This forces the water to flow from bottom to the boundary, while simulating a constant water table above the soil region.

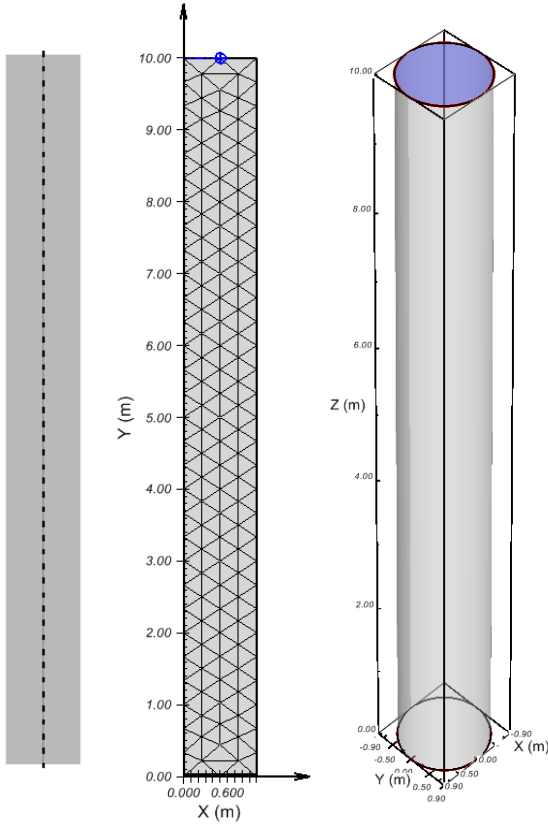


Figure 5-3: Oil sands column 1 model geometry in 1D, 2D and 3D. Note: only 25% of nodes are shown for the 1D analysis for the sake of clarity.

5.1.3 Results

Figure 5-4 shows a comparison of the interface heights predicted and those found experimentally by Jeeravipoolvarn et al (2008) with the modeling results from SVOOffice. The SVOOffice predictions are very similar to the results predicted by Jeeravipoolvarn et al (2008), although these results are not consistent with the experimental results. Furthermore, it can be seen that the 1D, 2D and 3D Weibull results are identical. This was expected, as the side boundary conditions of a column test would not impact the degree of consolidation significantly. Also it can be seen that the Power function predicts slightly more consolidation than the Weibull function. Figure 5-5, Figure 5-6, and Figure 5-7 compare the height profiles of the effective stress, excess pore-water pressure, and void ratio found

through experimental testing and modeling predictions by Jeeravipoolvarn et al (2009) and the results obtained by SVOOffice in a 1D analysis. It can be seen that the results are nearly identical. SVOOffice does predict slightly higher effective stress values, yet these values are still very low in comparison to the total stress and pore-water pressure.

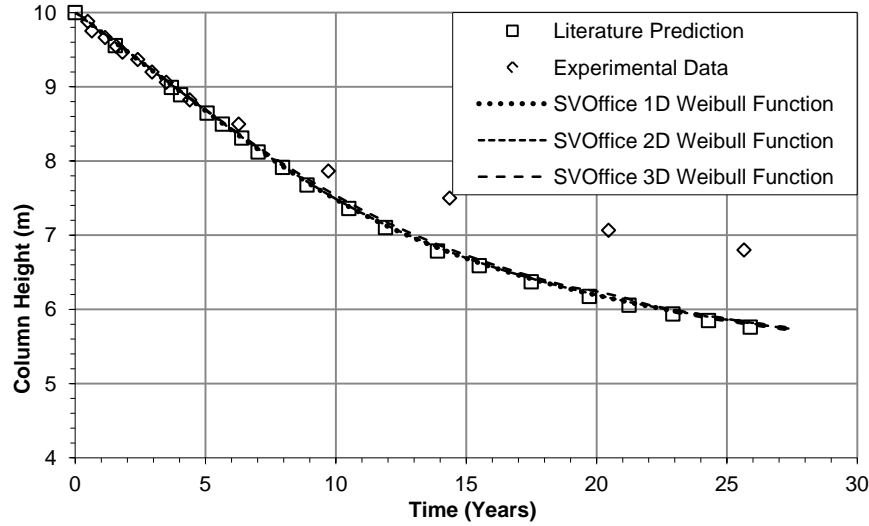


Figure 5-4: Oil sands column comparison of 1D, 2D and 3D column test results.

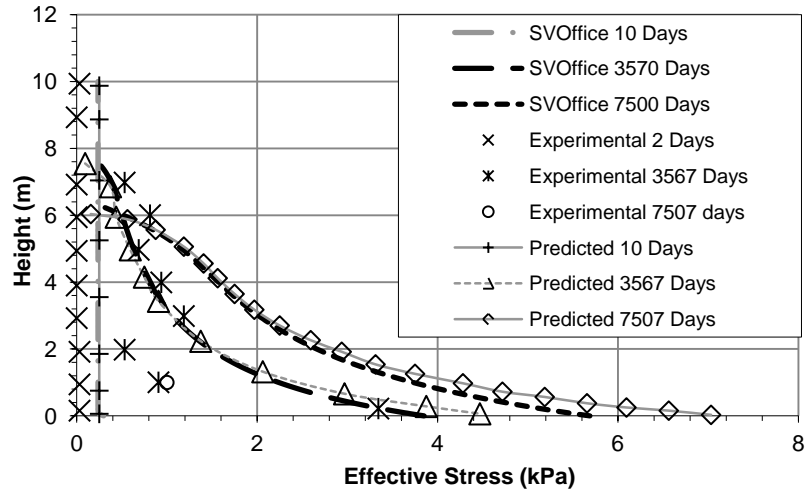


Figure 5-5: SVOOffice, experimental and literature prediction effective stress profiles at various times

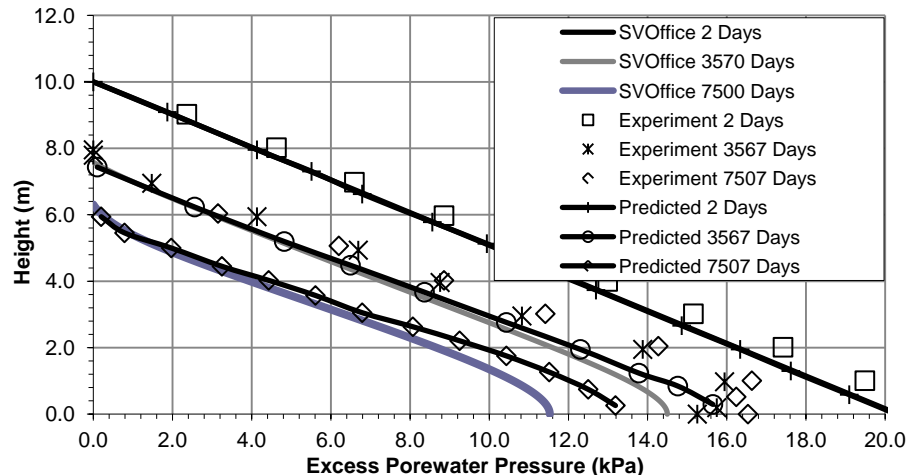


Figure 5-6: SVOOffice, experimental and literature prediction excess pore-water pressure profiles at various times

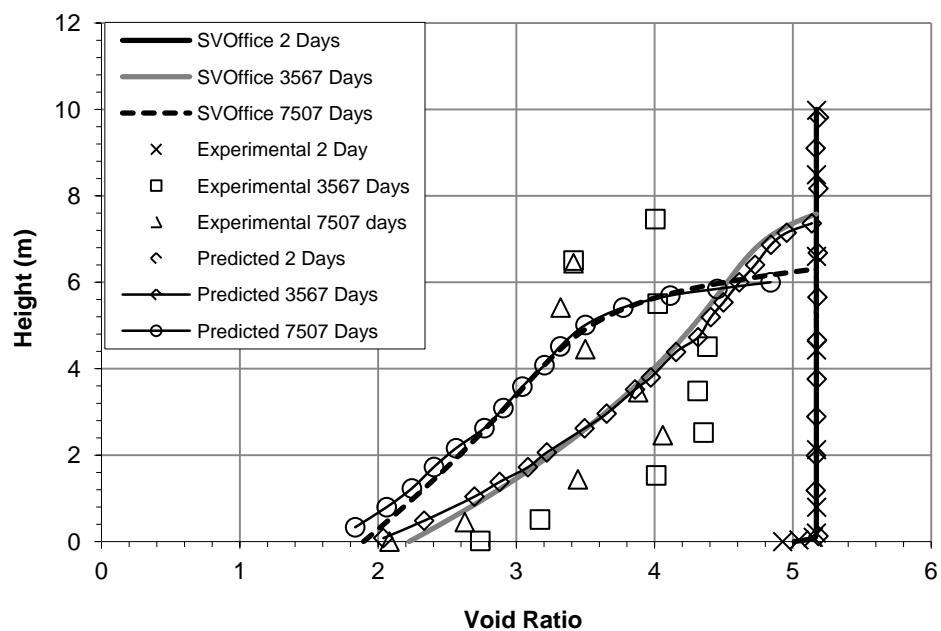


Figure 5-7: SVOOffice, experimental and literature prediction void ratio profiles at various times

5.1.4 Discussion

The use of the same material parameters and model geometry within SVOOffice is found to produce the same results as Jeeravipoolvarn et al. `s (2008) modeling. The fact that these parameters do not produce the same results as were observed in the experiment mean that the parameters do not properly reflect the material behavior and thus further material testing needs to be performed to develop more representative parameters.

The fact that the same results are observed when the model is considered in multiple dimensions as the 1D case indicates that for this system there are no significant multidimensional effects when models are extrapolated into multiple dimensions. For multi-dimensional column tests, this is the correct result, as one dimensional models are meant to represent the results of a real world column test, which does exist in three dimensional space. Jeeravipoolvarn (2010) performed a similar experiment in 1D and 2D using his multidimensional formulation and observed the same result.

5.2 2D Tailings Impoundment

To examine some of the effects of modeling an impoundment in two dimensions, an extrapolation of the Caldwell et al. (1984) one dimensional model, which is discussed in Section 4.1 and presented in detail in Appendix A, was created using the same filling curve and material parameters as the one dimensional model. This allows for comparisons to be made to the results of the one dimensional model and incorporates material parameters and a filling curve known to exist in the real world. This allows the investigation on the effects of side boundary conditions. Also, based on data for both the sulphide and gossan tailings produced at this site, an alternate deposition scenario can be used to investigate the effects of spatial variability of tailings.

5.2.1 Geometry and Boundary Conditions

The original model consists of a 47.15m column of sulphide tailings. The main impoundment is filled over 20 years, therefore staged filling needs to be applied. This is a more realistic long term management simulation as opposed to instantaneous filling. SVOOffice uses a phased approach whereby regions are added at specified time increments. Therefore, the filling curve provided from Caldwell et al (1984) (Figure 5-12) was used to determine a number of irregular increases in tailings height. Each step was phased at the halfway point between the start and end time of the respective phase, thereby resulting in a stepwise filling scheme.

Deformation is fixed along the bottom boundary. There are no restrictions with respect to deformation applied to the top boundary. The bottom boundary is set to be impermeable, while the water level on top of the pool is held constant at 47.15 m throughout filling resulting in a completely saturated system. Caldwell et al. (1984) also states that the tailings were deposited below water.

A 2V:1H sloped side impoundment geometry has been assumed for this simulation to allow for the investigation of sloping boundary conditions, which can only be applied to uniform slopes (Figure 5-9). For this scenario, the sidewalls remain impermeable, although the use of different boundary conditions could be used to simulate the presence of low hydraulic conductivity embankments or various hydraulic conditions. This is discussed further in Section 5.3.

5.2.2 Material Parameters

Caldwell et al (1984) provided the effective stress – void ratio – hydraulic conductivity relations used in their calculations. These were digitized and subsequently

extended power functions were fit to the data. These are shown in 5-9. The sulphide tailings are stated to have a specific gravity of 4.2 and an initial void ratio of 1.1, while the gossan tailings have a specific gravity of 3.2 and an initial void ratio of 2.0.

The constitutive equations for the compressibility and permeability of the sulphide tailings are given in equations 5-4 and 5-5 respectively, while those of the gossan tailings are given in equations 5-6 and 5-7.

$$e = 1.29(\sigma' + 9.402)^{-0.071} \quad 5-4$$

$$k = 1.6572e^{6.7026} \quad 5-5$$

$$e = 1.97(\sigma' + 0.86)^{-0.099} \quad 5-6$$

$$k = 0.154e^{4.8205} \quad 5-7$$

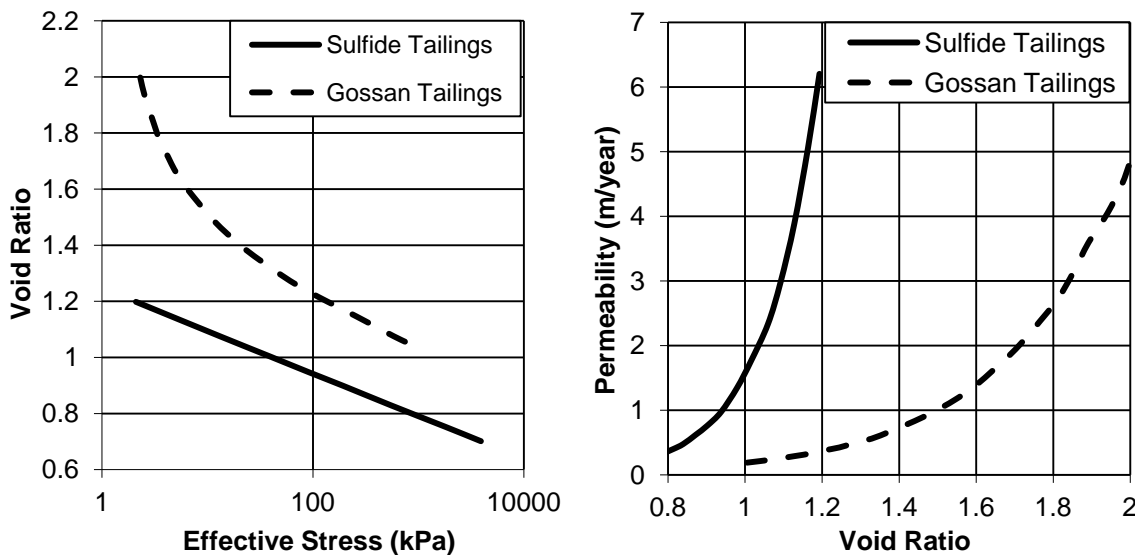


Figure 5-8: Compressibility and permeability relationships of sulfide and gossan tailings

A Poisson's ratio of 0.30 was assumed although there was no value provided in the report. A sensitivity analysis is presented in Section 4.2.1 to determine the effect of the Poisson's Ratio on the one dimensional results.

5.2.3 Sloping Boundary Conditions

Consolidation along a slope is an area that has not been fully investigated. Jeeravipoolvarn (2010) used fixed side boundaries to simulate consolidation along the inside of a conical containment vessel. It is acknowledged that this is a simplification. An alternative approximation that has been implemented in SVOFFICE is to allow the boundary to deform within the bounds of the system along a frictionless slope.

Figure 5-10 and Figure 5-11 demonstrate the deformed mesh after 20 years of the fixed and sliding boundary conditions respectively. The void ratio distribution within the impoundment is also shown. The boundary conditions prove to have a significant impact upon the observed behaviour. The fixed condition results in a concave surface, with very little consolidation observed at the sloped boundaries, as would be expected when they are not allowed to deform. When the sliding boundary condition is introduced, the opposite is observed, there is a convex surface, with greater consolidation occurring near the side slopes.

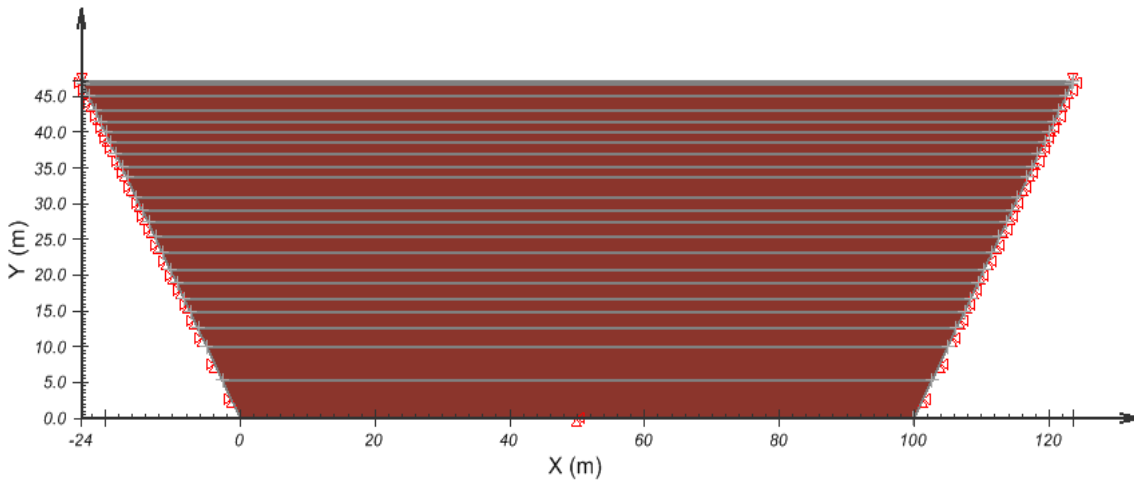


Figure 5-9: Geometry of 2-D tailings impoundment model

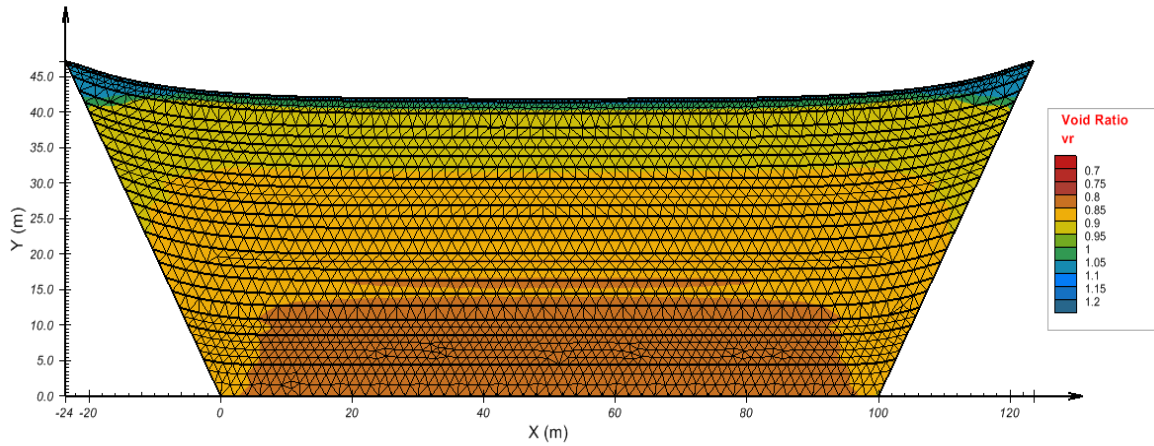


Figure 5-10: Fixed geometry deformation after 20 years with void ratio profile.

Figure 5-12 compares the surface height predictions at the center of the 2D impoundment for the fixed and sliding sloped boundaries to those of the 1D column. Both show good correlation to the 1D prediction of Caldwell et al (1984). The fixed model predicts slightly more consolidation at the center than the sliding boundary condition. This could be caused by the fact that when a fixed boundary is applied, less consolidation occurs along the sides, meaning that the excess pore water pressure is able to dissipate to a lesser extent horizontally as well as vertically. The flow vectors are depicted in Figure 5-13 and show that there is drainage occurring towards the edges.

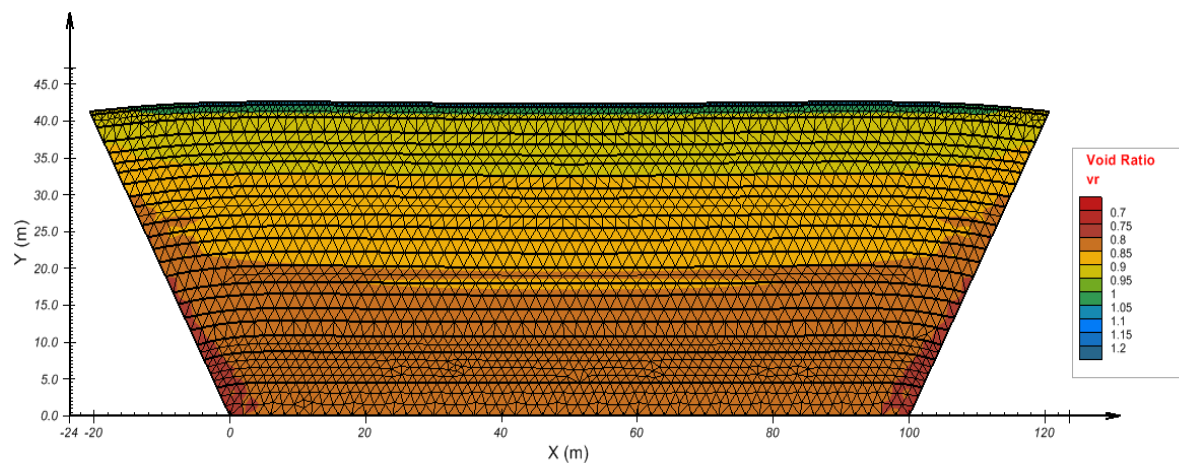


Figure 5-11: Sliding geometry deformation after 20 years with void ratio profile.

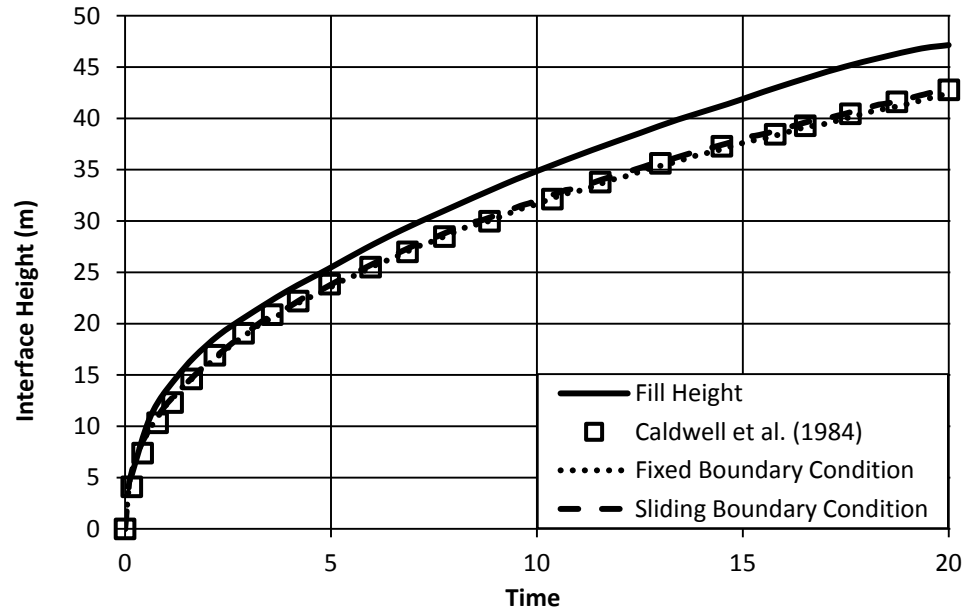


Figure 5-12: Comparison of 2D impoundment heights at center of deposit for fixed and sliding boundary conditions against the filling curve and Caldwell et al. (1984) prediction.

5.2.4 Effect of an Underdrain

To further extend the two dimensional model, the effect of a drain layer along the bottom of the impoundment is investigated. To simulate a free draining surface, the bottom

boundary condition is defined as having a water head of 0 meters. The sloping sides remain impermeable, and the fixed boundary condition is used.

Figure 5-14 shows the deformed mesh and void ratio profile after 20 years when an underdrain is included. The void ratio profile is more uniform, than when the lower boundary remains impermeable (Figure 5-10). For this geometry and material parameters, the presence of the underdrain was found to have a very small impact when considering settlement of the surface. While an underdrain is expected to increase consolidation over time, Anstey and Williams (2007) also found that for accumulating metals tailings, the underdrain did not significantly affect consolidation, but rather that the hydraulic conductivity of the tailings is the determining factor.

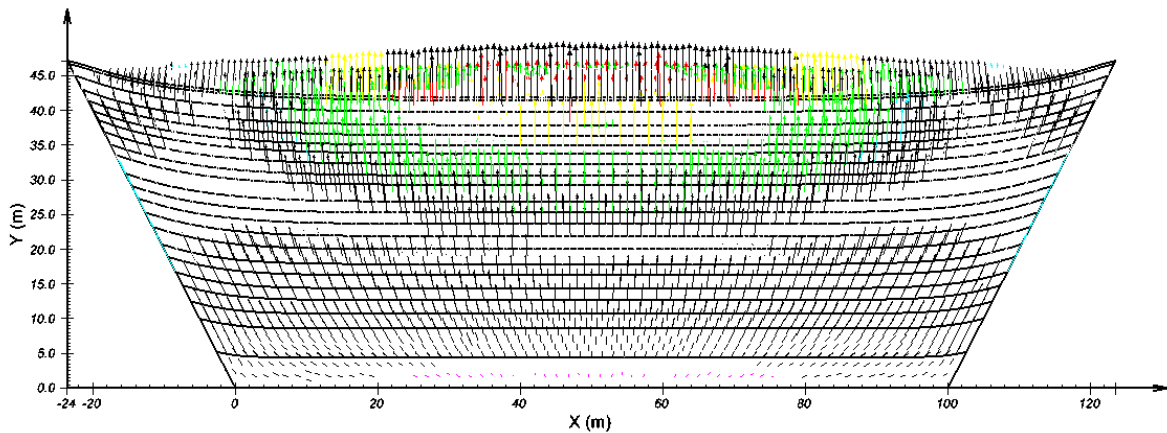


Figure 5-13: Flux vectors in the fixed boundary condition scenario.

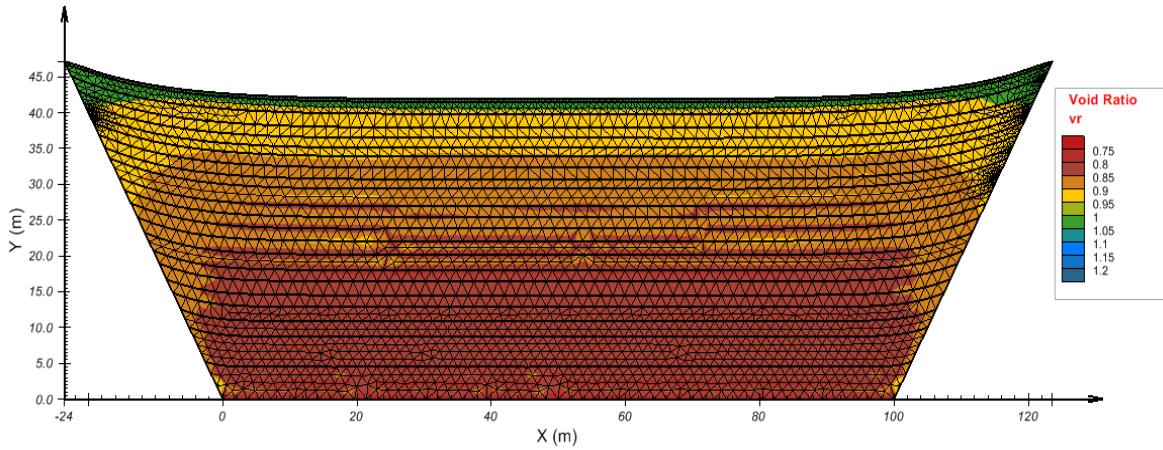


Figure 5-14: 2D deformation with under drain after 20 years with void ratio profile.

5.2.5 Spatial Variability

As was previously mentioned there were both gossan (exposed oxidized portion of the mineral vein) and sulphide tailings produced at this location, with the gossan tailings being produced earlier in the mine life. One disposal scenario, which was initially considered, was to deposit the gossan tailings underneath the sulphides. As the gossan tailings have a much lower specific gravity and a completely different set of index and consolidation parameters, these tailings would behave differently than the sulphides. Although this scenario was questioned by reviewers at the time due to potential overturning of the tailings due to the gossan tailings having lower specific gravity, it does present an interesting finite strain model that can be evaluated.

It is assumed that the first two lifts, totalling 10 meters, are made up of the gossan material. The same filling curve was used from the main impoundment. A diagram of the model after 20 years is shown in Figure 5-15, while the tailings height predictions are shown in Figure 5-16. The two material model shows significantly more consolidation than the base fixed boundary scenario.

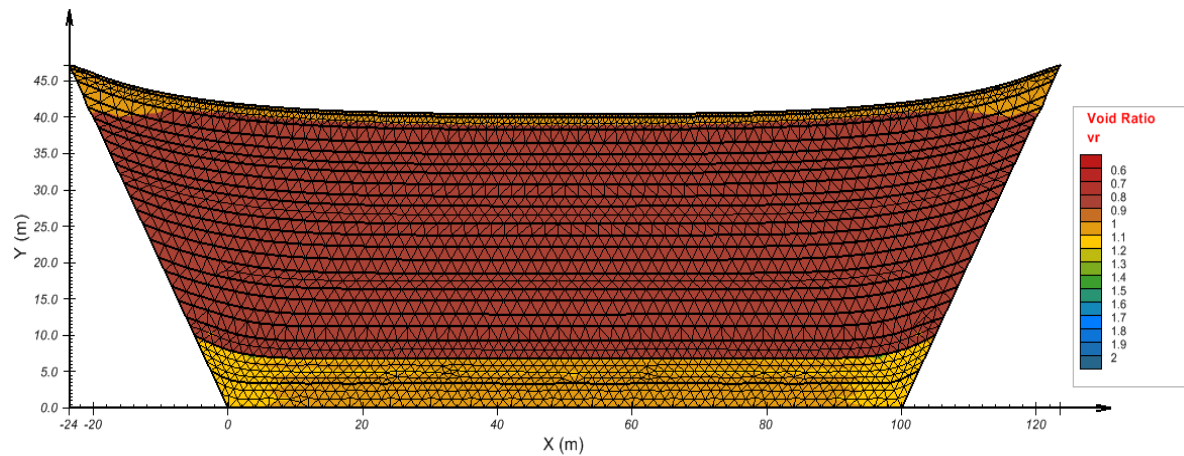


Figure 5-15: Two material disposal scenario after 20 years with void ratio profile.

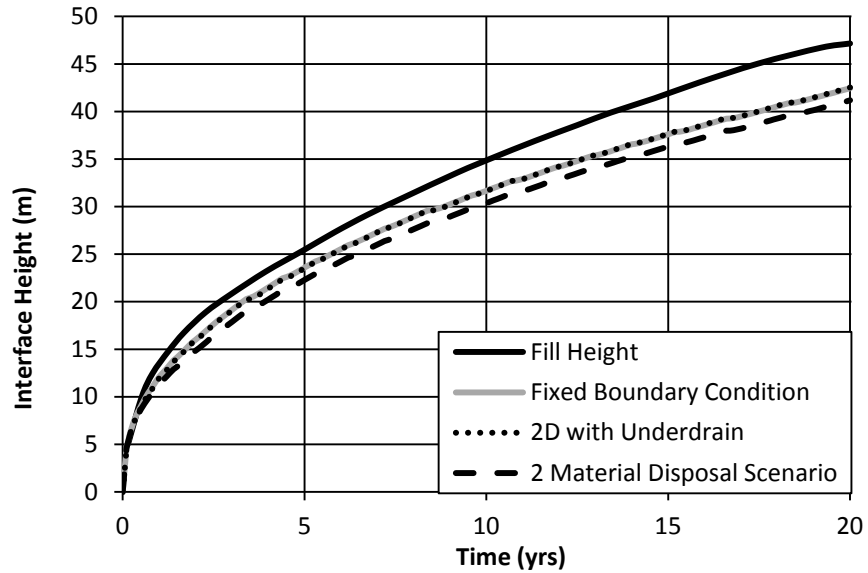


Figure 5-16: Filling height comparison of the effect of the under drain and the 2 material disposal scenario.

5.3 2D Tailings Pit

In their 2007 paper, Anstey and Williams introduced two case studies examining large strain consolidation being applied to in-pit tailings disposal. They studied both gold and nickel tailings impoundments and found that using a large strain formulation in the

program Plaxis, they could model the impoundments in two dimensions. While the Plaxis formulation is different to that used by SVOOffice, it was possible to make a comparison between the methodologies by modeling the gold tailings impoundment using SVOOffice. This required a number of assumptions to be made regarding the functions used to fit the material properties; however, it is believed that the results obtained can be used to further the examination of modeling in two dimensions. Plaxis also uses an ALE (Arbitrary Lagrangian Eulerian) coordinate system (Fredlund, 2011), while the modeling performed in SVOOffice uses a Lagrangian coordinate system. Generally ALE formulations are preferred for very large deformations, as they allow for very large deformations to be modeled without the need for constant re-meshing as the mesh is either allowed to move according to Lagrangian principles or remains static according to Eulerian (Donea, Huerta, Ponthot, & Rodriguez-Ferrari, 2004). Comparisons between the methodologies are made, although it must be remembered that it is possible that significantly different material parameters are being modeled. The procedure used to extrapolate material properties is provided for each tailings impoundment.

A rebuttal paper was written in 2010 by McDonald and Lane, which argued that these models should be completed using the modified Cam-Clay methodology. While the results obtained are found to show good correlation to the field observations, it is believed that the Cam-Clay model doesn't adequately consider the material behavior as it linearizes the compressibility relationship and uses a constant hydraulic conductivity. The results of this are discussed further in Section 5.3.5

5.3.1 Geometry

The geometry for the gold tailings impoundment is given in Figure 5-17. The tailings pit was filled in a number of stages using a linear rate of filling. An interesting aspect of the Anstey and Williams (2007) analysis is that the hydraulic conductivity of the surrounding bedrock was included, so that lateral drainage through the bedrock could be incorporated into the analysis.

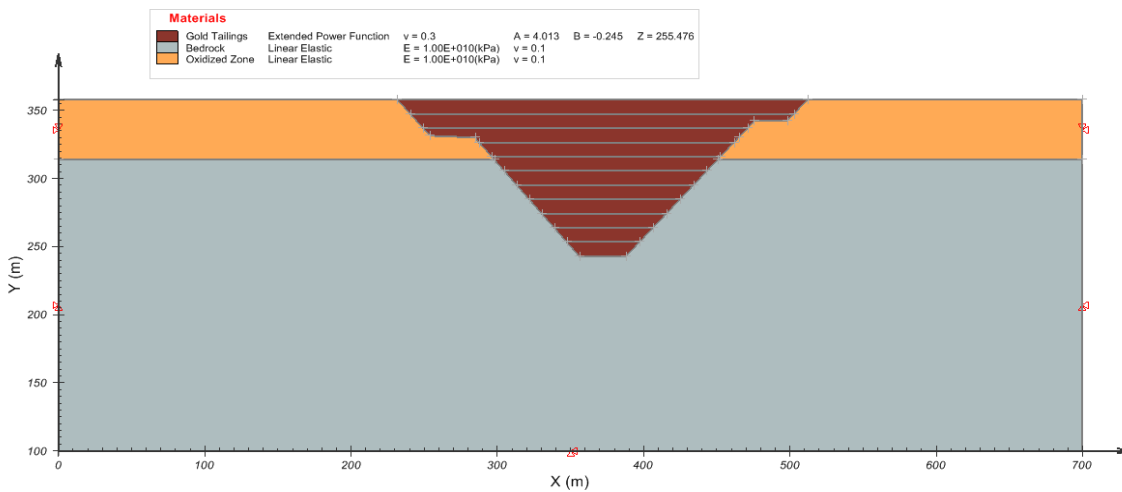


Figure 5-17: Gold tailings impoundment geometry (Anstey and Williams, 2007).

5.3.2 Extrapolation of Material Parameters

The method with which Anstey and Williams (2007) incorporated the compressibility and hydraulic conductivity relationships of the tailings is unclear. Their paper does, however, provide information about the minimum and maximum void ratios and the stresses at which they occur, as well as the corresponding minimum and maximum compressibility (a_v) and hydraulic conductivity values (k). It is therefore possible to solve for power functions that correspond to these parameters. Representing the hydraulic conductivity relationship with a power function is simple, as there are two variables and two equations.

The compressibility relationship required additional manipulation to be fit to an extended power function. To do this, the definition of compressibility (equation 5-8) was used.

$$a_v = \frac{de}{d\sigma'} \quad 5-8$$

Taking the derivative of the extended power function, it is possible to define compressibility as is shown in equation 5-9.

$$a_v = AB * (\sigma' + Z)^{B-1} \quad 5-9$$

This provides 4 equations, with which to solve for the three variables of the extended power function. Microsoft Excel Solver was used to solve the system of equations. The following sections summarize the interpolated parameters.

The gold tailings studied by Anstey and Williams (2007) have a specific gravity of 2.64 and an initial void ratio of 1.03. Based upon the void ratio and compressibility data provided, equations 5-10 and 5-11 were developed.

$$e = 4.013(\sigma' + 255.5 \text{ (kPa)})^{-0.245} \quad 5-10$$

$$k = 0.00283(e)^{4.84} \left(\frac{m}{day} \right) \quad 5-11$$

These equations are presented visually in Figure 5-18 and Figure 5-19. A comparison of the literature and calculated parameters is presented in Table 5-1.

Table 5-1: Comparison of literature and calculated material parameters for the gold tailings compressibility function at the minimum and maximum void ratios.

| Parameter | Literature | Calculated |
|-------------|------------|------------|
| e_1 | 1.031 | 1.031 |
| e_2 | 0.553 | 0.553 |
| a_{v1} | -0.00098 | -0.001 |
| a_{v2} | -2.6E-05 | -4.2E-05 |
| K_1 (m/d) | 3.28E-03 | 3.28E-03 |
| K_2 (m/d) | 1.61E-04 | 1.61E-04 |

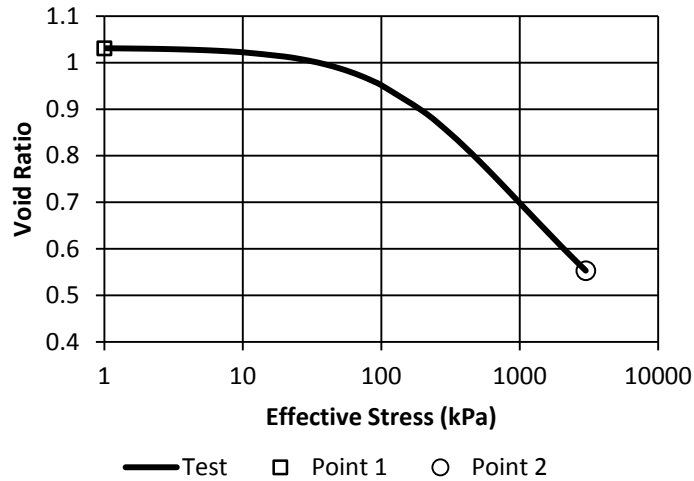


Figure 5-18: Compressibility function fitted to gold tailings parameters.

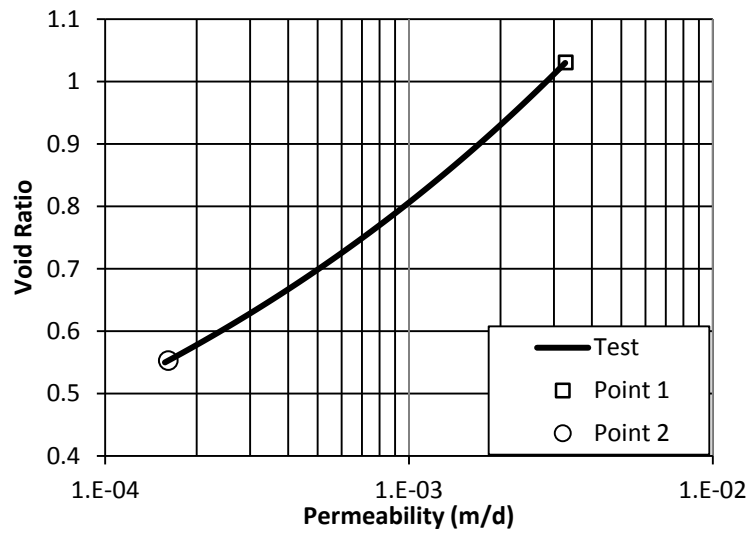


Figure 5-19: Hydraulic conductivity function fitted to gold tailings.

5.3.3 Boundary Conditions

The impoundments defined by Anstey and Williams (2007) are surrounded by pervious fractured bedrock. The influences of this are therefore modeled. The hydraulic conditions are maintained as normal, with zero flux boundaries at the extents of the bedrock and a head boundary equal to the maximum height of the tailings, to ensure the model

remains saturated. Deformation at the model edges is also restricted on the sides, bottom and upper bedrock. The top of the tailings is allowed to deform. There are no conditions placed upon the intersection of the tailings and bedrock, as these conditions are covered by the defined material parameters.

5.3.4 Results

The gold tailings scenario was allowed to run for a period of approximately 41 years following filling. It was found that 90% of total settlement had been reached after 13 years while 99% was reached after approximately 19.5 years. Figure 5-20 illustrates the final deformed mesh spacing of the tailings impoundment of the tailings and surrounding bedrock. Figure 5-21 and Figure 5-22 chart the changes in surface elevation and cumulative settlement of the tailings over time.

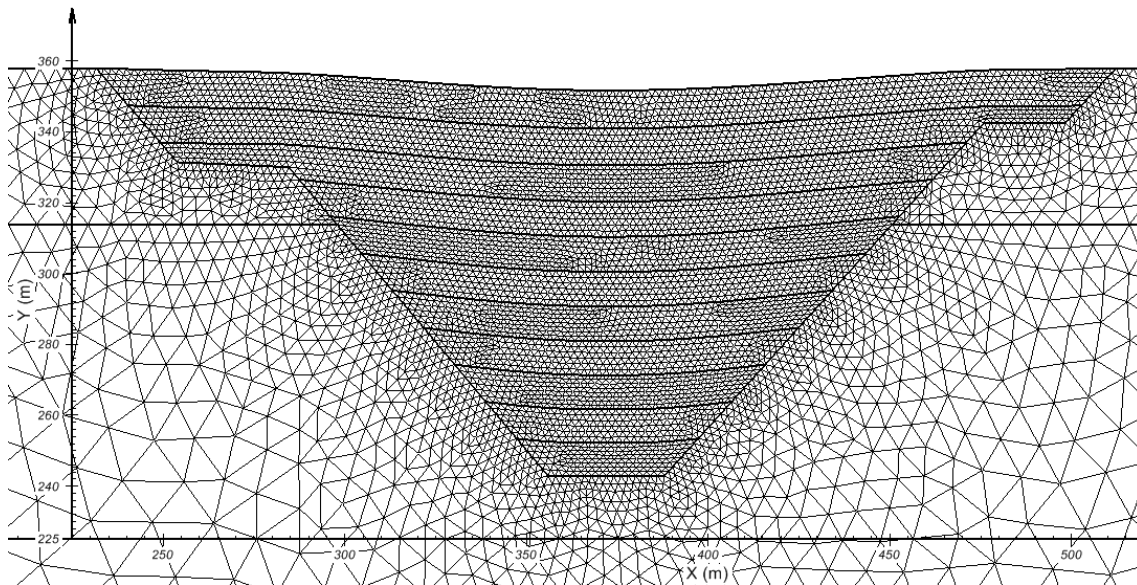


Figure 5-20: Deformed mesh of the gold tailings impoundment after 30 years of consolidation

5.3.4.1 Settlement

The tailings were found to settle to a maximum of 6.2 meters below the maximum fill height at the center of the impoundment. This compares to a prediction of 6.8 meters by Anstey and Williams (2007), who also predict that it would take 109 years to reach 90% consolidation. To illustrate the process of consolidation Figure 5-23 and Figure 5-24 show time series of the distribution of displacement and void ratio respectively, within the impoundment. Note: all time values in subsequent diagrams given in years.

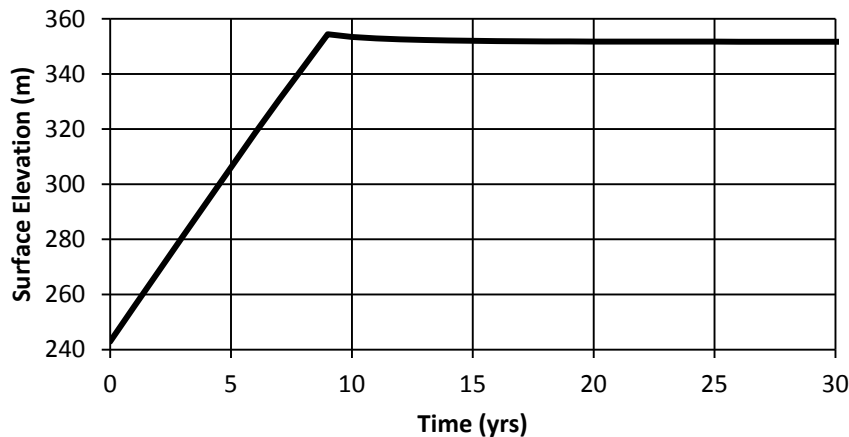


Figure 5-21: Tailings surface elevation through filling to a final time of 30 years

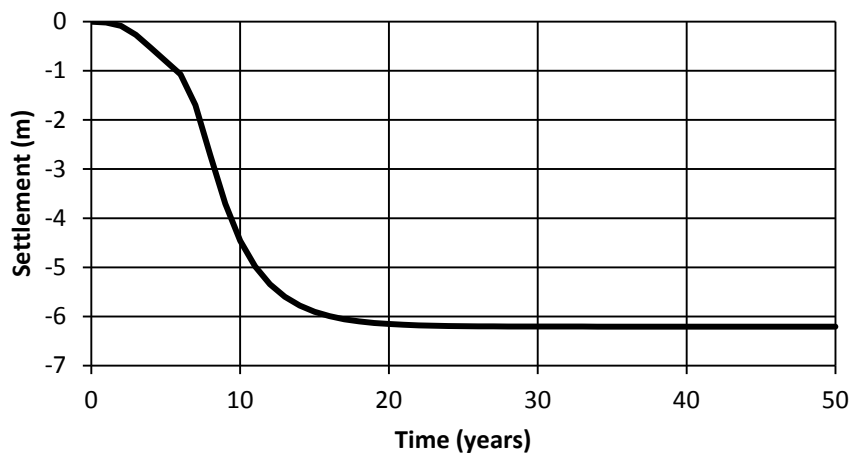
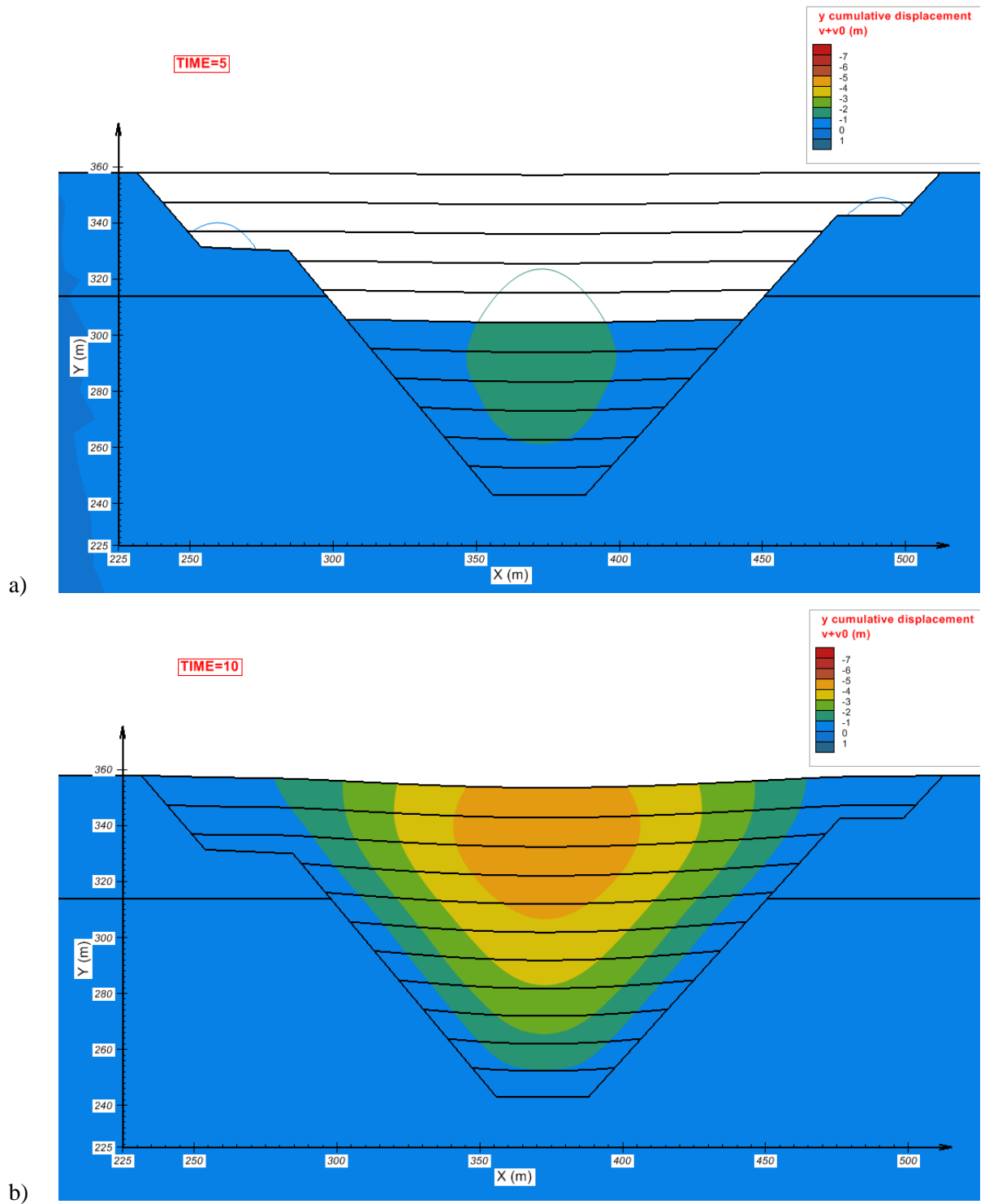
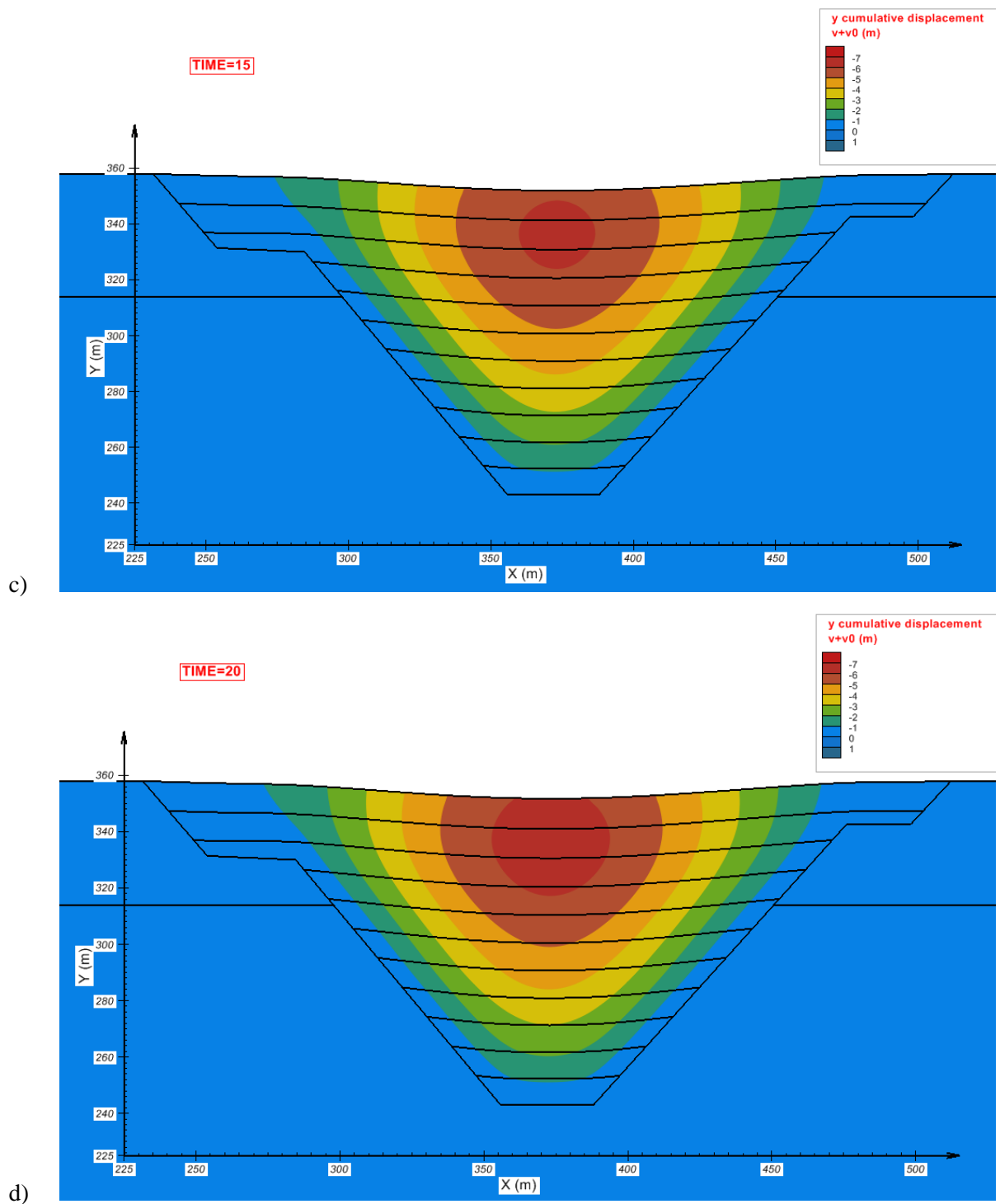
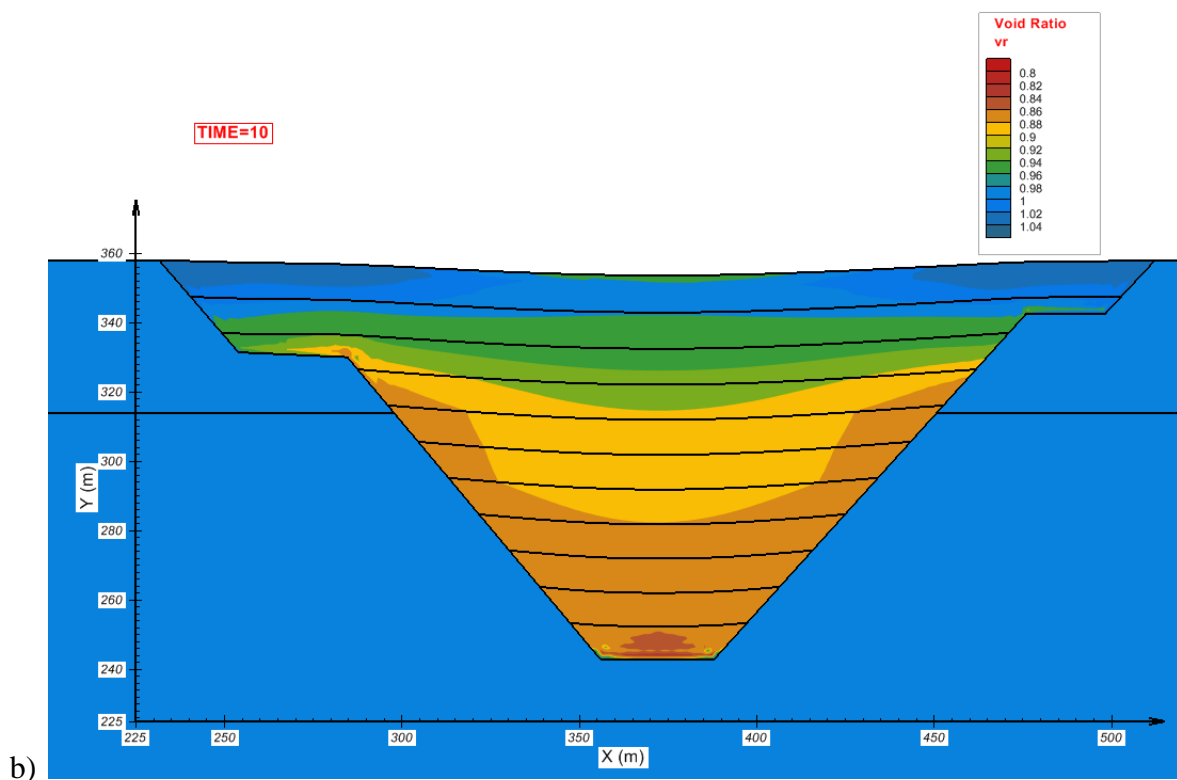
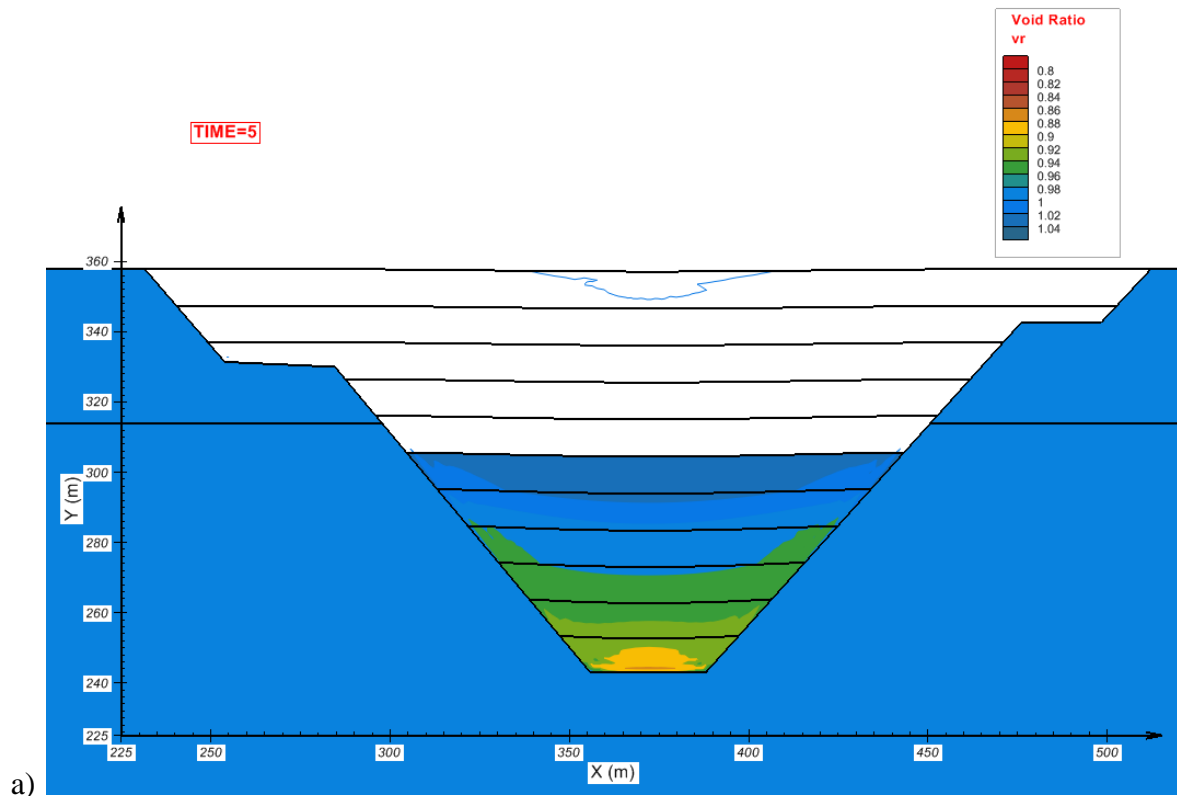


Figure 5-22: Cumulative tailings settlement over 30 years





**Figure 5-23: Time series of displacement distribution for times a) 5 years b) 10 years
c) 15 years and d) 20 years**



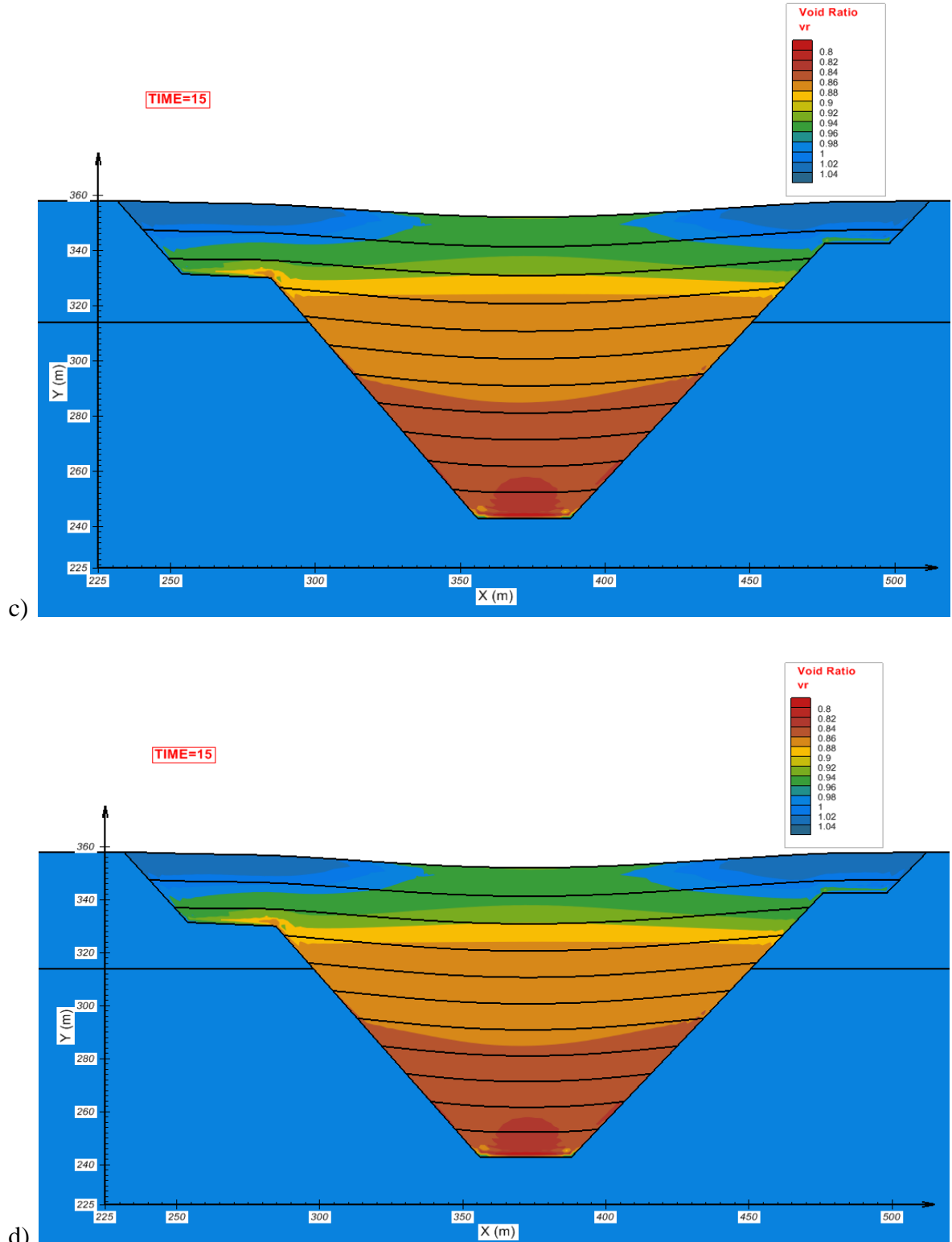


Figure 5-24: Void ratio distribution for times a) 5 years b) 10 years c) 15 years and d) 20 years

5.3.4.2 Pore-water Pressure Dissipation

The pore-water pressure dissipation within the gold tailings leads to an interesting phenomenon when considered in 2D. Figure 5-25 compares the pore-water pressure dissipation at two points to the settlement observed at the surface of the impoundment. Figure 5-25 shows how the pore-water pressure peaks over time at two heights along the centerline of the impoundment. While there is no discernible difference here, when the excess pore-water pressure generated over time is plotted, as in Figure 5-26, it can be seen that the maximum pore-water pressure actually occurs at the point slightly above the base of the impoundment. This is further depicted when observing the relative progression of excess pore-water pressure over time, which is shown in Figure 5-27. The two peaks that are observed in the pressure-time plots are caused by the way that staged filling is handled, with the pore-water pressure being able to dissipate between stages, especially when the drainage pathways remain short and the material is unconsolidated (higher hydraulic conductivity) early in the model. For this scenario, the same number of stages was used as in Anstey and Williams (2007); however it is believed that by adding more stages, these effects could be decreased.

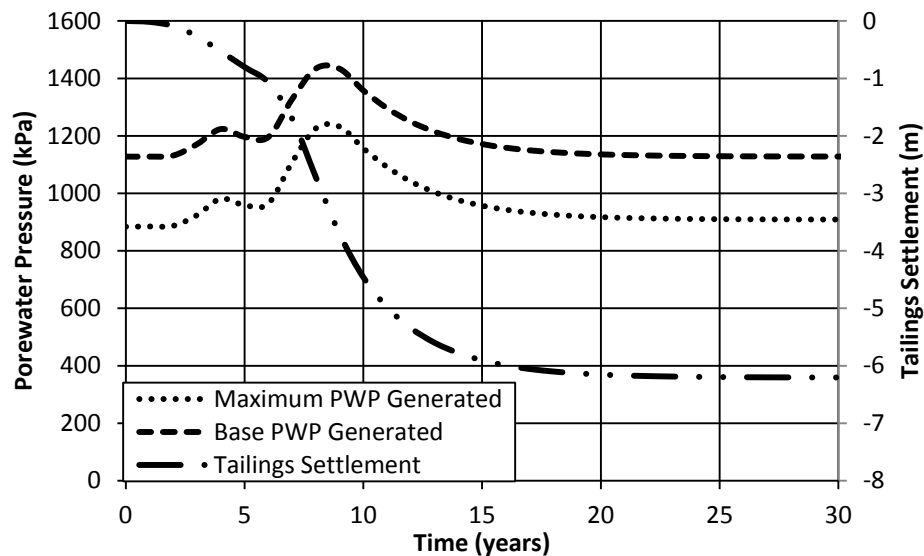


Figure 5-25: Pore-water pressure variation over time at the base of the gold tailings and slightly above, where the maximum pwp is observed

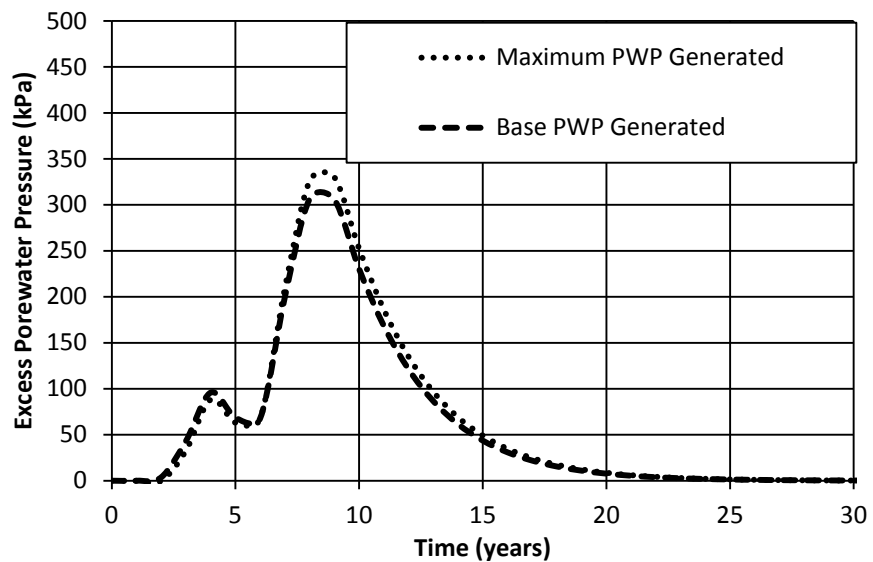
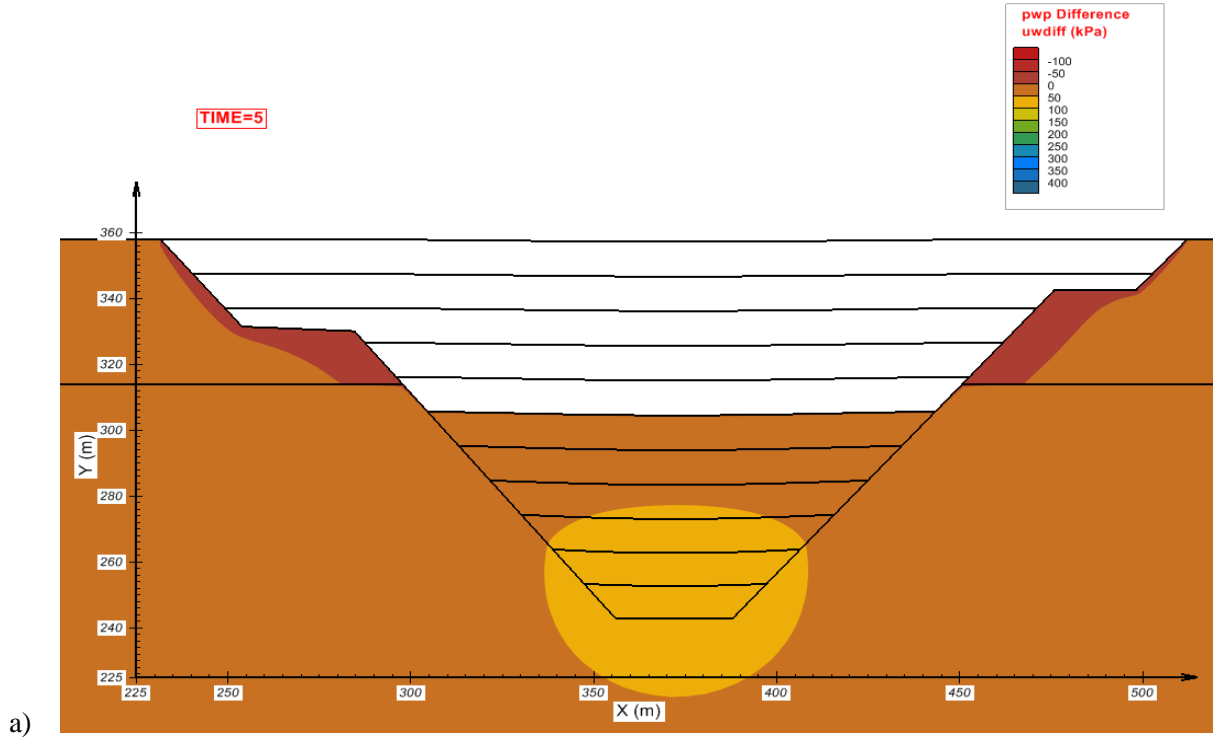


Figure 5-26: Excess pore-water pressure variation over time at the base of the gold tailings and slightly above, where the maximum pwp is observed.



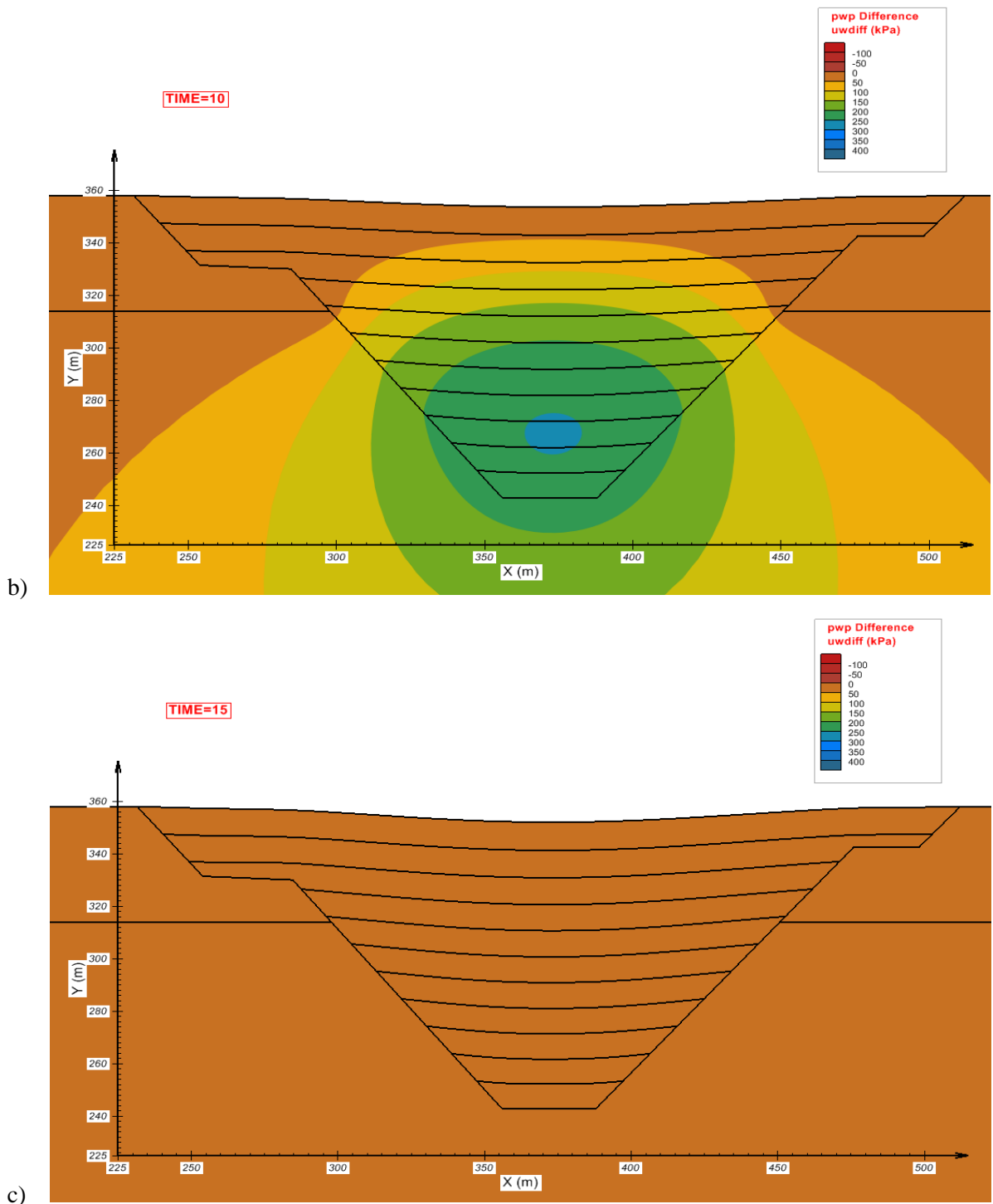


Figure 5-27: Excess pore-water pressure distributions for times a) 5 years, b) 10 years, and c) 15 years (excess pore-water pressure has almost completely dissipated).

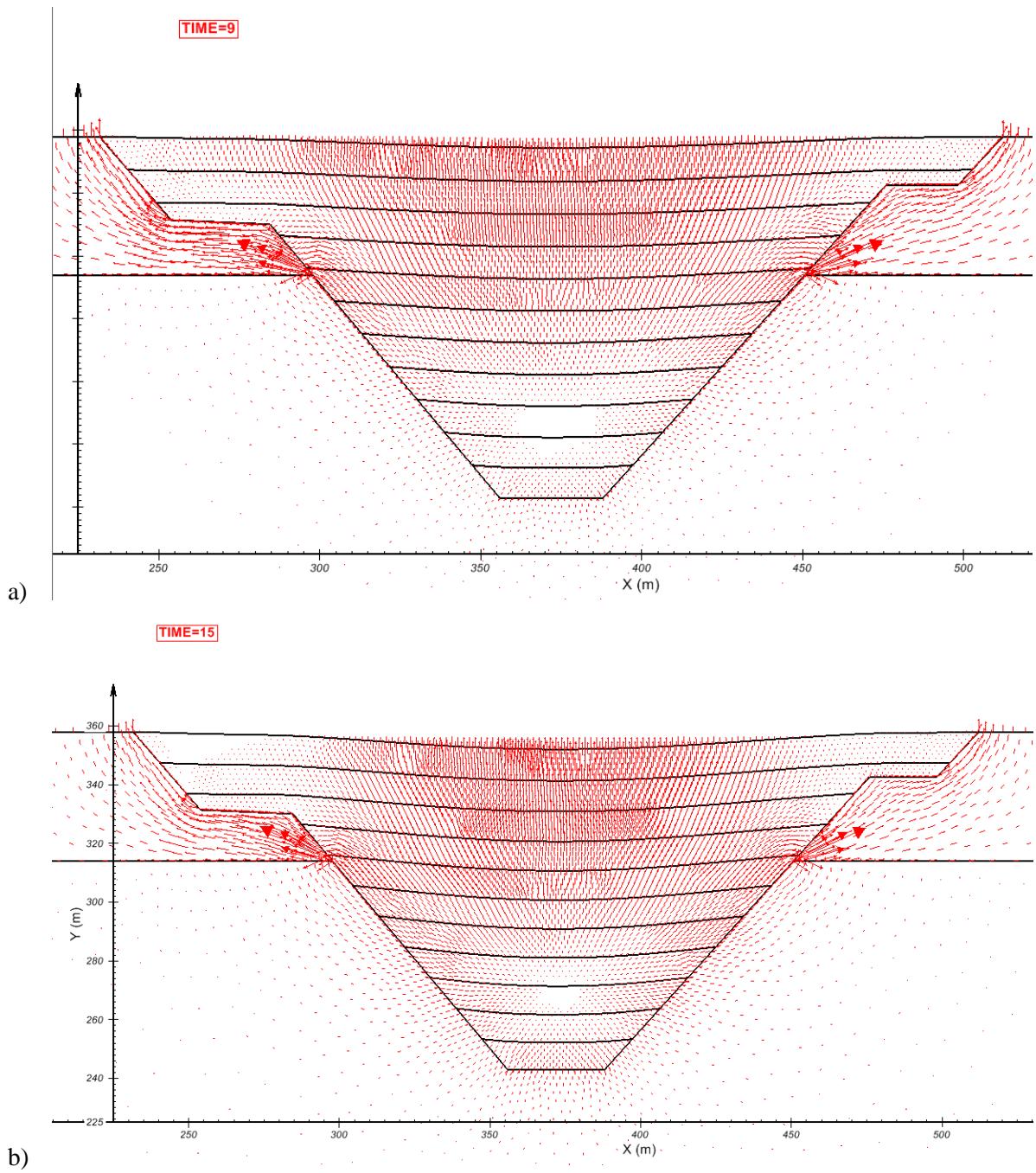


Figure 5-28: Groundwater flux vectors at times a) 9 years and b) 15 years.

5.3.4.3 Impact of Lateral Drainage

Lateral drainage through the surrounding bedrock is a factor which can only be analyzed when it is considered in two or three dimensions. To investigate what effect drainage into the surrounding bedrock has on the tailings impoundment, the gold tailings model was rerun, except that the bedrock regions were deleted and the side boundaries were set to be fixed and impermeable. Figure 5-29 and Figure 5-30 show that the addition of the bedrock does not change the amount of final settlement observed. It does however change the rate at which the tailings are found to drain. This is interesting as Anstey and Williams (2007), as well as in section 5.2.4 found that considering underdrainage does not significantly alter the rate at which tailings consolidation occurs. When the bedrock is not considered, the tailings are found to reach 90% consolidation after approximately 16 years and 99% after 27 years vs. 20 years when the bedrock hydraulic conductivity is included.

Figure 5-31 and Figure 5-32 show the pore-water and excess pore-water pressure distributions when the bedrock is and is not considered. The addition of the bedrock reduces both the maximum and base pore-water pressures. Figure 5-27 shows that the maximum pore-water pressures exist slightly above the base when the bedrock is considered. There are two peaks to both of the pressure dissipation graphs, which are likely due to dissipation of excess pore-water pressure occurring during the time between filling stages when the drainage pathways are short. The excess pore-water pressure distribution (Figure 5-33) shows that the largest excess pore-water pressures occur at the bottom of the deposit and increase vertically, particularly at the center of the impoundment, as should be expected, as the most consolidation would occur at the deepest point in the impoundment. Figure 5-34

shows that when the bedrock isn't considered, all of the flux vectors are directed in the vertical direction.

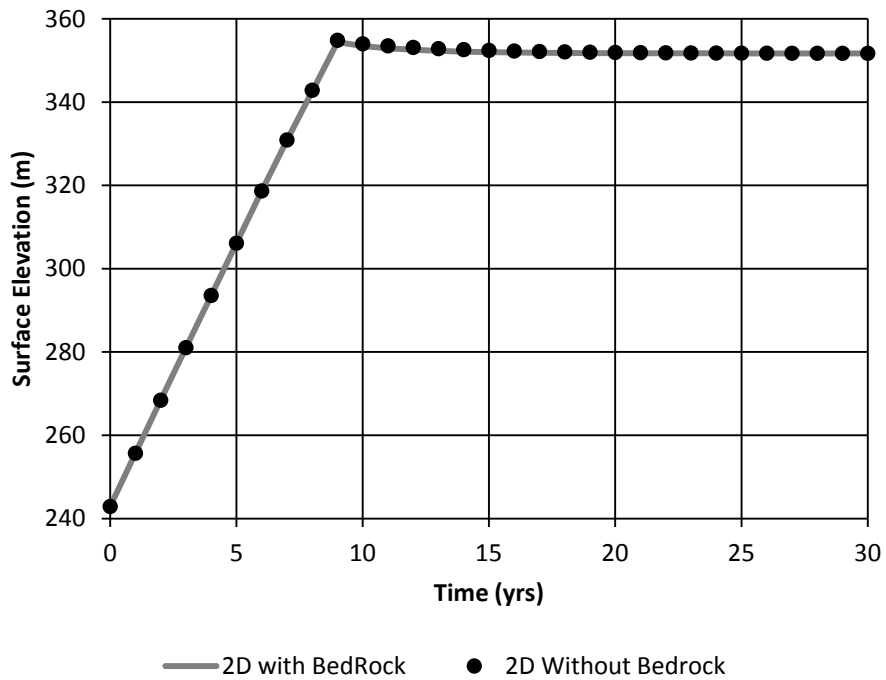


Figure 5-29: Tailings surface elevation through filling to a final time of 30 years

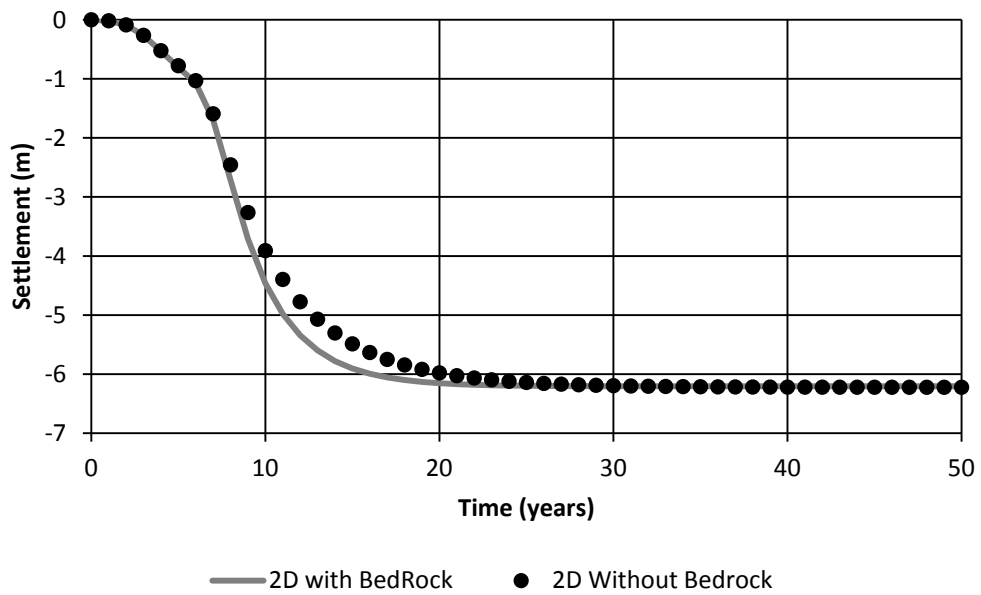


Figure 5-30: Cumulative tailings settlement over 30 years

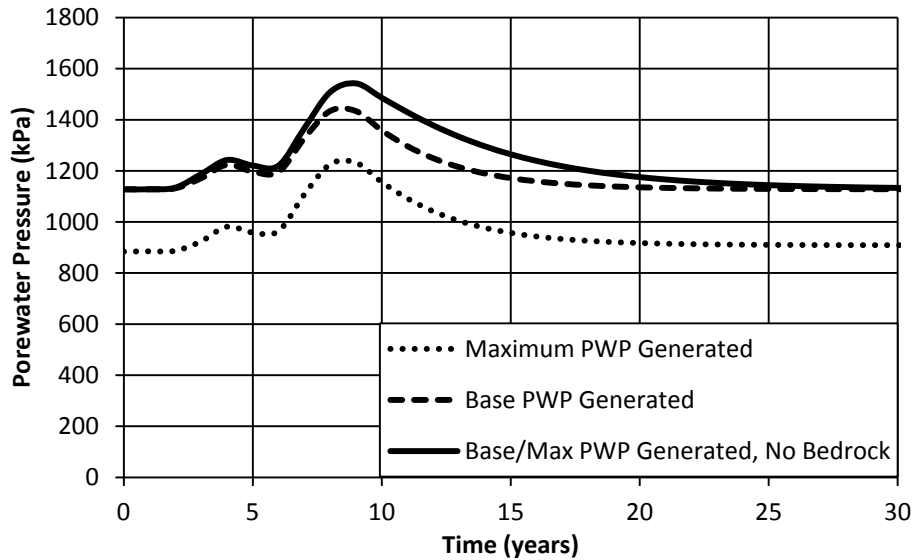


Figure 5-31: Pore-water pressure variation with time when the bedrock hydraulic conductivity is and is not considered by the model

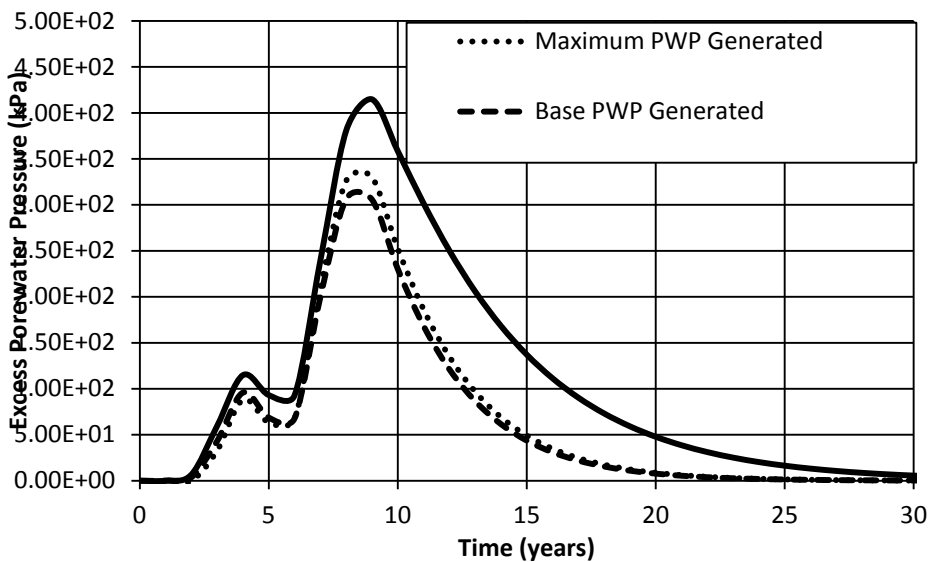
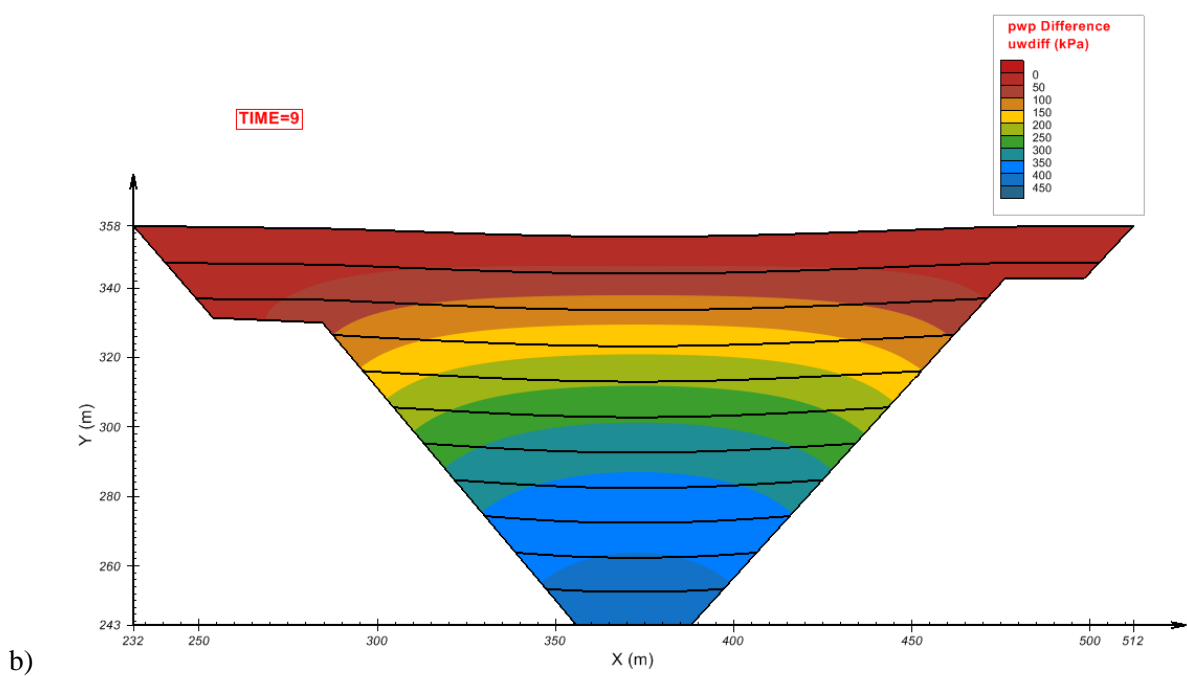
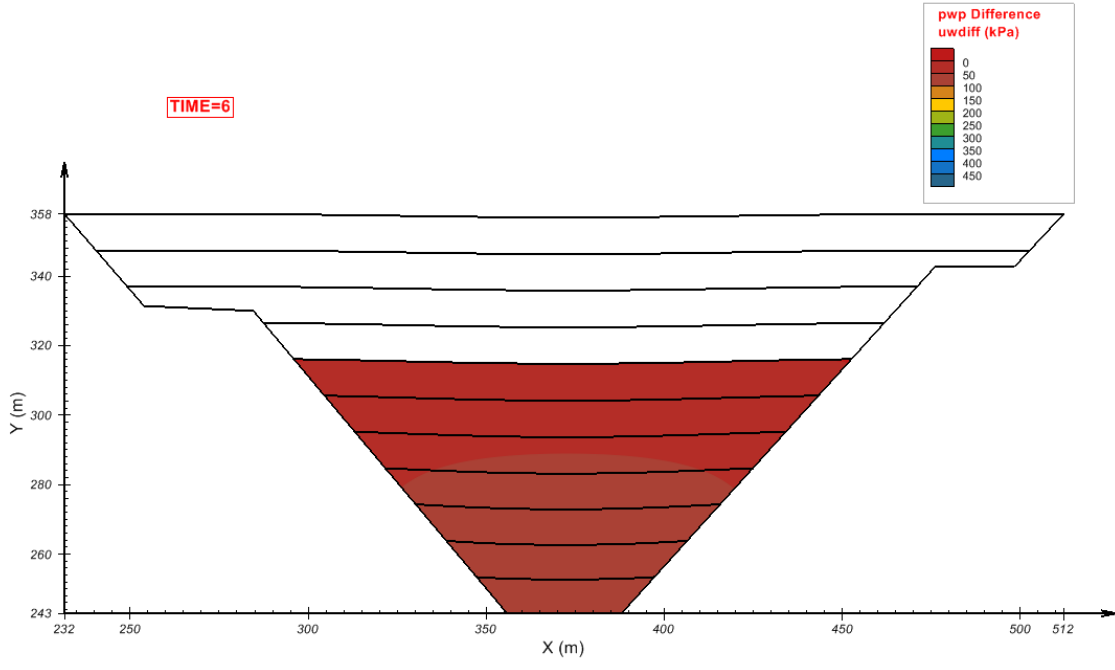


Figure 5-32: Excess pore-water pressure variation with time when the bedrock hydraulic conductivity is and is not considered by the model



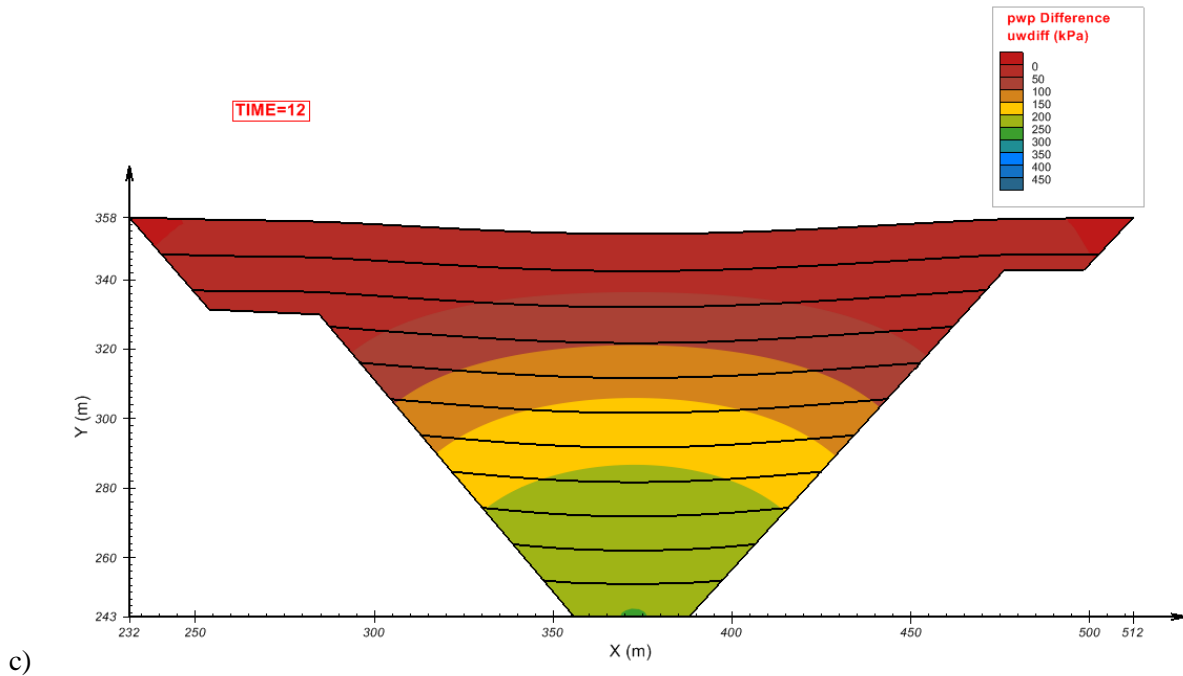


Figure 5-33: Excess pore-water pressure distribution when the hydraulic conductivity of the surrounding bedrock is not considered for times a) 6 year b) 9 years and c) 12 years.

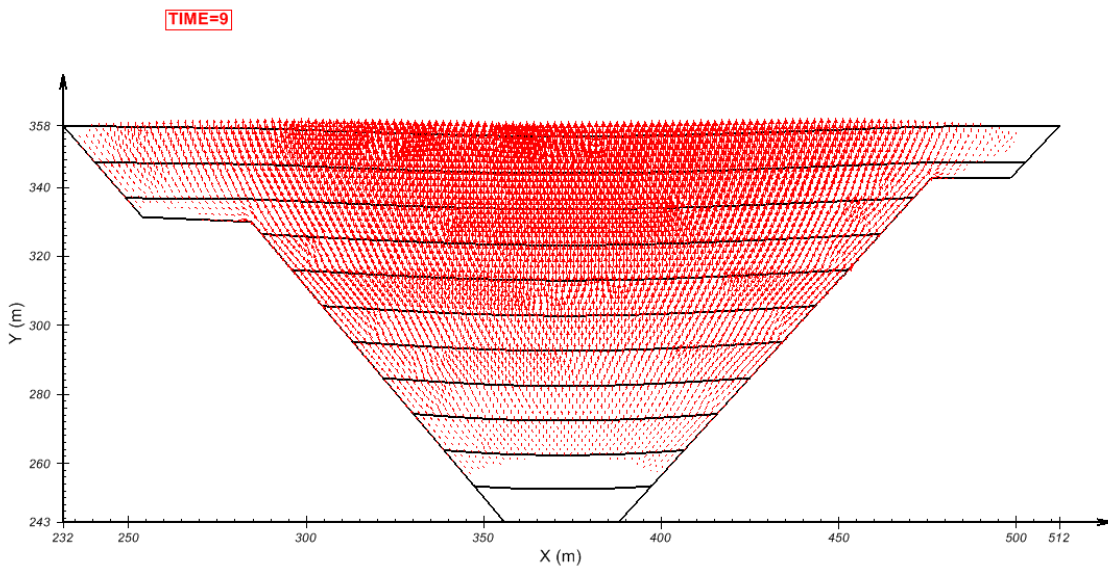


Figure 5-34: Groundwater flux vectors after 9 years when bedrock is not considered.

5.3.5 Discussion

Slightly less overall settlement is predicted by SVOffice when compared to Anstey and William's (2007) prediction. Furthermore, SVOffice predicted that the tailings would take significantly less time to consolidate than Anstey and William's model.

Anstey and Williams (2007) use a semi sliding boundary condition, where the sides are composed of a number of small steps, allowing each layer to deform vertically. SVOffice does not allow sliding boundary conditions to be applied to internal boundaries. Therefore, the side boundaries were held as fixed against the bedrock. This could possibly lead to a scenario where drag along the side of the impoundment hinders consolidation (i.e. the sides of the tailings cannot consolidate and the mesh is forced to stretch as it settles thus settlement near the center is hindered). This wasn't observed to have a significant effect on the settlement in the 2D comparison of fixed vs. sliding boundaries performed in Section 5.2.1, as there, the impoundment was sufficiently wide and the mesh spacing sufficiently dense, that these effects would not occur. It also has the effect of maintaining high void ratios along the edges of the impoundment, creating a preferential drainage pathway, which can increase the rate of consolidation. Furthermore, the model in Section 5.2.1 was only allowed to consolidate until the end of filling. Therefore there could be some effects that become visible after deposition has ceased. However, in the narrow mine pit modeled in Section 5.3, with most of the tailings surface exposure being to the sloped sides, it appears that this factor may become more significant.

The prediction by Anstey and Williams (2007) that the gold tailings would take 110 years to consolidate was rebutted in a later paper. McDonald and Lane (2010) used the modified Cam-Clay model, implemented in Plaxis, to study similar deposits of gold tailings

stored in mined out pits. McDonald and Lane (2010) found that the gold tailings would take approximately 1 year to consolidate following end of operation. The field data that had been collected also corroborated their findings.

While the McDonald and Lane (2010) results are comparable to field observations, their methodology differs significantly in that hydraulic conductivity remains constant, therefore predicting much faster rates of drainage. More importantly however, it is believed that unsaturated influences would also need to be considered in order for this to be properly modeled using large strain theory, as Morgan and Lane (2010) show that the water levels in piezometers in the bedrock surrounding the pit decrease to well below the surface of the impoundment after filling, therefore the assumption made by SVOOffice, that deposition and consolidation is performed in a saturated, subaqueous environment would not hold true.

While SVOOffice does predict smaller values of the time to reach final consolidation of the tailings than Anstey and Williams (2007), the version provided does not include unsaturated effects that would occur due to the lowering water table over time. There is therefore a need to account for the unsaturated consolidation effects occurring when the water levels within a pit are allowed to subside. The current prediction of a consolidation period of 7-10 years following the end of deposition is believed to be a reasonable time period for a mine operator to monitor the site. This time period would be reduced were the model to include the increased lateral gradients due to drawdown of the water table.

As a final note, while the material parameters are believed to be reasonably representative of the material, they are based upon interpolation. Therefore, these parameter values should be viewed as a potential basis for comparison and not be considered a design specification. It was also noted that Plaxis, which was used by Anstey and Williams (2007),

uses a slightly different formulation referred to as ALE (Arbitrary Lagrangian Eulerian) (Fredlund M., October 2011), while the modeling performed herein was based upon a Lagrangian coordinate system.

5.4 3D Modeling Considerations

When creating a three dimensional model, the software requires the user to define the geometry as regions and surfaces. A region defines the horizontal extent of the geometry, while a surface defines the vertical extent. The software then generates mesh to fill the area between surfaces. A layer refers to the mesh contained in between two surfaces. One requirement of the program is that surfaces must be defined at every point within the model. Region data is entered using Cartesian coordinates, similar to 2D, while surface data is applied to all points within a region. This means that the surface elevation can either be defined as a constant value, a plane, a mathematical expression or using a Kriging technique to generate a variable grid based upon spatial data that is entered.

When modeling an irregular tailings impoundment, the least complicated way to do this is to enter initial topographic data and define a Kruged surface of the impoundment geometry when empty, then to define additional surfaces as flat layers at the fill heights and to have the surfaces wrap up along the sides according to the original topography. An analogy for this would be to think of nested bowls stacked on a kitchen shelf.

Similar to the way two dimensional regions are staged over periods of time, so too are surfaces. Therefore to complete a staged analysis, surfaces of constant height are defined at various increments, similar to 2D. The problem with this approach is that the constant surfaces will overlap the bowl shaped topography; therefore a minimum thickness between layers needs to be defined. This minimum thickness along the edges creates a thin layer

along the sides of the tailings impoundment for each layer. This is illustrated in Figure 5-35. Therefore adding more layers dramatically increases the mesh required to define the geometry. Alternative possibilities include defining exact pinch-out intersections where each layer intersects the pit wall.

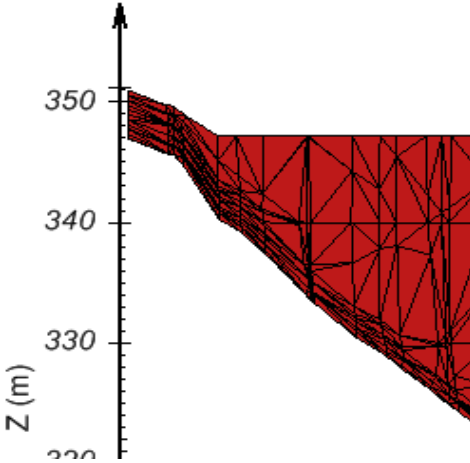


Figure 5-35: Cross-section illustrating the effect of layering deposits in three dimensions. Note: model is exaggerated 10 times in the vertical direction.

The thin layers created by implementing the minimum thickness approach results in very thin mesh layers. Therefore some optimization is required using a number of meshing parameters available within SVOOffice. Under ideal circumstances, the minimum thickness is set as small as possible. It was found that thicknesses between approximately 0.5 and 1 meter were able to mesh, when other meshing parameters were adjusted. These parameters and their effects are:

- MergeDist: Specifies the minimum spacing between nodes. Nodes closer than this are grouped together
- Mesh Spacing: Specifies the maximum spacing between nodes.
- Ngrid: Specifies the number of Mesh Rows in each dimension
- Aspect Ratio: controls the maximum ratio of width to height of a cell

The solution required variation of these parameters in order to attain a system that was capable of meshing.

This was the mesh generation method which met with the most success at the present time. This does not, however, rule out the possibility that there are alternative methods which could be used to better simulate the layering, that exist within the current framework of the SVOffice software. It is noted that research at SoilVision Systems Ltd. is on-going with implementing new methodologies for handling increasingly difficult pinch-out schemes in layering scenarios.

5.5 3D Tailings Impoundment Model

To investigate the ability of the software to model a 3D tailings impoundment, a model was created using topography data taken from the Caldwell et al (1984) paper for the scenario used as a 1-dimensional benchmark and the idealized 2D pit model.

5.5.1 Geometry

Figure 5-36 shows the geometry of the Caldwell et al. (1984) tailings impoundment. The shape was interpolated using a topographical map provided in the original paper. Some data manipulation was required to smooth out the shape and to ensure that at no point on the base surface, the unconsolidated fill height was exceeded. One point that should be noted is that the pictures show the impoundment exaggerated by a factor of 10 in the vertical direction. As is the case in many impoundments, the impoundment extents are much greater in the horizontal directions than in the vertical.

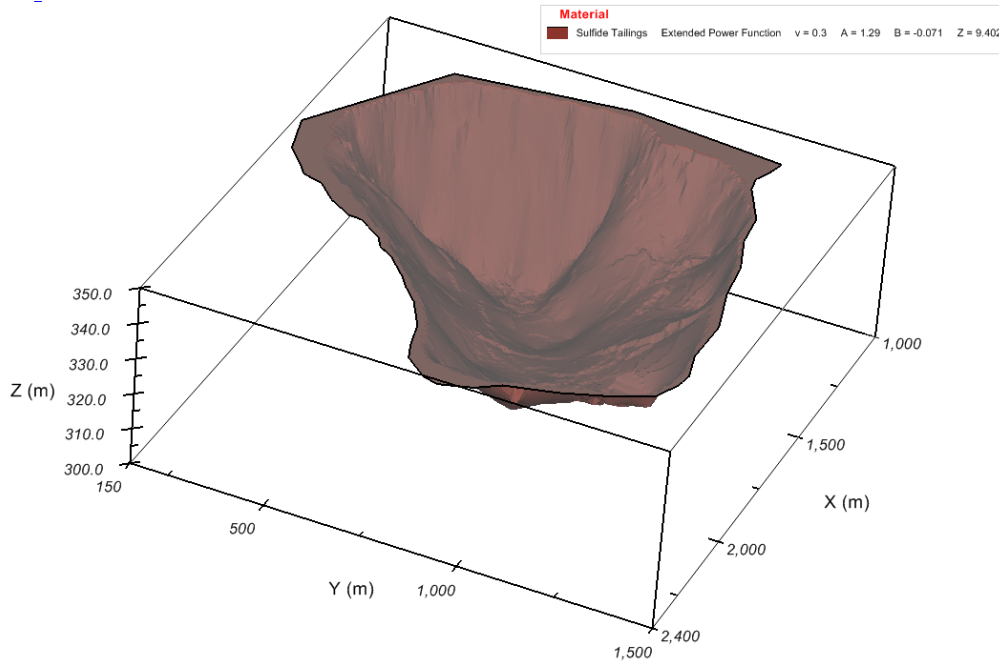


Figure 5-36: Caldwell et al. (1984) 3D tailings impoundment interpolated geometry.
Note: model is exaggerated 10 times in the vertical direction.

As this model consists of a staged analysis, multiple layers were required. For the 1D and idealized 2D geometries, 21 layers were used. However for the 3D model, due to the meshing restrictions discussed in Section 5.4, only four layers were used, as is shown in Figure 5-37. Filling of the impoundment in four layers of equal depth was calculated using the same filling curve as the 1D and 2D analyses presented in Appendix A and section 5.2 respectively. As can be expected, this is an approximation; however, it is necessary when considering the meshing required to simulate the thin layers when the minimum thickness is implemented. The meshing of a cross section view of the impoundment is shown in Figure 5-38.

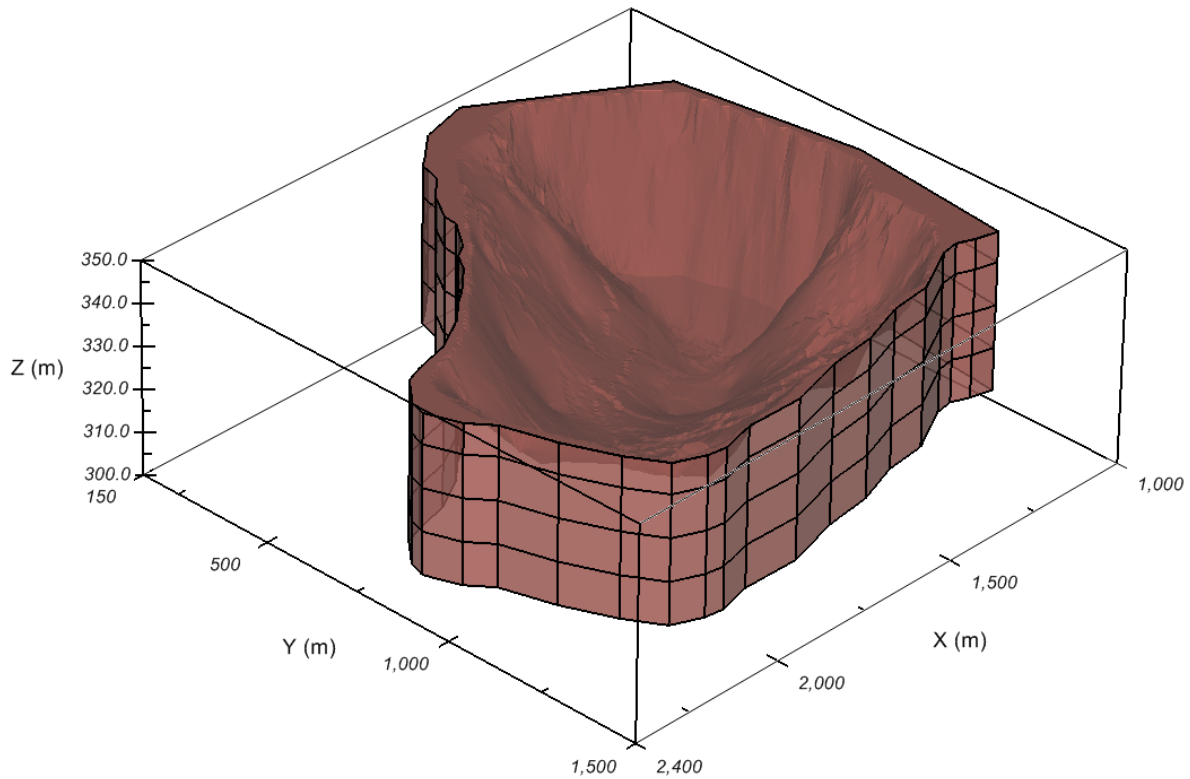


Figure 5-37: 3D Caldwell et al. (1984) impoundment showing the 4 layers used to simulate staged filling. Note: model is exaggerated 10 times in the vertical direction.

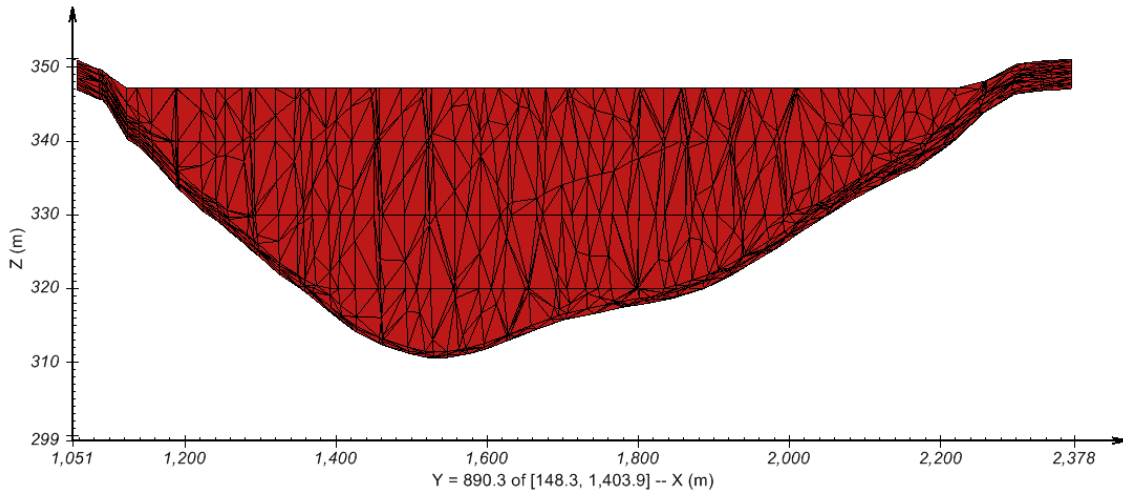


Figure 5-38: Cross-section of mesh generated for the 3D Caldwell et al. (1984) tailings impoundment. Note: model is exaggerated 10 times in the vertical direction.

5.5.2 Material Parameters

The material parameters for this scenario are the same as those used for the 1D Caldwell (1984) sulphide tailings benchmark presented in Appendix A and the idealized 2D pit model presented in Section 5.2.

5.5.3 Boundary Conditions

As this geometry consists of a 3D irregular deposit, the only deformation boundary available for the bottom surface is the fixed boundary condition. As usual the other surfaces are free to deform in all directions. The vertical region boundaries are set to zero deformation as well to simplify the calculation. These are not expected to influence the results significantly. Similarly only flux through the upper surface is allowed. This is controlled by a head boundary equal to the initial elevation of the top surface.

5.5.4 Results and Discussion

Based upon the modeling of the 3D tailings impoundment, using the Caldwell et al (1984) geometry, the model was found to show general agreement with the 1 dimensional results presented in the original publication be Caldwell et al (1984). The magnitude of settlement at the deepest point of the impoundment is similar to the 1D predictions made by Caldwell et al (1984) (Figure 5-39), and can be seen to underestimate the Caldwell et al (1984) values at earlier times and overestimate at later times. Given that the 1D analysis represents a uniform depth tailings impoundment with drainage only occurring through the surface and no edge effects, this is considered to be a suitable level of agreement. Errors can also be attributed to several of the assumptions required for 3D analysis, such as the coarse vertical mesh spacing and fact that only four layers were considered during filling. The reasons for these assumptions were discussed previously in Section 5.4. Drag along the

impoundment edges is not believed to play a significant factor in these analyses, as the impoundment is much larger in the horizontal direction than in the vertical. There is however a need to further investigate what effects deformation boundary conditions will have in 3D analysis and how different ways of setting up the model layering and boundary conditions will affect this phenomenon.

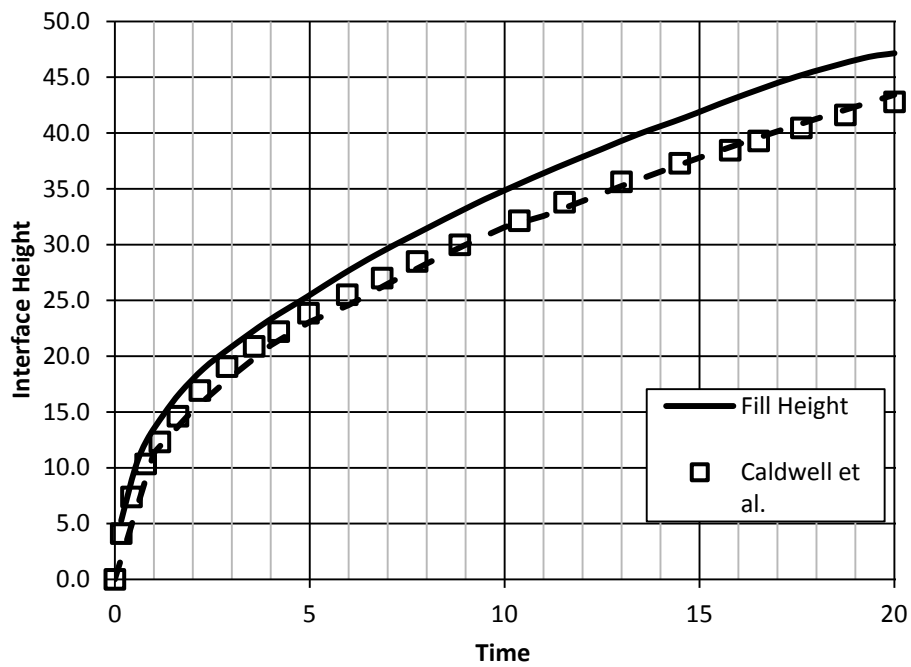
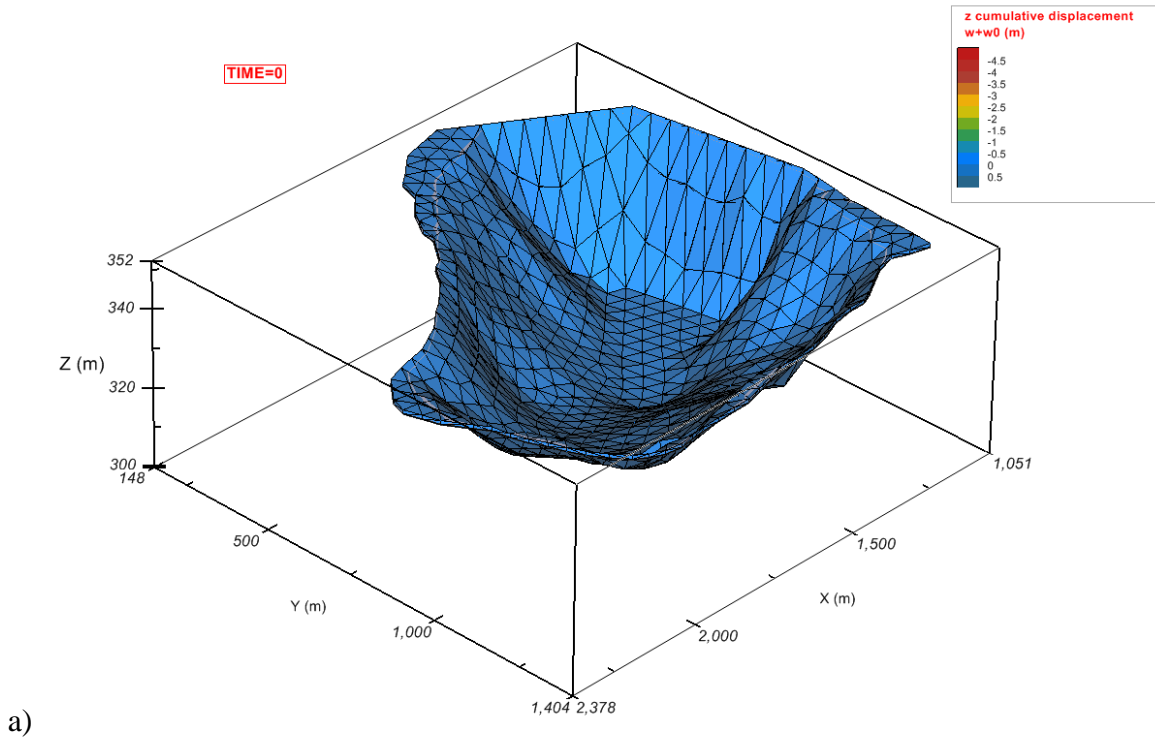
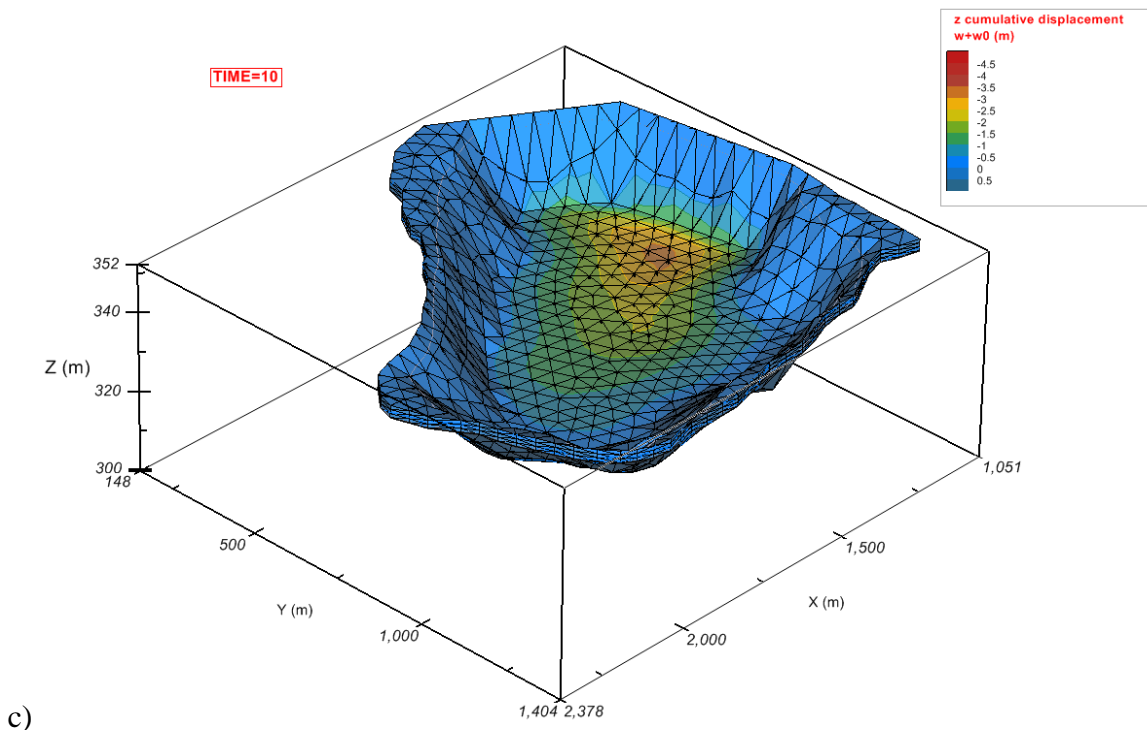
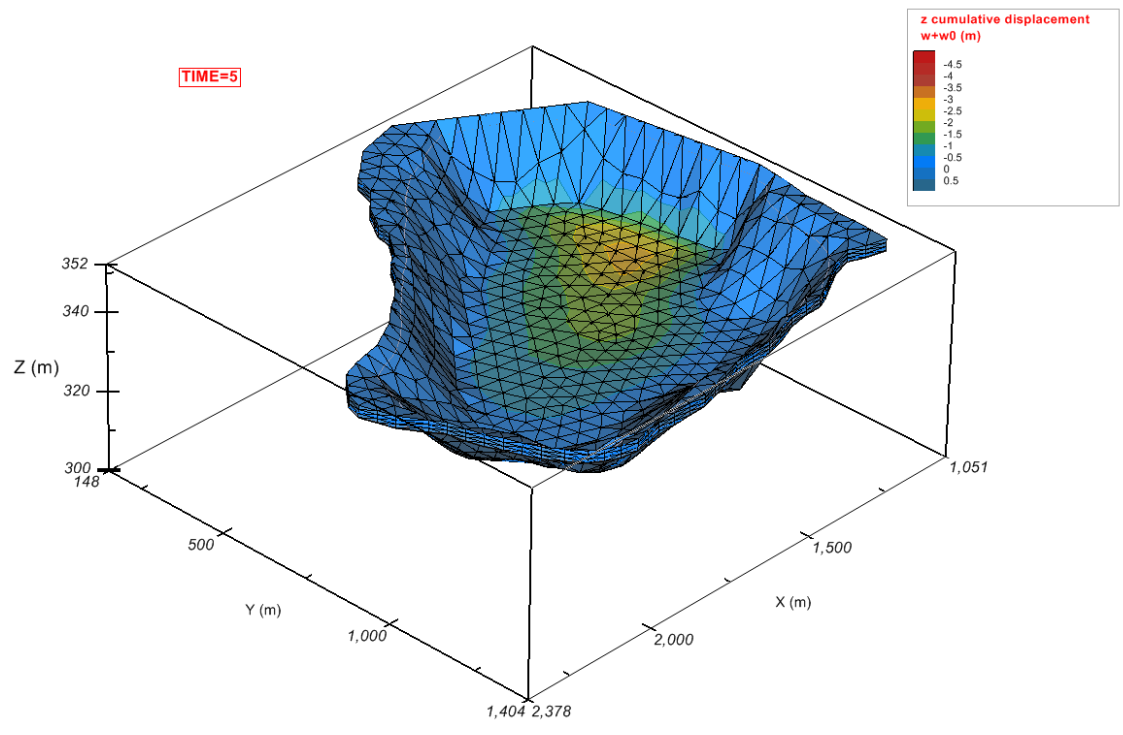


Figure 5-39: Interface height at the lowest point for 3D impoundment geometry as compared to the fill height and the predictions made by Caldwell et al.

Figure 5-40 shows the 3D displacement at the surface of the impoundment for various time intervals. Figure 5-41 shows the final displacement map of the top surface of the tailings impoundment. This allows for a better prediction as to the volume of the tailings that the tailings impoundment will contain when it reaches final consolidation, rather than simply assuming that everything consolidates to the same degree. To depict the variation in parameters at the deepest point in the impoundment, 2D cross section images were gathered.

The location where these images were taken is at the deepest point in the impoundment (Figure 5-42). The cross-sectional displacement map is shown in Figure 5-43. Diagrams depicting the cross-sectional void ratio distribution, pore-water pressure and excess pore-water pressure at various times are presented in Figure 5-44, Figure 5-45 and Figure 5-46.





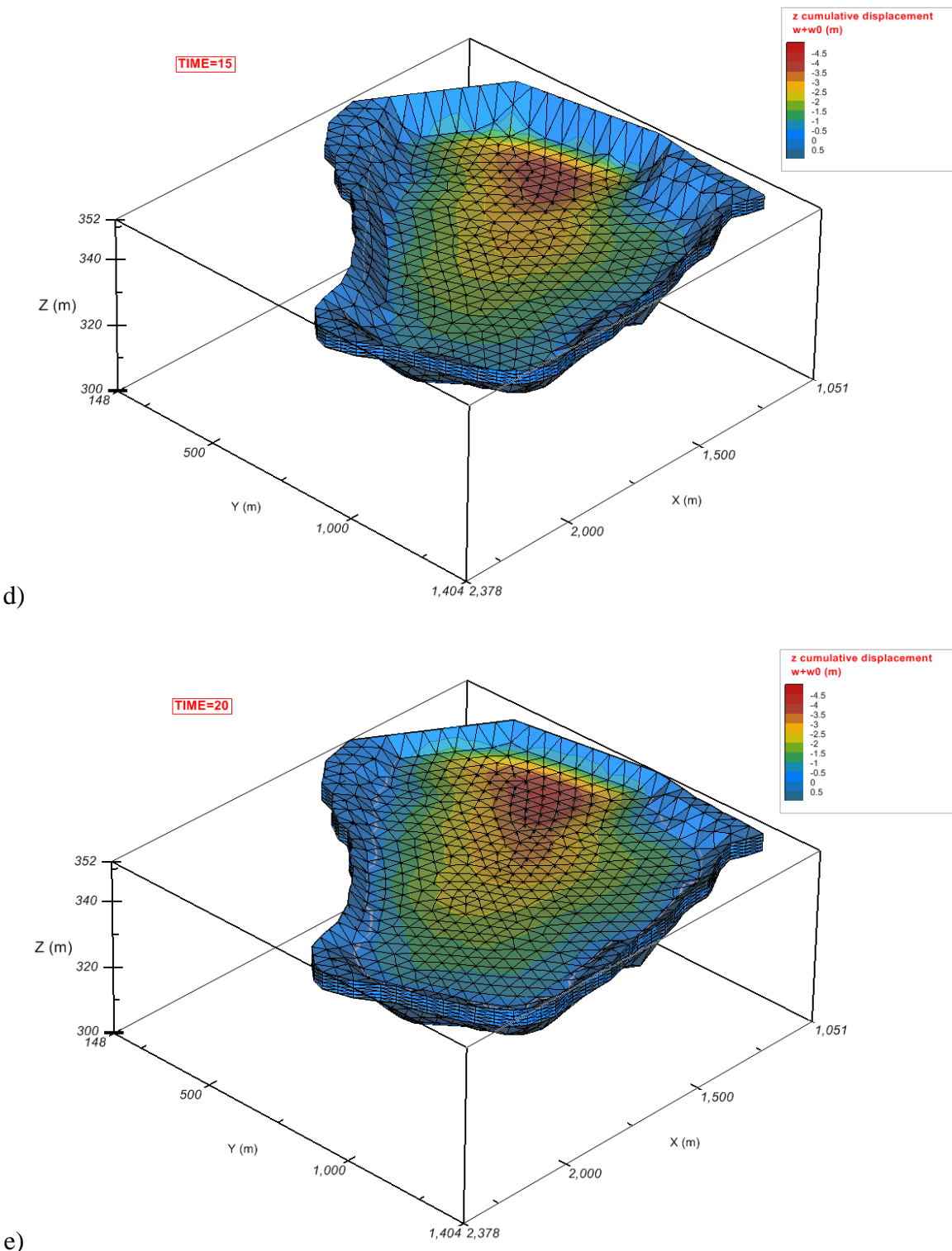


Figure 5-40: 3D time series of impoundment filling and settlement for times a) 0 years, b) 5 years, c) 10 years, d) 15 years and e) 20 years. Note: model is exaggerated 10 times in the vertical direction.

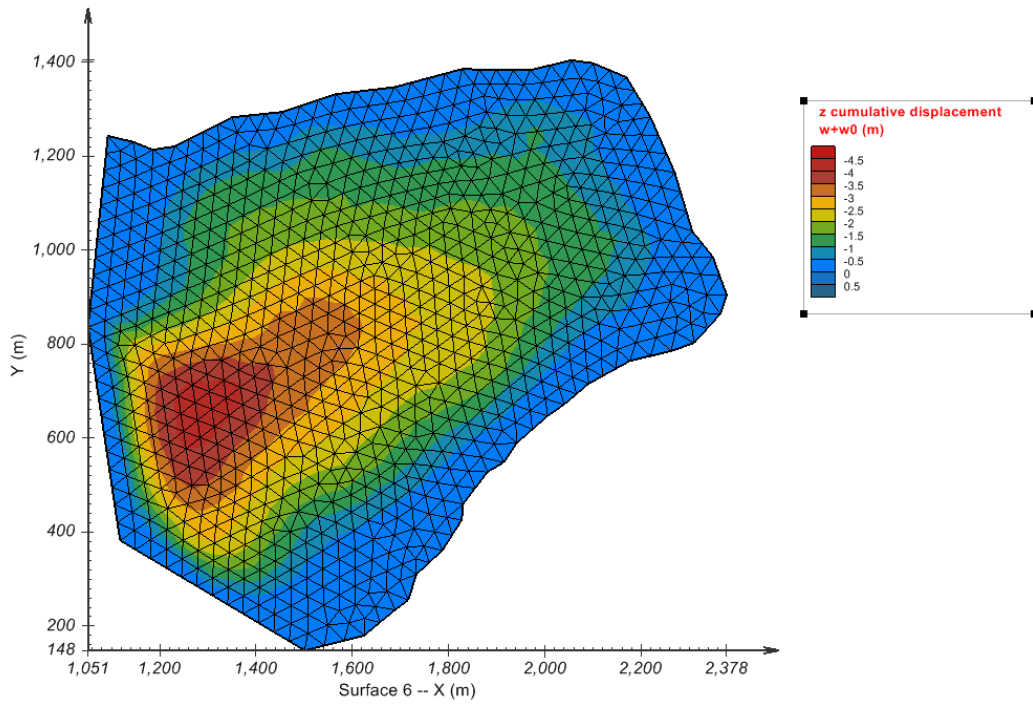


Figure 5-41: Top surface displacement at the end of filling (20 years).

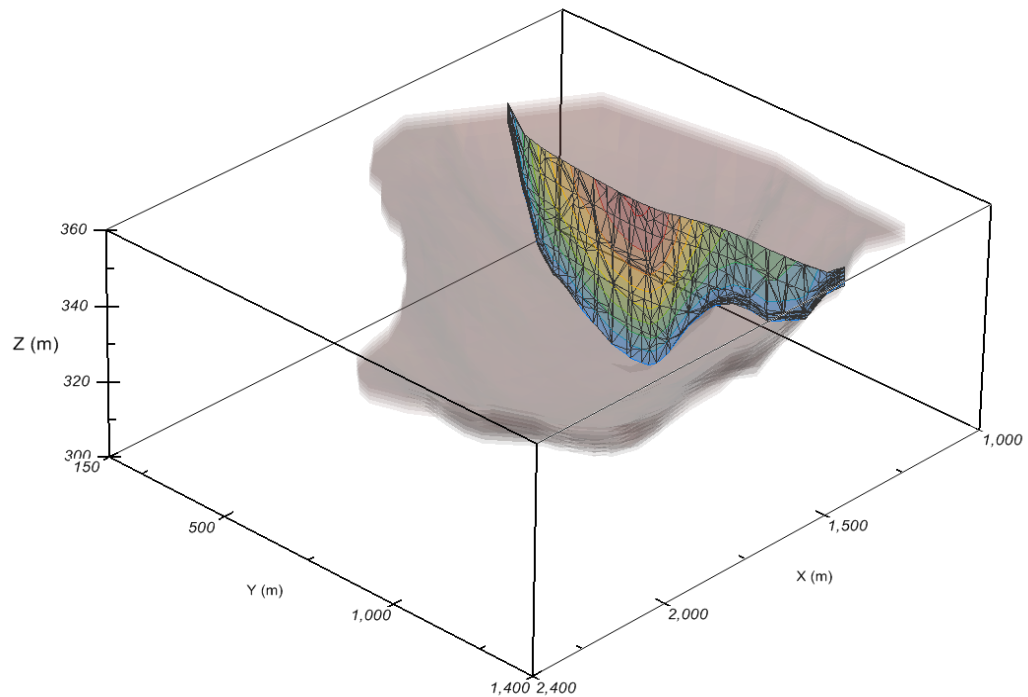


Figure 5-42: Location within the impoundment of the cross-sectional view point.

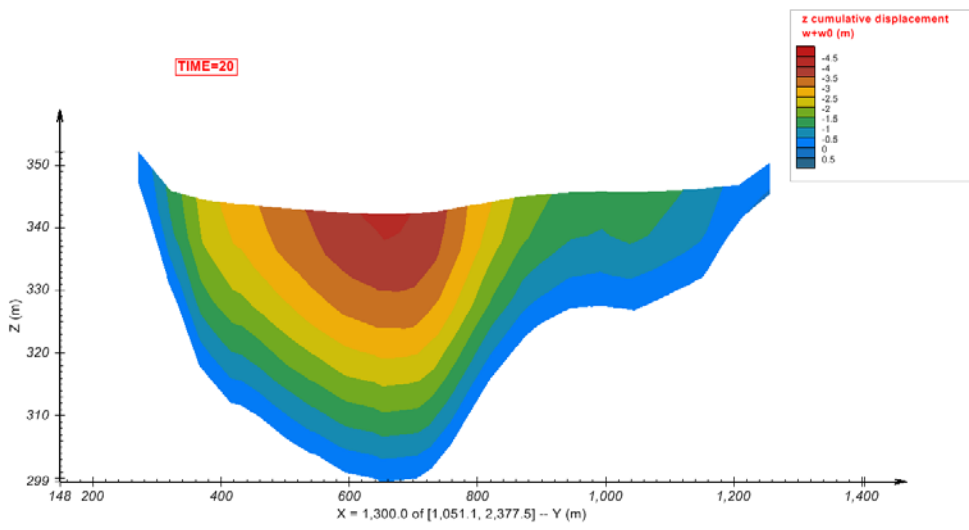
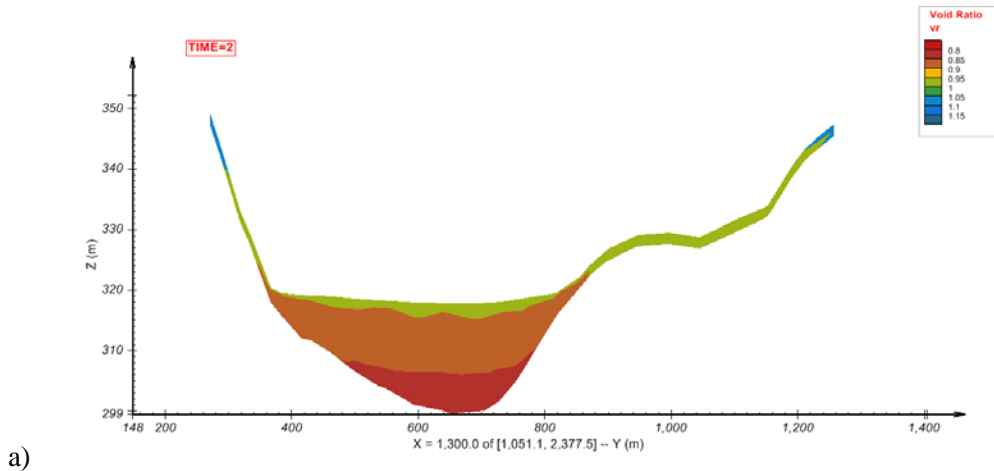
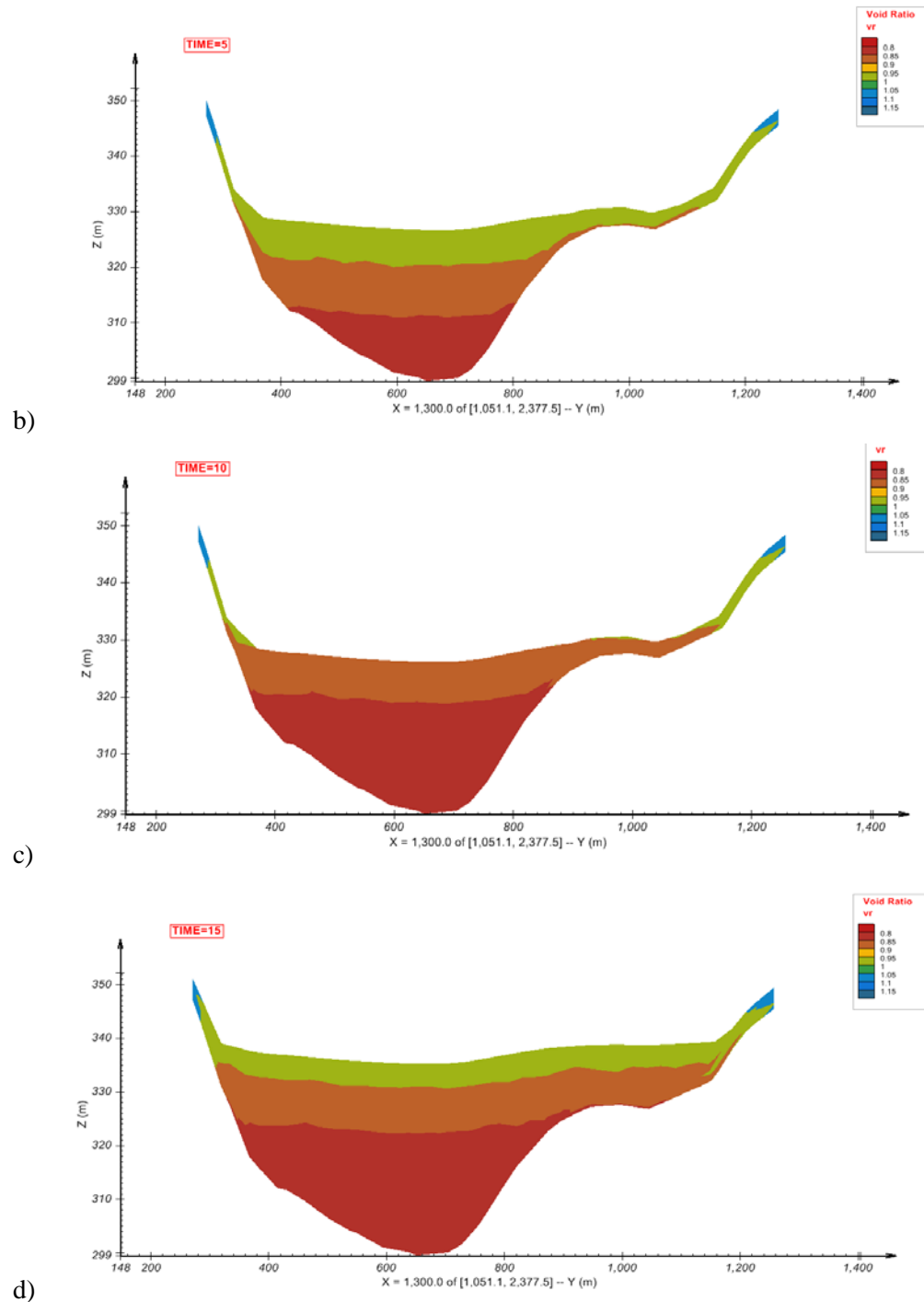
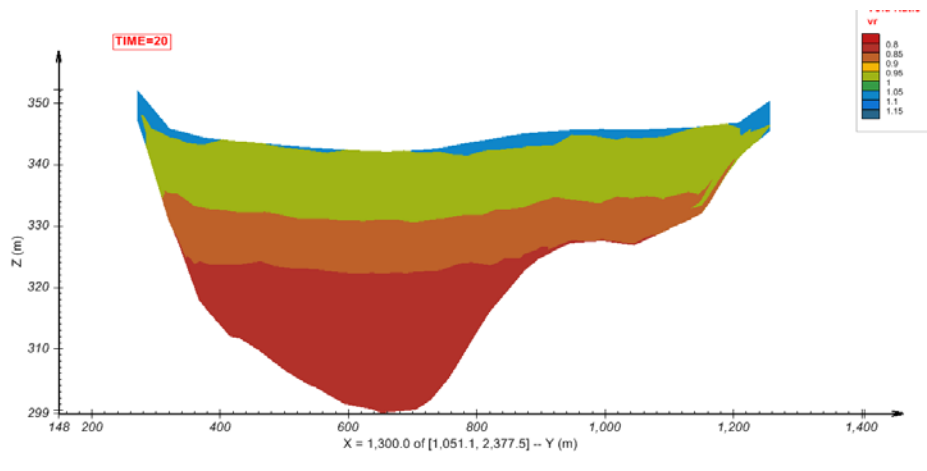


Figure 5-43: Cross section of surface displacement for X=1300 meters at the end of filling (20 years).

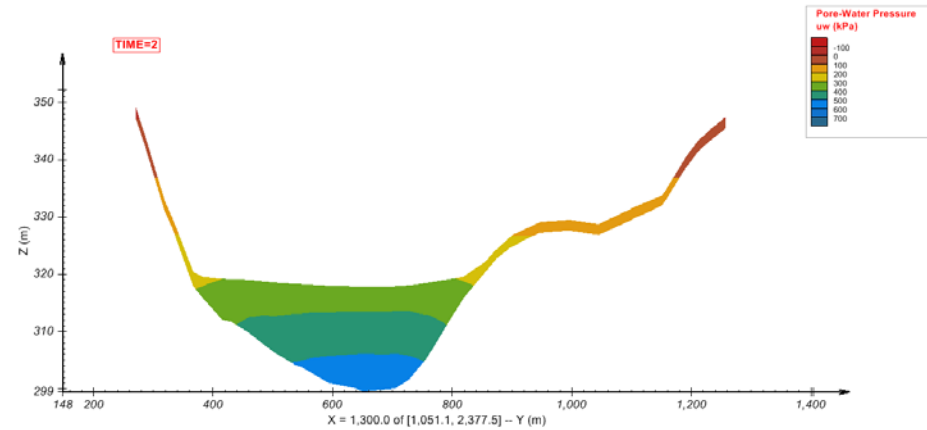




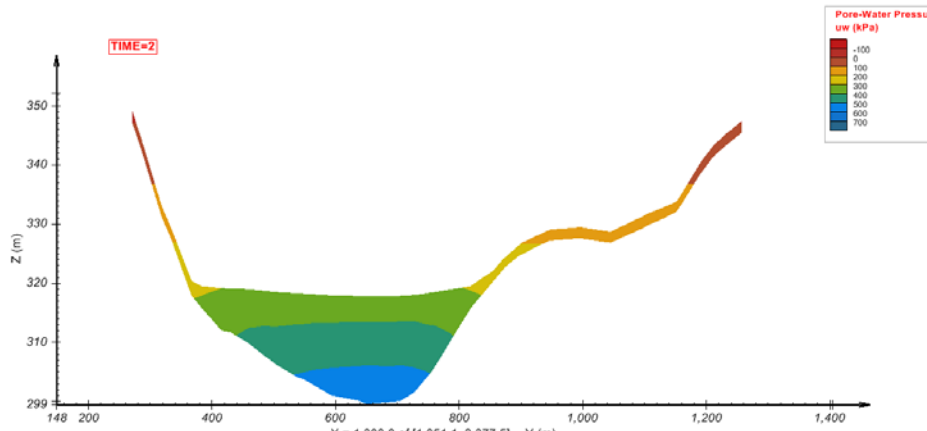


e)

Figure 5-44: Void ratio profile of impoundment cross-section at times a) 2 years b) 5 years c) 10 years d) 15 years e) 20 years.



a)



b)

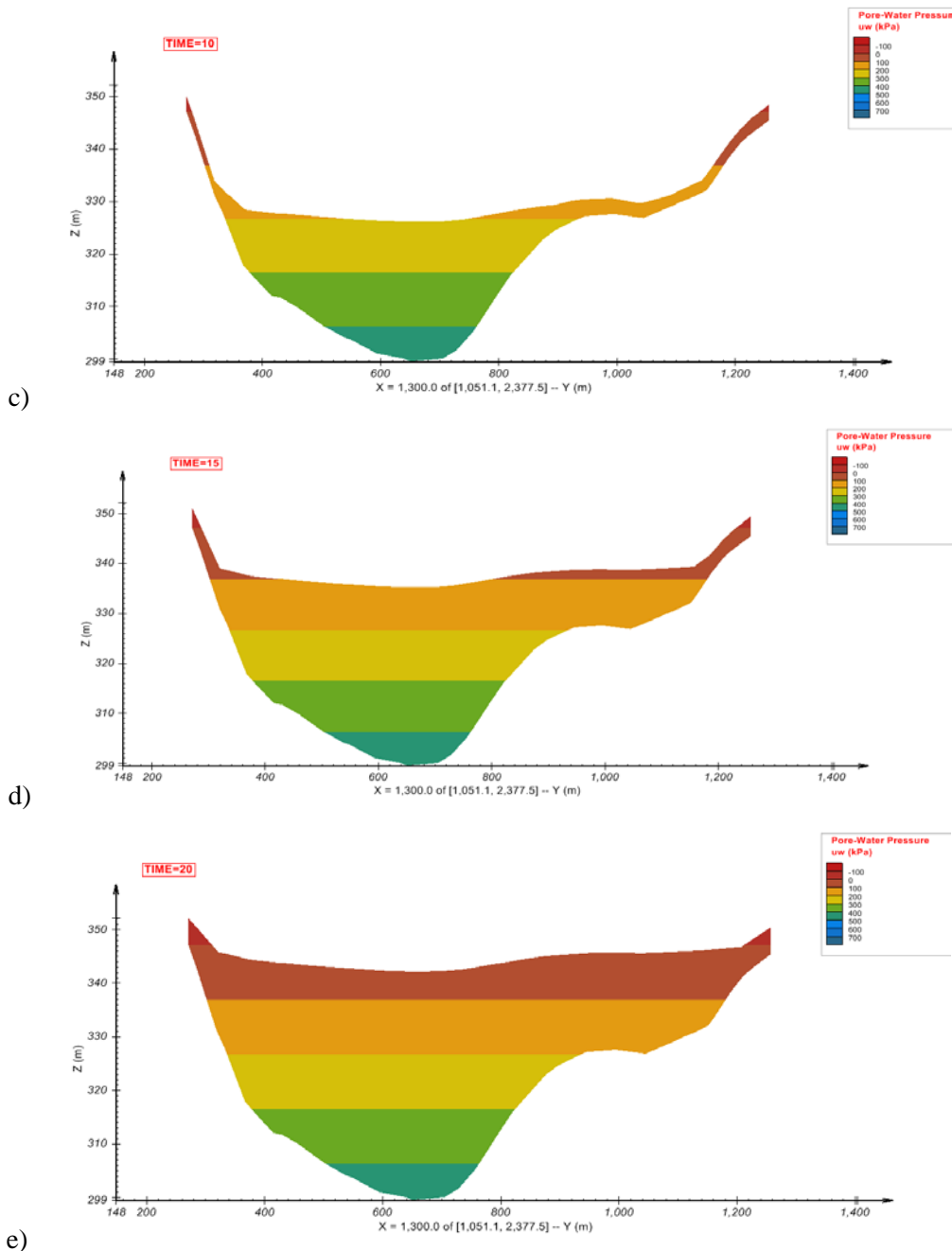


Figure 5-45: Pore-water pressure profile of impoundment cross-section at times a) 2 years b) 5 years c) 10 years d) 15 years e) 20 years.

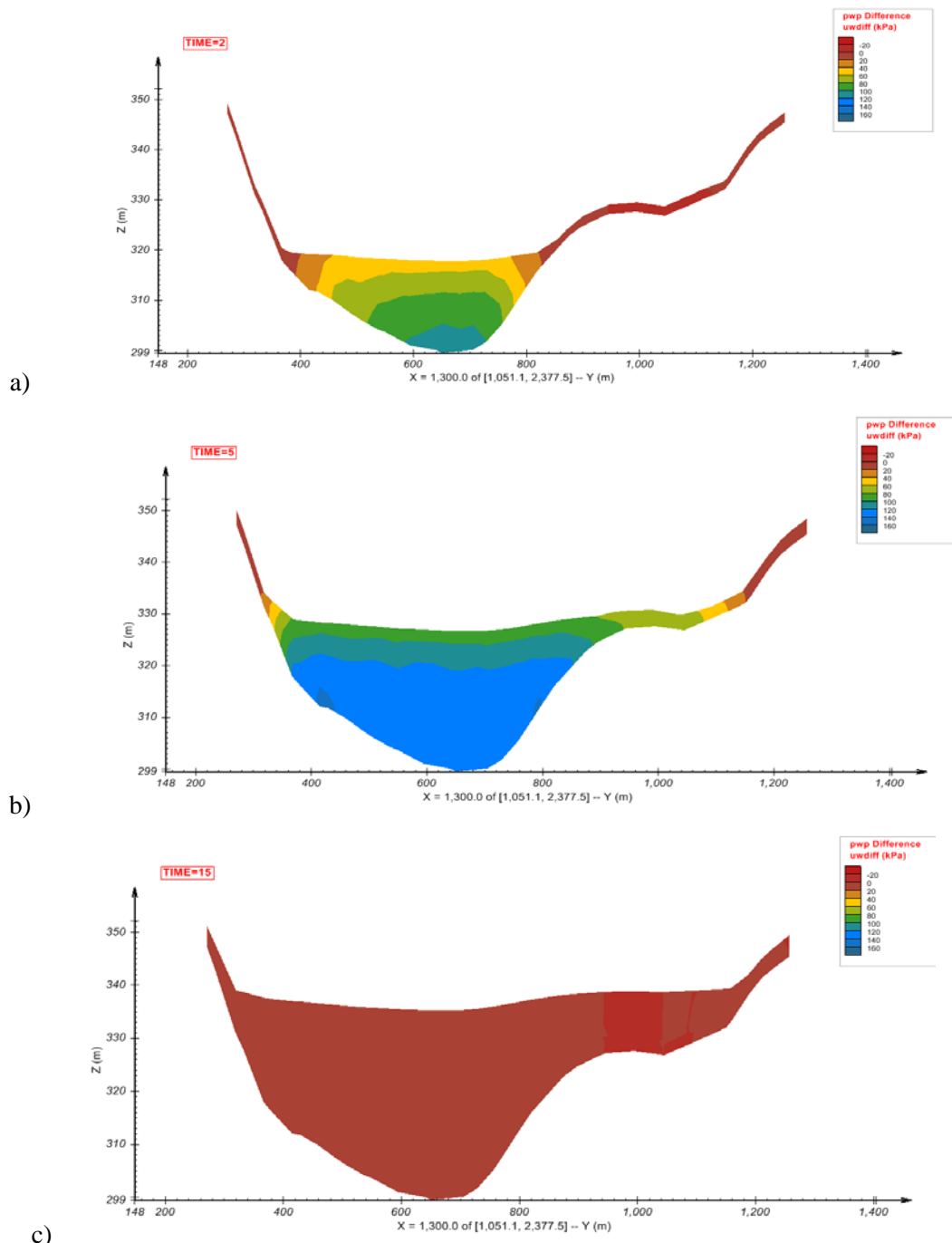


Figure 5-46: Excess pore-water pressure profile of impoundment cross-section at time a) 2 years b) 5 years and c) 15 years (excess pore-water pressure has almost completely dissipated).

5.5.5 Conclusions

Modeling three dimensional tailings impoundments requires many assumptions to be made regarding the geometry of the impoundment. While the current meshing procedure is not perfect, the ability to incorporate three dimensional filling practices into the impoundment design is extremely valuable. Many of these advantages can also be seen in two dimensions, where there is greater control of the meshing of the impoundment, however, in some cases, where complex geometry exists, such as highly permeable regions in the underlying geology and wick drains, there is a need to be able to consider the influence of these factors and to compare them to the one and two dimensional results. When applied to a specific case and using only a modest amount of additional geometric data, the software is able to generate a good correlation to the one and two dimensional results, while still retaining the advantages of the 3D analysis. It is expected that with further refinement of the methodology, greater accuracy and computational efficiency will be achieved.

5.6 Summary

The modeling of multidimensional tailings impoundments allows for greater consideration of the geometrical influences that affect deposited tailings. When considered in two dimensions, factors, such as lateral flux, sloping sides and spatial variability can be considered. Three dimensions also allows for more complex geometry to be studied. Within this chapter, a summary of modeling performed on several example tailings impoundments is presented. Along with the results of this modeling, there is discussion as to how the modeling is performed and the assumptions that are being made to complete this modeling.

It is concluded that SVOFFICE will allow for more in depth investigations into large strain consolidation of tailings impoundments. While some assumptions must be made in

applying the program regarding the boundary conditions and mesh generation algorithms, it is capable of modeling a wider variety of conditions than any other program available to date.

Chapter 6: Discussion of Multidimensional Modeling using SVOFFice

Modeling multi-dimensional tailings impoundments introduces new factors which need to be considered in order for the analyses to be deemed defendable. While this thesis investigates how these factors can be handled by the software, there is still room for further work as to what procedure works best under different circumstances. The following sections provide a brief discussion and literature review of best practice for several factors which are considered, in the author's opinion, most important when considering how the tailings will behave in the actual impoundment.

6.1 Geometry and Material Parameters

Whether modeling in one, two or three dimensions, by far the most important aspects are the model geometry and material parameters. While the impoundment geometry should be fairly straightforward to gather and idealize, it is important to make sure that the mesh spacing is suitable for the analysis. The material parameters require careful thought and consideration before being applied. Although an in-depth investigation of large strain consolidation testing techniques is outside the scope of this thesis, there is a brief outline of testing presented in Chapter 2 and summary of testing procedures in Appendix B.

6.1.1 Poisson Ratio

The Poisson's ratio parameter is not generally required when considering large strain consolidation. However, the SVOFFice formulation does require it to be specified, even for 1D analysis. As was shown in Section 4.2.1, Poisson's ratio can have a significant impact upon the amount of consolidation that is calculated. Although, it can be measured during triaxial compression testing (Rassam & Williams, 1999), some trends were observed for the

magnitude of the Poisson's ratios which provided comparable results for the various case studies. Table 6-1 provides a summary of the values of Poisson's ratio, type of tailings and initial void ratio of the material used for each case study. Higher void ratio materials, such as phosphate clay and fine oil sands tailings generally require higher Poisson's ratios from 0.4 to 0.49.

Table 6-1: Comparison of Poisson's Ratio for different case studies.

| Case Study | Type of Tailings | Initial Void Ratio | Poisson's Ratio |
|---|--------------------------------------|---------------------------|------------------------|
| (Jeeravipoolvarn, Scott, & Chalaturnyk, 2008) | Oil Sands Fine Tailings | 5.17 | 0.40 |
| CONDESO | Phosphate Tailings | Greater than 10 | 0.49 |
| (Caldwell, Ferguson, Schiffman, & Zyl, 1984) | Copper and Gold Tailings | 1.1 to 2.0 | 0.3-0.4 |
| (Townsend & McVay, 1990) | Phosphate Tailings | 6.0 - 14.8 | 0.49 |
| (Bartholomeeusen, et al., 2002) | Intermediate Plasticity Dredged Silt | 2.42 | 0.35 |

Literature studies of the Poisson's ratios of other types of tailings are compiled in Table 6.2. Here a similar trend is observed, with the Poisson's ratio decreasing with increasing confining pressures (Rassam & Williams, 1999) and an initial value of 0.5 being assumed for oil sands tailings (Hughes, Campanella, & Roy, 1997). Hughes et al (1997) also suggests that Poisson's ratio can be written as a function of compressibility.

The results of the literature study suggest that in the absence of other data, assuming a Poisson's ratio of approximately 0.3-0.4 is an appropriate estimate. Although there is not any literature available supporting the theory that the Poisson's ratio of high void ratio materials is close to 0.5, it should be noted that the Poisson's ratio of incompressible materials, such as water is 0.5. It would therefore appear logical that materials that have large amounts of water within the soil matrix should exhibit the same behavior.

Table 6-2: Values of assumed and measured Poisson`s Ratio taken from literature.

| Type of Tailings | Poisson`s Ratio | Source |
|--------------------|---|--------------------------------------|
| Gold Tailings | 0.34 at $\sigma_3=50$ kPa 0.17 at $\sigma_3=500$ kPa | (Rassam & Williams, 1999) |
| Potash Tailings | 0.3 (assumed) | (Fredlund, Zhang, & MacDonald, 1993) |
| Oil Sands Tailings | 0.0-0.5 (assumed) | (Hughes, Campanella, & Roy, 1997) |
| Bauxite Tailings | 0.3 (assumed for cohesion-less soils) | (Consoli & Sills, 2000) |

Further research is required into the Poisson`s ratio of phosphate and other high void ratio materials. Further benchmarking should be performed for cases where the Poisson`s ratio is known and not assumed.

6.2 Boundary Conditions

6.2.1 Sloping Deformation Boundary Conditions

The side slopes of tailings impoundments present an interesting problem and need to be considered on the basis of the tailings behavior that is observed. Fixing deformation along the side boundaries is a simple solution, which may or may not adequately mimic the behavior observed within the tailings. However, it is suspected to lead to a scenario where settlement is hindered slightly by the lack of deformation at the impoundment boundaries (Section 5.3.5). Further research is required into what magnitude this effect has on various scenarios. A possible testing methodology would be to vary the side slope in a uniform 2D impoundment and measure the variations in stress and settlement.

An alternative boundary condition that can be used along sloping boundaries was introduced in Section 5.2.1. Deformation is allowed along the slope, although there is no consideration for frictional effects. This boundary condition can only be applied in 2D to uniform slopes and is found to only be suitable when considering steep sided impoundments

where the slope can be approximated as a straight line. A similar method, where the sloping sides of the impoundment are not expected to influence the results would be to consider the side boundaries as being vertical and to model them accordingly (i.e. they would be fixed horizontally, while being free to deform vertically). There is however a tradeoff as the sliding conditions can only be applied to external boundaries, which means that lateral flux cannot be considered when sliding boundary conditions are applied. Judgment and experimentation is required to determine which phenomenon will have the largest impact upon the model.

There are currently no clear approaches regarding how deformations should be modeled along the edges of the tailings impoundment. Using the 1D geometrical discretization method allows Coffin's (2010) formulation and FS CONSOL to avoid this problem when looking at more complicated geometry. However, this does not allow the impact of localized geometric phenomena to be considered and therefore, it would be advantageous for a more robust formulation to be developed.

6.2.2 Lateral Flux

Lateral flux can only be modeled in two and three dimensional analyses. It is one of the primary advantages of SVOffice. Both the effects of under-drains and of the surrounding impoundments were examined. In Section 5.3.4.3, the impact of considering lateral drainage through fractured bedrock is shown to be significant. The time to reach 90% consolidation is improved from 16 years to 13. It is therefore valuable to consider the surrounding groundwater table and hydraulic effects in more advanced analyses. While it is more conservative to not consider lateral drainage when planning for the time to reach final closure, reducing this time is desirable and would allow for mining companies to reduce their

time estimates for the post-closure monitoring period and the time when they will have the full value of any financial assurance returned.

6.3 Spatial Variability

Spatial Variability refers to considering materials with different parameters in the same model. This allows for much more flexibility when designing tailings impoundments with multiple materials or materials with different consolidation parameters, and also when monitoring existing impoundments where the variability in void ratios and hydraulic conductivity is better understood. Although a common assumption is to assume that materials are spatially homogeneous, this may not be a good assumption when considering segregated tailings.

Segregated tailings are found to commonly occur in metal tailings impoundments due to faster settlement of coarse particles, while finer particles remain suspended in the fluid longer. This creates a decrease in hydraulic conductivity with distance from the deposition point. To effectively model this system, regions of lower hydraulic conductivity would need to be created within the impoundment.

6.4 Advantages of Multidimensional Modeling

SVOffice implements a true 3D finite element mesh when modeling and is not limited to using a 1D geometrical discretization scheme as is seen for the Coffin (2010) formulation and FSConsol. It also does not make the assumption of zero horizontal deformation as Jeeravipoolvarn (2010) does in his multidimensional formulation of the large strain consolidation problem (Fredlund M., September 2011).

Consideration for the impacts of tailings geometry will aid greatly in determining tailings impoundment capacity and spatial consolidation over time. Using 1D columns to

determine the consolidation occurring at the deepest point will result in a significant overestimate of impoundment capacity, especially in cases where most of the impoundment is resting upon the side slope material.

Consolidation of the side slopes, which can refer to manmade embankments or the local topology, is a factor not considered in other analyses. Although not specifically considered herein, by knowing the loading due to the deposition of tailings, it would be possible to use supporting analyses to determine the consolidation of the underlying materials.

One shortcoming of this research is the focus placed upon modeling tailings settlement and void ratio. Equally important is examining the changes in hydraulic conductivity within the impoundment, volume of seepage over time and the dissipation of excess pore-water pressure. All of these parameters can be examined and plotted in a similar manner to settlement and void ratio.

Examining seepage is another factor where multidimensional analyses are very useful. Especially in cases where water treatment is required, gaining an estimate of seepage production over time is a necessary part of the design process. By specifying external hydraulic conditions, such as the hydraulic conductivity of the surrounding materials, the local water table conditions and an estimate of the local climate, it would be possible to build a model where the total amount of seepage could be examined and the design of seepage collection systems, such as spine and wick drains, be performed.

6.5 Areas of Further Refinement

The way which SVOffice handles the filling of impoundments is somewhat complex when considered in multiple dimensions. It is also noted that the meshing requirements for

handling 2D and 3D analysis are exponentially more complex than a simple 1D analysis. The question of when an impoundment will reach capacity becomes difficult to answer when considering a 2D or 3D impoundment with fixed sides.

A direct comparison between Coffin (2010) and SVOFFICE was not completed due to difficulties reproducing the filling scheme created by Coffin in 2 and 3 dimensions. Coffin (2010) refines the original CONDES0 filling methodology to use a Lagrangian filling scheme, filling is related using the Lagrangian z coordinate, which denotes the volume of solids rather than the column height. This is found to significantly affect the degree of consolidation observed over time (Coffin, 2010). As SVOFFICE has been benchmarked against the original form of CONDES0, there is a need for consideration as to how to implement a similar scheme within SVOFFICE. In the future, it is recommended that a comparison between the two methodologies be examined further.

The procedure used to model a 3D impoundment, where staged filling is considered, is limited in the number of layers that can be used and requires careful adjustment of the meshing parameters. While this is a challenge of any system where the horizontal extent is much greater than the vertical, the specification of a methodology to define impoundments based upon topographic information would be advantageous. Furthermore, since deformation and flux are primarily concerned with the vertical direction, the ability to increase the mesh density vertically, while maintaining a coarse horizontal spacing would be very advantageous in terms of computational efficiency and the time required to gather results.

Chapter 7: Conclusion

The finding of this thesis is that the SVOOffice consolidation software is a viable tool for modeling the 1D consolidation of tailings materials, using accepted practices to calculate large strain consolidation. This is shown through the completion of a wide variety of benchmarks to literature case studies. Furthermore, the software allows for new areas of large strain consolidation to be investigated, such as the effects of multi-dimensional analysis on individual tailings impoundments. Modeling of tailings impoundments in 2D and 3D shows that consideration for multidimensional effects, such as side boundary conditions and lateral drainage can change the observed behavior of the impoundment. It is expected that the ability to create these models will greatly improve professionals' understanding of the problem to better design and manage tailings impoundments.

7.1 Practical Applications

The primary application of the large strain consolidation software is the design and monitoring of tailings impoundments used by the mining industry. With greater focus being placed on designing for closure, knowing how an impoundment will behave decades or even centuries later is of great importance. When applied to these cases, the SVOOffice software will aid in the prediction of the tailings impoundment capacity over the life of the mine. It can also aid in determining how long it will take the deposit to reach a stable state, where further consolidation effects can safely be considered insignificant. Current practice is to use various testing and 1D modeling procedures to develop tailings density predictions. These can then be implemented in filling plans for impoundment design and scheduling of dam construction (Coffin, 2010).

Modeling the discharge of water from the tailings is another large aspect of the consolidation analyses. The changing hydraulic conductivity will greatly affect the seepage through dams. Other possible applications exist when designing structures using dredged materials where fill will be deposited in subaqueous environments, such as for building artificial islands, using deposited material.

Current research in the Canadian Oil Sands is focusing on the consolidation of Oil Sands tailings to meet the ERCB Directive 074, which requires the tailings to meet certain strength requirements. The segregation occurring within metal tailings impoundments, where zones of varying hydraulic conductivity develop, makes being able to model spatial variability within an impoundment very useful. Integration of SVOffice with ongoing research would be advantageous to both the researchers, by providing them with a tool to incorporate multidimensionality into large strain analyses, but also to the program itself, which would benefit from the practical application.

7.2 Potential for Future Research

In the future, there is a need for better understanding of the behavior of tailings and integration with other processes. Consolidation is only part of the tailings management process and sedimentation and unsaturated effects need also be considered. Potential linkages to these processes already exist in research, as is discussed in Chapter 2. There is, however, a need to study how these factors, when implemented in a finite element model capable of solving the large strain consolidation equation will relate to real world conditions.

As is observed in the Jeeravipoolvarn et al. (2008) benchmark presented in Appendix A, the software can only be relied upon to be as good as the data which is provided. There is an ongoing need to improve the theories related to the material behavior and the laboratory

testing procedure used to gather the data. As new methods of analysis become available, there will be a need to implement them into the software. One area where further work is required is in determining how Poisson's ratio varies with tailings composition and void ratio. This research has found that Poisson's ratio of 0.5 shows good correlation to the literature predictions for very high void ratio slurries observed in phosphate tailings. However, there is not research available to corroborate this hypothesis.

Future research using this software needs to investigate how the sloping boundaries should be modeled and which boundary condition is appropriate under different scenarios. There is a need to determine when fixing the boundaries is appropriate, and when a sliding boundary condition needs to be considered. Through the use of different flux boundary conditions, it may be possible also be possible to model discharge of lateral flux while considering a sliding boundary condition.

7.3 Closing Remarks

The findings of this research present extensive benchmarking of the SVOOffice large strain consolidation software against literature case studies. This indicates that the software is capable of meeting and exceeding the standard methodologies in use today. However, the application of this software to new scenarios, which have not been previously benchmarked, needs to be performed with extreme care. Practitioners need to gain an appreciation for how the choice of material parameters, mesh spacing and boundary conditions, as well as time increments and error limits will affect their model results. While the operation may seem as simple as entering numbers into a calculator, finding the correct solution of these models can, at times, be more akin to using a finely tuned and sensitive piece of equipment.

With the advent of any new technology, there are technical challenges which will need to be addressed in the future. There is a need to apply SVOFFICE to real world tailings impoundments to find how the multidimensional aspects compare under these circumstances. The incorporation of other factors, such as sedimentation, evaporation and unsaturated flow, will aid in determining what factors are of critical importance when designing for closure of tailings impoundments.

While the results here show great promise, it is the author's opinion that the best form of verification is through real world applications. SoilVision Systems Ltd is known to publish case studies of applications of their software and it is hoped that academia and industry will be supportive of this in the future.

Bibliography

- Abu-Hejleh, A. N., Znidarcic, D., & Barnes, B. L. (1996). Consolidation Characteristics of Phosphatic Clays. *Journal of Geotechnical Engineering*, 295-301.
- Anstey, D. M., & Williams, D. J. (2007). Predicting Consolidation of In-Pit Tailings. *ACG Total Tailings Management Seminar*. Australian Center for Geomatics.
- Azam, S., Jeeravipoolvarn, S., & Scott, J. D. (2009). Numerical Modeling of Tailings Thickening for Improved Mine Waste Management. *Journal of Environmental Informatics*, 111-118.
- Bartholomeeusen, G., Sills, G. C., Znidarcic, D., Kesteren, W. v., Merckelbach, L. M., Pykes, R., et al. (2002). Sidere: numerical prediction of large-strain consolidation. *Geotechnique*, 639-648.
- Caldwell, J. A., Ferguson, K., Schiffman, R. L., & Zyl, D. v. (1984). Application of Finite Strain Consolidation Theory for Engineering Design and Environmental Planning of Mine Tailings Impoundments. *Sedimentation Consolidation Models - Predictions and Validation*, (pp. 581-606). San Francisco.
- Carrier, W. D., Bromwell, L. G., & Somogyi, F. (1983). Design Capacity of Slurried Mineral Waste Ponds. *Journal of Geotechnical Engineering*, 699-716.
- Coffin, J. (2010). *PhD Thesis; A 3D Model for Slurry Storage Facilities*. Boulder, Colorado: University of Colorado.
- Consoli, N. C. (1991). *Numerical Modelling of the Sedimentation and Consolidation of Tailings*. Montreal, Quebec: Concordia University.
- Consoli, N. C., & Sills, G. C. (2000). Soil formation from tailings: comparison of predictions and field measurements. *Geotechnique*, 25-33.
- Cryer, C. W. (1963). A Comparison of the Three-Dimensional Consolidation Theories of Biot and Terzaghi. *Journal of Mechanics and Applied Math*, 401-412.
- Davies, E. H., & Raymond, G. P. (1965). A Non-linear Theory of Consolidation. *Geotechnique*, 161-173.
- Donea, J., Huerta, A., Ponthot, J., & Rodriguez-Ferrari, A. (2004). Arbitrary Lagrangian-Eulerian Methods. In *Encyclopedia of Computational Mechanics*. John Wiley and Sons.

- Fredlund, D. W., Zhang, Z. M., & MacDonald, K. (1993). Analyses for the stability of potash tailings piles. *Canadian Geotechnical Journal*, 491-505.
- Fredlund, M. D., Donaldson, M., & Gitirana, G. G. (2009). Large Strain 1D, 2D and 3D Consolidation Modeling of Tailings. *Tailings and Mine Waste2009*. University of Alberta Geotechnical Program.
- Fredlund, M. (2011, October). Personal Correspondence.
- Fredlund, M. (September 2011). Personal Correspondence.
- Garrido, P., Burgos, R., Concha, F., & Burger, R. (2002). Software for the design and simulation of gravity thickeners. *Minerals Engineering*, 85-92.
- Gibson, R. E., English, G. L., & Hussey, M. J. (1967). The Theory of One Dimesnional Consolidation of Saturated Clays. *Geotechnique*, 17, 261-273.
- Gibson, R. E., Schiffman, R. L., & Cargill, K. W. (1981). The Theory of One-Dimensional Consolidation of Saturated Clays. II Finite Nonlinear Consolidation of Thick Homogeneous Layers. *Canadian Geotechnical Journal*, 280-293.
- Gjerapic, G., & Znidarcic, D. (2007). A Mass-Conservative Numerical Solution for Finite-Strain Consolidation During Continuous Soil Deposition. *GeoDenver 2007: New Peaks in Geotechnics*, (pp. 1-10). Denver.
- Gjerapic, G., Johnson, J., Jeffrey, C., & Znidarcic, D. (2008). Determination of Tailings Impoundment Capacity via Finite-Strain Consolidation Models. *GeoCongress 2008* (pp. 798-806). New Orleans: ASCE.
- GWP, S. (2007, July). *FSConsol Home Page*. Retrieved October 2011, from FSConsol: <http://www.fsconsol.com/>
- Hughes, J. M., Campanella, R. G., & Roy, D. (1997). A simple understanding of the liquefaction potential of sands from self boring pressuremeter tests. *14th International Conference on Soil Mechanics and Foundation Engineering*, (pp. 515-518). Hamburg.
- Jeeravipoolvarn, S. (2010). *Geotechnical Behaviour of In-Line Thickened Oil Sands Tailings - PhD Thesis*. Edmonton: Faculty of Graduate Studies, University of Alberta.
- Jeeravipoolvarn, S., Chalaturnyk, R. J., & Scott, J. D. (2008). Consolidation Modeling of Oil Sands Fine Tailings: History Matching. *GeoEdmonton'08*, (pp. 190-197). Edmonton.

- Jeeravipoolvarn, S., Scott, J. D., & Chalaturnyk, R. J. (2008). 10 m Standpipe Tests on Oil Sands Tailings: Long-term Experimental Results and Prediction. *Canadian Geotechnical Journal*, 875-888.
- Koppula, S. D., & Morgenstern, N. (1982). On the consolidation of sedimenting clays. *Canadian Geotechnical Journal*, 19, 260-268.
- Lee, K. (1979). *An Analytical and Experimental Study of Large Strain Soil Consolidation*. Oxford, UK: Linacre College, University of Oxford.
- Liu, J.-C., & Znidarcic, D. (1991). Modelling One-Dimensional Compression Characteristics of Soils. *Journal of Geotechnical Engineering*, 162-169.
- McDonald, L., & Lane, J. C. (2010). Consolidation of in-Pit tailings. *Mine Waste 2010* (pp. 49-62). Perth Australia: Australian Center for Geomatics.
- McNamee, J., & Gibson, R. E. (1960). Plane Strain and Axially Symmetric Problems of the Consolidation of a semi-infinite Clay Stratum. *Journal of Mechanics and Applied Math*, 210-227.
- Monte, J. L., & Krizek, R. J. (1976). One-Dimensional Mathematical Model for Large Strain Consolidation. *Geotechnique*, 495-510.
- Morris, P. H. (2002). Analytica; Solutions of Linear Finite-Strain One-Dimensional Consolidation. *Journal of Geotechnical and Geoenvironmental Engineering*, 319-326.
- Oliveira-Filho, W. L., & van Zyl, D. (2006). Modeling Discharge of Interstitial Water from Tailings Following Deposition. *Solas c Rochas*, (pp. 199-209). Sao Paulo.
- Priestley, D., Fredlund, M., & van Zyl, D. (2010). Benchmarking Multi-dimensional Large Strain Consolidation Analyses. *Uranium 2010 Proceedings* (pp. 271-288). Saskatoon: Met Soc.
- Rassam, D. W., & Williams, D. J. (1999). Engineering properties of gold tailings. *International Journal of Surface Mining, Reclamation and the Environment*, 91-96.
- Schiffman, R. L. (1982). The Consolidation of Soft Marine Sediments. *Geo-Marine Letters*, 199-203.
- Schiffman, R. L., Vick, S. G., & Gibson, R. E. (1988). Behaviour and Properties of Hydraulic Fills. *Hydraulic Fill Structures* (pp. 166-202). Fort Collins, Colorado: ASCE.
- Townsend, F. C., & McVay, M. C. (1990). SOAs LARGE STRAIN CONSOLIDATION. *Journal of Geotechnical Engineering*, 116 (2).

Yao, D. T., & Znidarcic, D. (1997). *Crust Formation and Dessication Characteristics for Phosphatic Clays: User's Manual for Computer Program CONDESO*. Polk County, Florida: Florida Institute of Phosphate Research.

Yao, D., & Znidarcic, D. (1997). *User's Manual for Computer Program CONDESO*. Bartow Florida: Florida Institute of Phosphate research.

Yao, D., Oliveira-Filho, W. L., Cai, X.-C., & Znidarcic, D. (2001). Numerical Solution for the Consolidation and Dessication og Soft Soils. *Internation Journal for Numerical and Analytical Methods in Geomechanics* , 139-161.

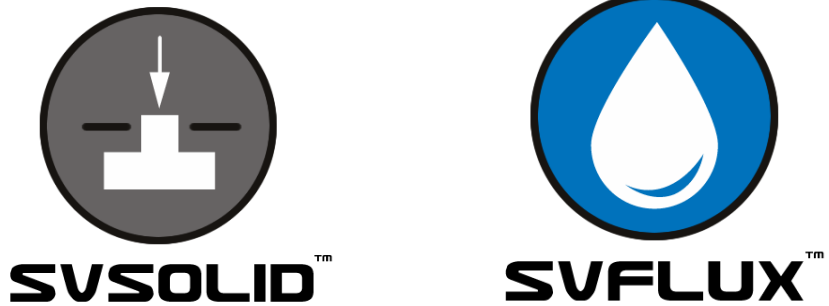
Znidarcic, D., Croce, P., Pane, V., Ko, H.-Y., Olsen, H. W., & Schiffman, R. L. (1984). The Theory of One-Dimensional Consolidation of Saturated Clays: III Existing Testing Procedures and Analyses. *Geotechnical Testing Journal* , 123-133.

Znidarcic, D., Shiffman, R., Pane, V., Croce, P., Ko, H.-Y., & Olsen, H. (1986). The theory of one-dimensional consolidation of saturated clays: part V, constant rate of deformation testing and analysis. *Geotechnique* , 227-237.

Appendices

Appendix A SVOFFICE Large Strain Consolidation Verification Manual - Draft

This appendix contains a draft version of the SVOFFICE Large Strain Consolidation Verification Manual written by the author of this thesis. This draft was submitted to SoilVision Systems Ltd. for their use as part of the ongoing benchmarking process of their software suite. All of the work contained herein was provided to SoilVision Systems and has been included in this thesis with their permission.



Large-Strain Consolidation

Verification Manual

DRAFT

Written by:
Daniel Priestley

SoilVision Systems Ltd.
Saskatoon, Saskatchewan, Canada

Software License

The software described in this manual is furnished under a license agreement. The software may be used or copied only in accordance with the terms of the agreement.

Software Support

Support for the software is furnished under the terms of a support agreement.

Copyright

Information contained within this Verification Manual is copyrighted and all rights are reserved by SoilVision Systems Ltd. The SVSOLID software is a proprietary product and trade secret of SoilVision Systems. The Verification Manual may be reproduced or copied in whole or in part by the software licensee for use with running the software. The Verification Manual may not be reproduced or copied in any form or by any means for the purpose of selling the copies.

Disclaimer of Warranty

SoilVision Systems Ltd. reserves the right to make periodic modifications of this product without obligation to notify any person of such revision. SoilVision does not guarantee, warrant, or make any representation regarding the use of, or the results of, the programs in terms of correctness, accuracy, reliability, currentness, or otherwise; the user is expected to make the final evaluation in the context of his (her) own problems.

Trademarks

Windows™ is a registered trademark of Microsoft Corporation.
SoilVision® is a registered trademark of SoilVision Systems Ltd.
SVOFFICE™ is a trademark of SoilVision Systems, Ltd.
CHEMFLUX™ is a trademark of SoilVision Systems Ltd.
SVFLUX™ is a trademark of SoilVision Systems Ltd.
SVHEAT™ is a trademark of SoilVision Systems Ltd.
SVAIRFLOW™ is a trademark of SoilVision Systems Ltd.
SVSOLID™ is a trademark of SoilVision Systems Ltd.
SVSLOPE™ is a trademark of SoilVision Systems Ltd.
ACUMESH™ is a trademark of SoilVision Systems Ltd.
FlexPDE® is a registered trademark of PDE Solutions Inc.

Copyright © 2011

by

SoilVision Systems Ltd.
Saskatoon, Saskatchewan, Canada
ALL RIGHTS RESERVED
Printed in Canada

TABLE OF CONTENTS

| | |
|---|----------|
| LARGE-STRAIN CONSOLIDATION | 1 |
| VERIFICATION MANUAL | 1 |
| DRAFT | 1 |
| 1 INTRODUCTION | 5 |
| 2 SATURATED CONSOLIDATION | 6 |
| 2.1 SIDERE: NUMERICAL PREDICTION OF LARGE STRAIN CONSOLIDATION..... | 6 |
| 2.1.1 <i>Model Description</i> | 6 |
| 2.1.1.1 Material Parameters..... | 6 |
| 2.1.1.2 Geometry/Boundary Conditions..... | 8 |
| 2.1.2 <i>Results</i> | 8 |
| 2.2 CONDESO VALIDATION – INSTANTANEOUS FILLING | 10 |
| 2.2.1 <i>Model Description</i> | 10 |
| 2.2.1.1 Material Parameters..... | 10 |
| 2.2.1.2 Geometry/Boundary Conditions..... | 11 |
| 2.2.2 <i>Results</i> | 12 |
| 2.3 CONDESO VALIDATION – STAGED FILLING ANALYSIS | 13 |
| 2.3.1 <i>Purpose</i> | 13 |
| 2.3.1.1 Geometry and Boundary Conditions..... | 13 |
| 2.3.1.2 Material Parameters..... | 14 |
| 2.3.2 <i>Results and Discussions</i> | 15 |
| 2.4 STANDPIPE TESTS ON OIL SANDS TAILINGS PART A | 17 |
| 2.4.1 <i>Model Description</i> | 17 |
| 2.4.1.1 Material Parameters..... | 17 |
| 2.4.1.2 Geometry/Boundary Conditions..... | 18 |
| 2.4.2 <i>Results</i> | 18 |
| 2.5 STANDPIPE TESTS ON OIL SANDS TAILINGS PART B – MULTI-DIMENSIONAL VERIFICATION | 21 |
| 2.5.1 <i>Model Description</i> | 21 |
| 2.5.1.1 Material Parameters..... | 21 |
| 2.5.1.2 Geometry/Boundary Conditions..... | 23 |
| 2.5.2 <i>Results</i> | 24 |
| 2.6 TOWNSEND SCENARIO A | 27 |
| 2.6.1 <i>Model Description</i> | 27 |
| 2.6.1.1 Material Parameters..... | 27 |
| 2.6.1.2 Geometry/Boundary Conditions..... | 28 |
| 2.6.2 <i>Results</i> | 29 |
| 2.7 TOWNSEND MODEL B | 33 |
| 2.7.1 <i>Model Description</i> | 33 |
| 2.7.1.1 Geometry and Boundary Conditions..... | 35 |
| 2.7.1.2 Material Parameters..... | 35 |
| 2.7.2 <i>Results and Discussions</i> | 35 |
| 2.8 TOWNSEND SCENARIO C | 38 |
| 2.8.1 <i>Model Description</i> | 38 |
| 2.8.1.1 Geometry/Boundary Conditions..... | 40 |
| 2.8.1.2 Material Parameters..... | 40 |
| 2.8.2 <i>Results</i> | 40 |
| 2.9 TOWNSEND SCENARIO D | 43 |
| 2.9.1 <i>Model Description</i> | 43 |
| 2.9.1.1 Material Parameters..... | 43 |
| 2.9.1.2 Geometry/Boundary Conditions..... | 44 |
| 2.9.2 <i>Results</i> | 45 |

| | |
|--|-----------|
| 2.10 CALDWELL CASE 1 STAGED FILLING ANALYSIS OF SULFIDE TAILINGS | 47 |
| 2.10.1 <i>Model Description</i> | 47 |
| 2.10.1.1 Geometry and Boundary Conditions | 48 |
| 2.10.1.2 Material Parameters..... | 49 |
| 2.10.2 <i>Results and Discussions</i> | 50 |
| 2.11 CALDWELL CASE 2 – STAGED FILLING ANALYSIS..... | 52 |
| 2.11.1 <i>Model Description</i> | 52 |
| 2.11.1.1 Geometry and Boundary Conditions | 53 |
| 2.11.1.2 Material Parameters..... | 54 |
| 2.11.2 <i>Results and Discussions</i> | 55 |
| 3 REFERENCES..... | 56 |

1 INTRODUCTION

The word "Verification", when used in connection with computer software can be defined as "the ability of the computer code to provide a solution consistent with the physics defined by the governing partial differential equation, PDE". There are also other factors such as initial conditions, boundary conditions, and control variables that also affect the accuracy of the code to perform as stated.

"Verification" is generally achieved by solving a series of so-called "benchmark" problems. "Benchmark" problems are problems for which there is a closed-form solution or for which the solution has become "reasonably certain" as a result of long-hand calculations that have been performed. Publication of the "benchmark" solutions in research journals or textbooks also lends credibility to the solution. There are also example problems that have been solved and published in User Manual documentation associated with other comparable software packages. While these are valuable checks to perform, it must be realized that it is possible that errors can be transferred from one's software solution to another. Consequently, care must be taken in performing the "verification" process on a particular software package. It must also be remembered there is never such a thing as complete software verification for "all" possible problems. Rather, it is an ongoing process that establishes credibility with time.

SoilVision Systems takes the process of "verification" most seriously and has undertaken a wide range of steps to ensure that the SVSOLID software will perform as intended by the theory of saturated-unsaturated stress and deformation.

The following models represent comparisons made to textbook solutions, hand calculations, and other software packages. We at SoilVision Systems Ltd. are dedicated to providing our clients with reliable and tested software. While the following list of example models is comprehensive, it does not reflect the entirety of models, which may be posed to the SVSOLID software. It is our recommendation that water balance checking be performed on all model runs prior to presentation of results. It is also our recommendation that the modeling process move from simple to complex models with simpler models being verified through the use of hand calculations or simple spreadsheet calculations.

2 SATURATED CONSOLIDATION

This Chapter will compare SVOFFICE to published research on saturated consolidation.

2.1 SIDERE: NUMERICAL PREDICTION OF LARGE STRAIN CONSOLIDATION

Reference: Bartholomeeusen et al. (2002)

Project: LS_SaturatedConsolidation
Model: sidp1, sidextendedp

Main Factors Considered:

One-Dimensional Consolidation

Correlation to D. Znidarcic's methodology

Relation to experimental and theoretical results

Comparison of Extended Power and Standard Power Functions to model void ratio-stress relationships

2.1.1 Model Description

The purpose of this model is to benchmark the coupled SVSolid/SVFlux analysis against experimental published results. Bartholomeeusen et al. created this benchmark in 2002 to correlate a number of other researcher's numerical models against experimental results. Numerous numerical models were used to estimate the soil parameters from other calibration experiments and then to apply them to another scenario for which the experimental results were not known. This setup was recreated using Znidarcic's formulation of soil parameters, as his results showed the highest correlation to the literature results. Both the extended and standard power functions were tested. In addition these results were compared to the program CONDESO. It was found that Znidarcic's results could be duplicated using his formulation of the soil parameters.

2.1.1.1 Material Parameters

The material used consists of sediment deposits taken from the Schelde River in Belgium. It has a specific gravity of 2.72 and an initial void ratio of 2.47. D. Znidarcic formulated the relations between the effective stress and void ratio as an Extended Power Function (Liu and Znidarcic, 1991). The void ratio – permeability relation is expressed as a standard power function. The curves are shown in Figure 1 and Figure 2 while their respective expressions are provided below ([1], [2]).

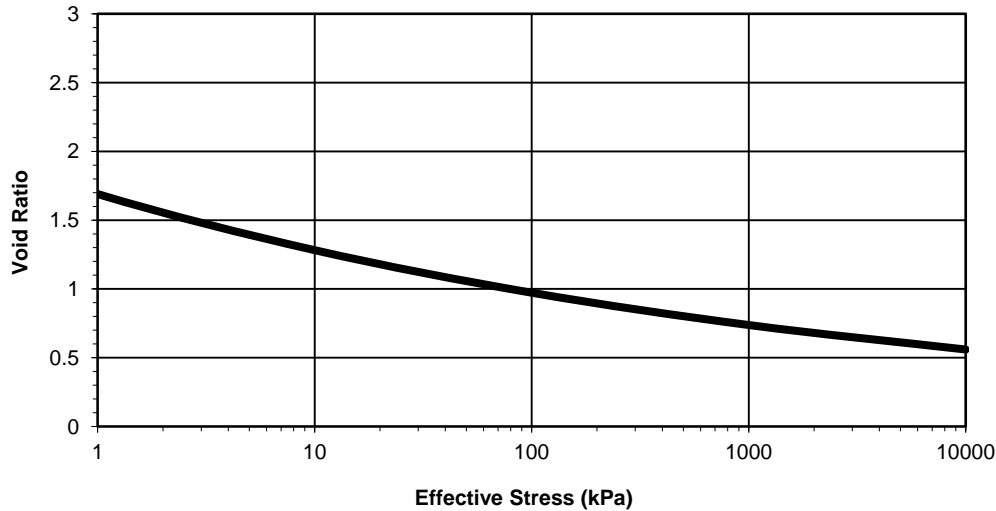


Figure 1 Sidere Effective Stress-Void Ratio Curve

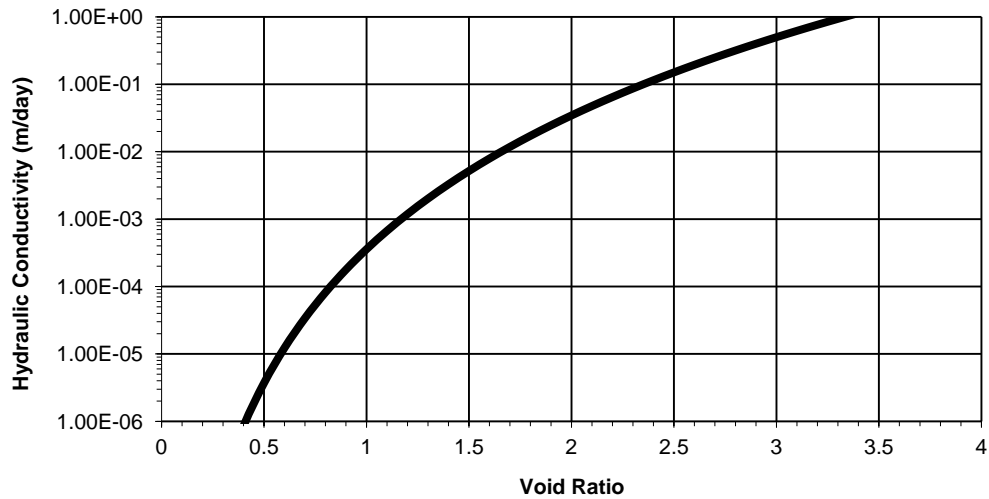


Figure 2 Sidere Void Ratio-Permeability Curve

Extended Power Function Model

$$e = 1.69(\sigma' + 0.046)^{-0.12} \text{ (kPa)} \quad [1]$$

$$k = 3.577 \times 10^{-4} e^{6.59} \text{ (m / day)} \quad [2]$$

The initial void ratio was calculated by setting the effective stress to 0 and calculating the void ratio. This simulates the void ratio at the boundary between sedimentation and consolidation (Gjerapic et al., 2007). The initial stress limit was set to be 0.019, as this is the minimum effective stress that should be observed. When set as a Power Function the effective stress-void ratio relation becomes:

Power Function Model

$$e = 1.69(\sigma')^{-0.12} (kPa)$$

[3]

The initial stress condition was defined so that the initial effective stress would be based upon the initial void ratio. This is applied to all cases of large strain slurry consolidation. It was set as:

Power Function Model

$$sy_0 = uw_0 + (vr_0 / 1.69)^{1/-0.12}$$

[4]

Extended Power Function Model

$$sy_0 = uw_0 + (vr_0 / 1.69)^{1/-0.12} - 0.046$$

[5]

$$sx_0 = sy_0$$

[6]

$$sz_0 = sy_0$$

[7]

An initial Poisson's ratio of 0.49 was assumed, since none was provided in the literature. Poisson's ratio can impact the results achieved in SVOOffice and should be investigated, whenever possible.

2.1.1.2 Geometry/Boundary Conditions

The model consists of a one-dimensional column, with a height of 0.565m. It is assumed that the material is initially homogeneous and is deposited instantaneously. The deformation boundary conditions consist of a lower boundary that is fixed in place and an upper boundary that is free to deform. The flux conditions consist of a constant head of 0.565m at the top boundary and a zero flux boundary at the bottom. No flow is allowed to leave through the sides of the column. This forces the water to flow from the bottom out through the top boundary, while simulating a constant water table above the soil region.

2.1.2 Results

Figure 3 shows a comparison of the interface heights predicted by Znidarcic and those found experimentally. Znidarcic's results were the closest to the experiment during the first seven days, but underestimated the amount of settlement after 8 days. It can be seen that SVOOffice was able to duplicate Znidarcic's results using the data points provided. The standard power function duplicated the results, while the extended power function predicted slightly different results.

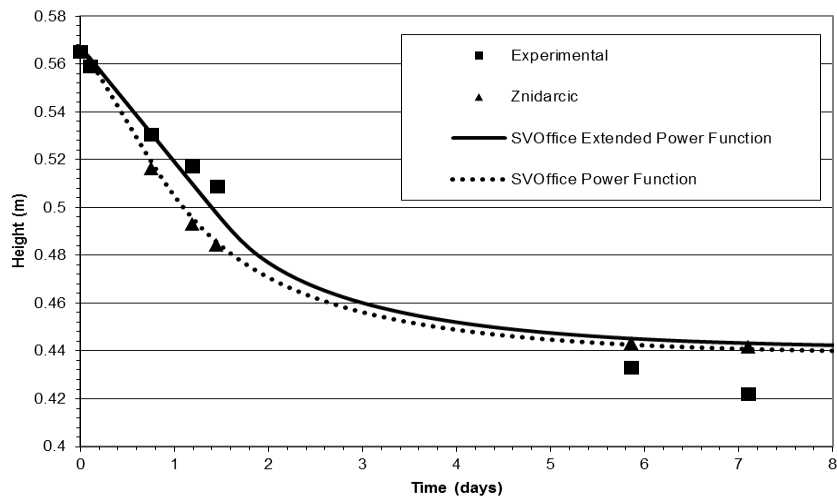


Figure 3 Sidere Results

Table 1: Summary of SIDP1 Model Parameters

| Initial Conditions: | |
|--|---|
| Model Run Time: | 8 Days |
| Maximum Time Increment: | 0.1 Days |
| Body Load Time: | 0.1 Days |
| Initial Height: | 0.565 m |
| Initial Void Ratio: | 2.47 |
| Specific Gravity: | 2.72 |
| Initial Water Level: | 0.565 m |
| Initial Stress Expression (Power Function Model): | $sy0=uw0+(vr0/1.69)^{1/(-0.12)}$, $sx0=sy0,sz0=sy0$ |
| Initial Stress Expression (Extended Power Function Model): | $sy0=uw0+(vr0/1.69)^{1/(-0.12)}-0.046$, $sx0=sy0,sz0=sy0$ |
| Initial Flux Condition: | Head Expression = 0.565 m |
| Flux Boundary Conditions: | |
| Bottom Boundary: | Zero Flux |
| Top Boundary: | Head Expression = 0.565 m |
| Deformation Boundary Conditions: | |
| Bottom Boundary: | Fixed |
| Top Boundary: | Free |
| Material Parameters: | |
| Effective Stress – Void Ratio: | Power Function |
| | $e = 1.69(\sigma')^{-0.12} (kPa)$ |
| | Extended Power Function |
| | $e = 1.69(\sigma'+0.046)^{-0.12} (kPa)$ |
| Hydraulic Conductivity – Void Ratio: | $k = 3.577 \times 10^{-4} e^{6.59} (m/day)$ |
| Poisson's Ratio: | 0.35 |
| Initial Stress Limit: | 0.019 |
| Unit Weight Option: | Based On Initial Void Ratio |

2.2 CONDESO VALIDATION - INSTANTANEOUS FILLING

Project: LS_SaturatedConsolidation
 Model: CONDESO_Trial_1

Main Factors Considered:

One-Dimensional Instantaneous Filling Consolidation
 Correlation to CONDESO
 Validation of Extended Power Function

2.2.1 Model Description

The purpose of this model is to benchmark the coupled SVSolid/SVFlux analysis against the program CONDESO. CONDESO was created in 1997 to solve for 1D Consolidation and Desiccation of tailings materials. It has been extensively benchmarked and is considered to be valid for 1D homogeneous applications.

2.2.1.1 Material Parameters

The material used was defined using an arbitrary definition. The extended power function is the only formulation available in CONDESO; therefore an extended function[7] was used for comparison. The hydraulic conductivity curve was defined using an ordinary power function[8]. The effective stress and void ratio – permeability curves are also shown in Figure 4 and Figure 5 respectively.

$$e = 4.0(\sigma' + 0.615)^{-0.08} \text{ (kPa)} \quad [8]$$

$$k = 6.0 \times 10^{-5} e^{4.0} \text{ (m/day)} \quad [9]$$

The initial void ratio was calculated by setting the effective stress to 0 and calculating the corresponding void ratio of 4.16. This simulates the void ratio at the boundary between sedimentation and consolidation (Gjerapic et al., 2007). The initial stress limit was set to be 0.0001, as the Z-term (0.615) allows the effective stress to be calculated down to zero. An initial Poisson's ratio of 0.49 was used as is discussed later.

The initial stress condition was defined in the same manner as in Section 2.1.

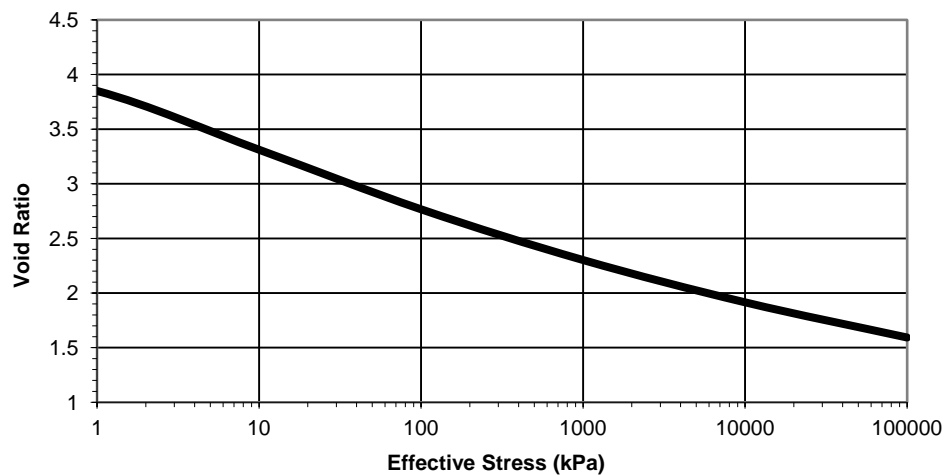


Figure 4: CONDESO_Trial_1 Effective Stress - Void Ratio Curve

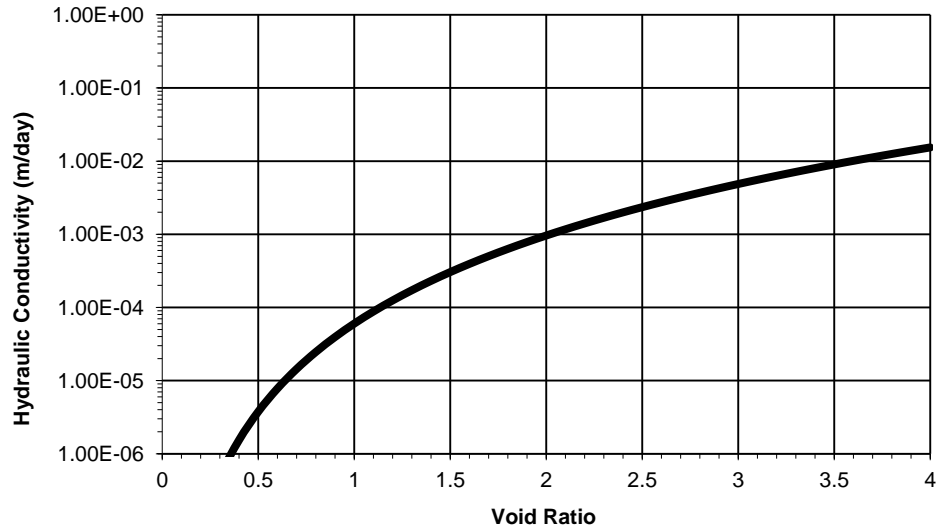


Figure 5: CONDESO_Trial_1 Void Ratio-Hydraulic Conductivity Curve

2.2.1.2 Geometry/Boundary Conditions

The model consists of a one-dimensional column, with a height of 10.0 m. The column is assumed to be instantaneously deposited and completely homogeneous at deposition. The top boundary is allowed to deform, while the bottom boundary is fixed. Flow is only allowed out of the system through the top surface. The water table is held constant at a height of 10.0 m.

Table 2: Summary of CONDESO Trial 1 Model Parameters

| Initial Conditions: | |
|--------------------------------------|---|
| Model Run Time: | 365 Days |
| Maximum Time Increment: | 5 Days |
| Body Load Time: | 2 Days |
| Initial Height: | 10 m |
| Initial Void Ratio: | 4.16 |
| Specific Gravity: | 2.5 |
| Initial Water Level: | 10 m |
| Initial Stress Expression: | $sy0=uw0+(vr0/4.0)^{1/(-0.08)}-0.615,$ $sx0=sy0,sz0=sy0$ |
| Initial Flux Condition: | Head Expression = 10 m |
| Flux Boundary Conditions: | |
| Bottom Boundary: | Zero Flux |
| Top Boundary: | Head Expression = 10 m |
| Deformation Boundary Conditions: | |
| Bottom Boundary: | Fixed |
| Top Boundary: | Free |
| Material Parameters: | |
| Effective Stress – Void Ratio: | Extended Power Function $e = 4.0(\sigma'+0.615)^{-0.08} (kPa)$ |
| Hydraulic Conductivity – Void Ratio: | $k = 6.0 \times 10^{-5} e^{4.0} (m / day)$ |
| Poisson's Ratio: | 0.49 |
| Initial Stress Limit: | 0.0001 |
| Unit Weight Option: | Based On Initial Void Ratio |

2.2.2 Results

As can be seen in Figure 6, SVOOffice is capable of duplicating the results found in CONDESO. In order to meet this benchmark it was necessary to set the Poisson's ratio to 0.49. Higher values of Poisson's ratio increase the amount of settlement by a significant amount. Poisson's ratios of 0.5 or higher are not practical; therefore it is found that CONDESO must assume a theoretical maximum Poisson's Ratio.

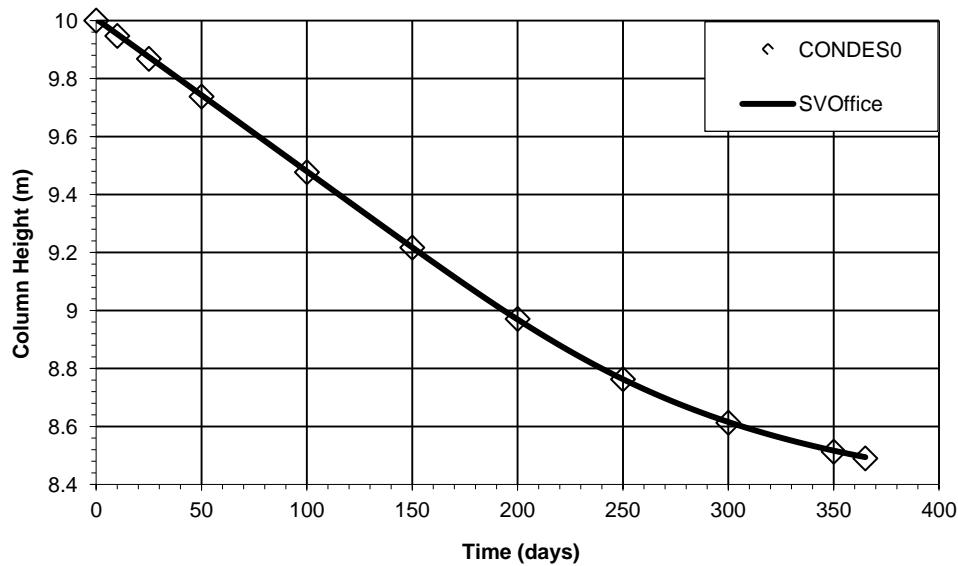


Figure 6: Column Height Comparison between SVOOffice and CONDESO

2.3 CONDESO VALIDATION - STAGED FILLING ANALYSIS

Project: Consolidation Benchmarks
 Model: CONDESO_Trials_2.svm

Main Factors Considered:

- One-Dimensional Staged Filling Analysis Consolidation
- Correlation to CONDESO
- Validation of Extended Power Function

Table 3: Summary of CONDESO Trial 2 Model Parameters

| Initial Conditions: | |
|--------------------------------------|---|
| Model Run Time: | 1000 Days |
| Maximum Time Increment: | 10 Days |
| Body Load Time: | 5 Days |
| Initial Height: | 2 m |
| Initial Void Ratio: | 4.16 |
| Specific Gravity: | 2.5 |
| Initial Water Level | 2 meters |
| Initial Stress Expression: | $sy0=uw0+(vr0/1.69)^{1/(-0.12)}$, $sx0=sy0,sz0=sy0$ |
| Initial Flux Condition: | Head Expression = 10 m |
| Flux Boundary Conditions: | |
| Bottom Boundary: | Zero Flux |
| Top Boundary: | Head Expression = 10 m |
| Side Boundaries: | Zero Flux |
| Deformation Boundary Conditions: | |
| Bottom Boundary: | Fixed |
| Top Boundary: | Free |
| Side Boundaries: | Fixed |
| Material Parameters: | |
| Effective Stress – Void Ratio: | Extended Power Function $e = 4.0(\sigma'+0.615)^{-0.08} (kPa)$ |
| Hydraulic Conductivity – Void Ratio: | $k = 6.0 \times 10^{-4} e^{4.0} (m/day)$ |
| Poisson's Ratio: | 0.495 |
| Initial Stress Limit: | 0.0001 |
| Unit Weight Option: | Based On Initial Void Ratio |

2.3.1 Purpose

The purpose of this model is to benchmark the coupled SVSolid/SVFlux analysis against the program CONDESO. CONDESO was created in 1997 to solve for 1-D Consolidation and Desiccation of tailings materials. It has been extensively benchmarked and is considered to be valid for most applications. It was found that when properly formatted the results can be duplicated in SVOOffice.

2.3.1.1 Geometry and Boundary Conditions

The model consists of a one-dimensional column, with a height of 10.0 m. The column is assumed to be deposited in 2 meter instantaneous increments every 200 days for a period of 800 days. This is followed by a further period of 200 days. The slurry is completely homogeneous at deposition. Figure 4 shows the model geometry.

The top boundary is allowed to deform, while the bottom boundary is fixed. Flow is only allowed out of the system through the top surface. The water table is held constant at a height of 10.0 m.

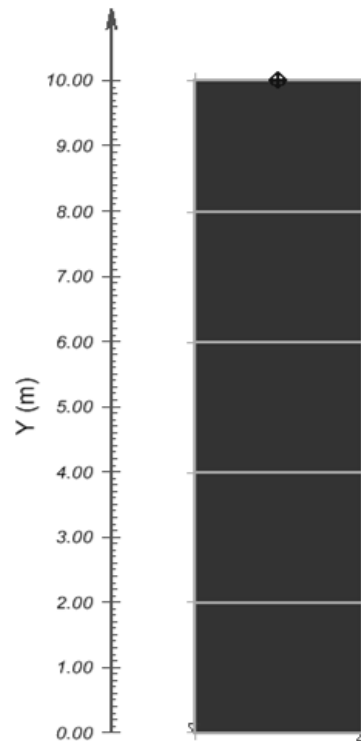


Figure 7: Example geometry

2.3.1.2 Material Parameters

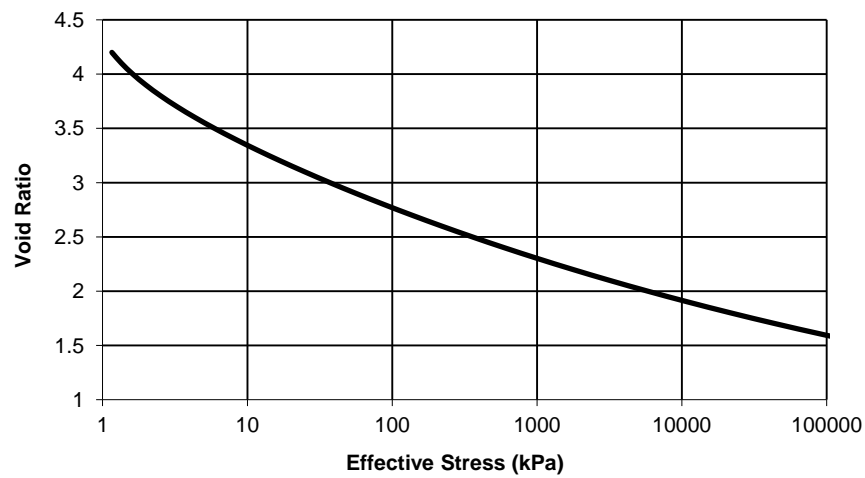


Figure 8: Effective Stress - Void Ratio Curve

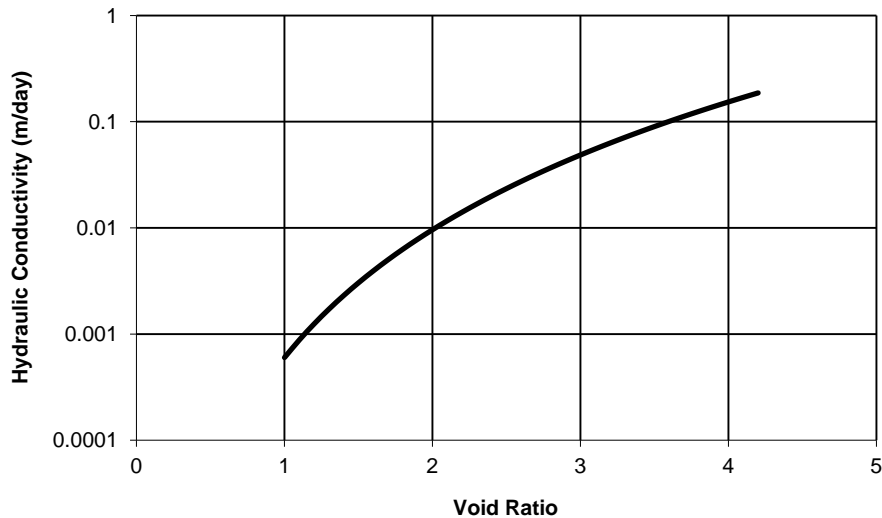


Figure 9: Void Ratio-Hydraulic Conductivity Curve

The material used was defined using an arbitrary definition. The extended power function is the only formulation available in CONDESO; therefore an extended function (9) was used for comparison (Figure 8). The hydraulic conductivity curve was defined using an ordinary power function (10). The void ratio – permeability relation is also shown in Figure 9.

$$e = 4.0(\sigma' + 0.615)^{-0.08} \text{ (kPa)} \quad (9)$$

$$k = 6.0 \times 10^{-5} e^{4.0} \text{ (m/day)} \quad (10)$$

The initial void ratio was calculated by setting the effective stress to 0 and calculating the corresponding void ratio of 4.16. This simulates the void ratio at the boundary between sedimentation and consolidation (Gjerapic et al., 2007). The initial stress limit was set to be 0.001, as the Z-term (0.615) allows the effective stress to be calculated down to zero. An initial Poisson's ratio of 0.49 was used as is previously discussed in Section 2.3.

2.3.2 Results and Discussions

As can be seen in Figure 10 and 11, SVOOffice is capable of duplicating the results found in CONDESO. In order to meet this benchmark it was necessary to set the Poisson's ratio to 0.495. Careful attention needs to be paid to time increments in stage filling analyses so that the data are represented properly. Each layer is brought in over the body load time period. This need to be sufficiently small so that there are no calculation errors. The maximum time increment should be set to approximately one fifth of the body load time for the material to be properly phased in. If layers fail to consolidate, it is likely that the time settings are too large.

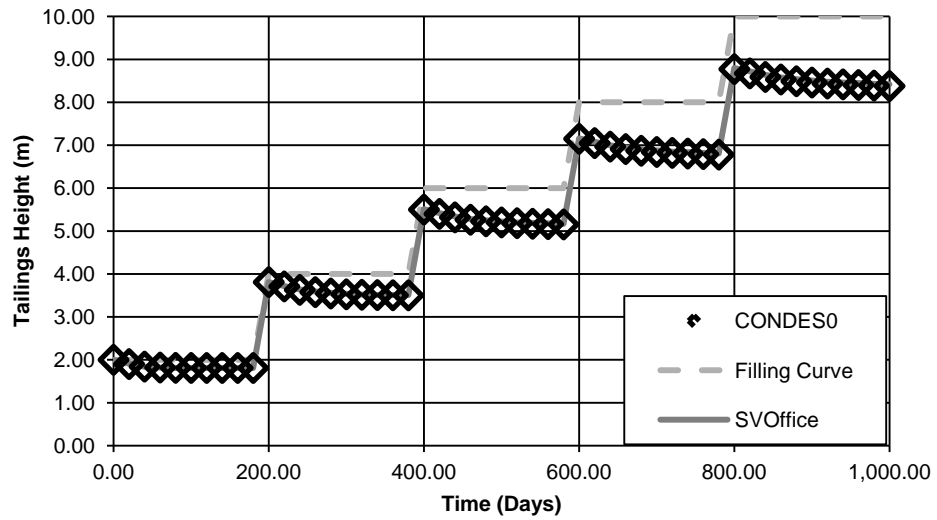


Figure 10: Column Height Comparison between SVOffice and CONDESO

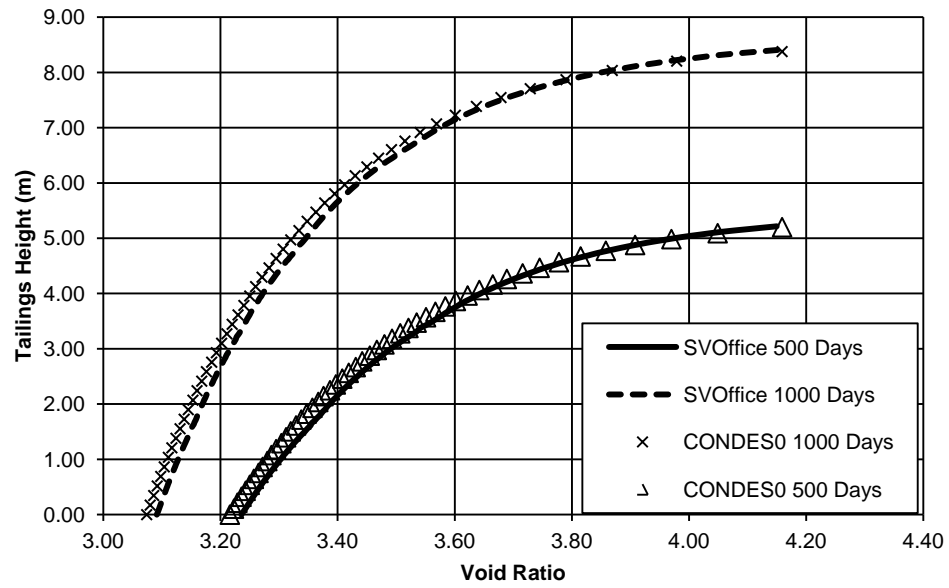


Figure 11: Void Ratio Profile Comparison at 500 and 1000 Days

2.4 STANDPIPE TESTS ON OIL SANDS TAILINGS PART A

Reference: Jeeravipoolvarn et al. (2009)

Project: LS_SaturatedConsolidation
 Model: Oil_Sands_Column_3

Main Factors Considered:

Correlation to Literature One-Dimensional Consolidation Model
 Validation of the Weibull Function

2.4.1 Model Description

Jeeravipoolvarn et al. created this benchmark in 2008 when the experimental results of a long-term consolidation test on oil sands tailings became available. The results from the experiment were then compared to another one-dimensional finite element model. This setup was recreated in SVOOffice using the Weibull function, which is recommended in the paper for oil sands tailings. This was used to validate the implementation of the Weibull function.

2.4.1.1 Material Parameters

The material used consists of oil sands tailings taken from Syncrude's Mildred Lake Tailings Impoundment in 1982. This sand was mixed with cyclone tailings sand to bring the percent sand in the mixture to 82%. It has a specific gravity of 2.58 and an initial void ratio of 0.87.

The effective stress - void ratio equation was plotted using a Weibull function, while the conductivity - void ratio was plotted using a power function. These are shown in Figure 12 and Figure 13 respectively. The Weibull function is provided in equation [9]. Equation [10] shows the permeability – void ratio relationship.

$$e = 1.08 - 0.77 \exp(-1.3\sigma'^{-0.29}) \text{ (kPa)} \quad [11]$$

$$k = 2.76 \times 10^{-3} e^{3.824} \text{ (m/day)} \quad [12]$$

The initial stress limit was set to be 1.00 kPa, as this is the minimum effective stress that should be observed based on equation 11 and the initial void ratio. A Poisson's ratio of 0.49 was assumed since none was specified in the literature.

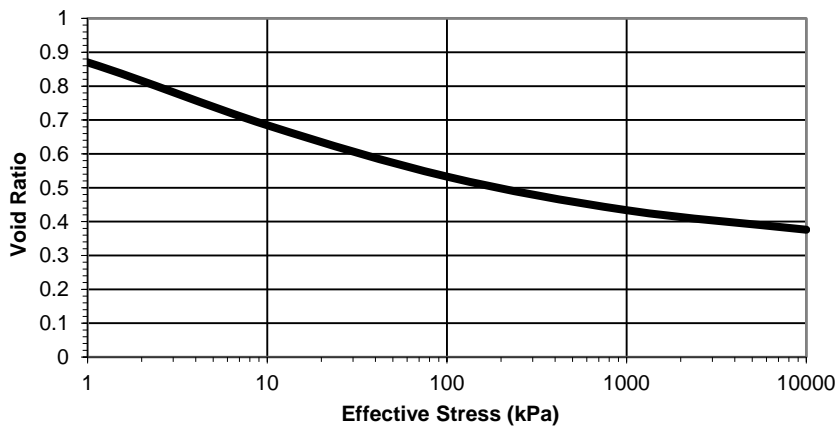


Figure 12: Oil_Sands_Column_3 Void Ratio-Effective Stress Curve

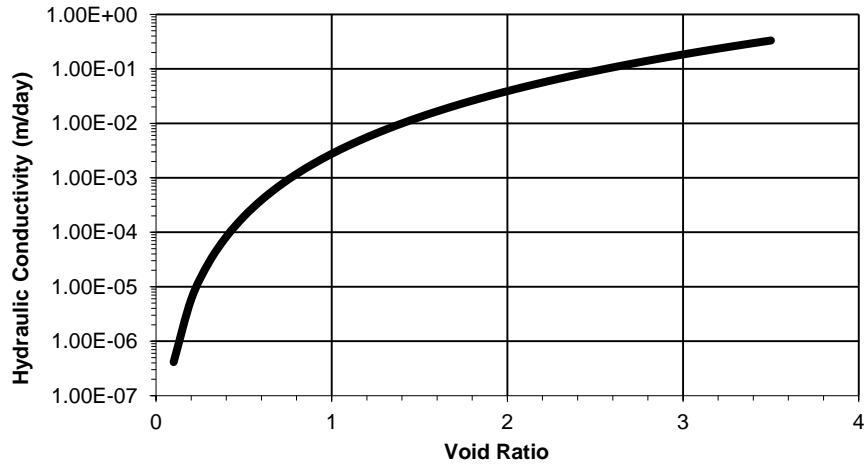


Figure 13: Oil_Sands_Column_3 Void Ratio-Hydraulic Conductivity Curve

2.4.1.2 Geometry/Boundary Conditions

The model consists of a column with a height of 10 m. It is assumed that the tailings are initially homogeneous and deposited instantaneously. The deformation boundary conditions consist of a lower boundary that is fixed in place, and an upper boundary that is free to deform. The flux conditions consist of a constant head of 10 m at the top boundary and a zero flux boundary on the bottom of the column. This forces the water to flow from bottom out through the top boundary, while simulating a constant water table above the soil region.

2.4.2 Results

Figure 14 shows a comparison of the interface heights predicted by Jeeravipoolvarn (2008) and those found experimentally in the same study. SVOFFICE was able to duplicate the results predicted using the Weibull function.

Figure 15, Figure 16, and Figure 17 show plots of Excess Porewater Pressure, Effective Stress, and Void Ratio Profiles at various times during consolidation. It can be seen that there is good agreement between the plots.

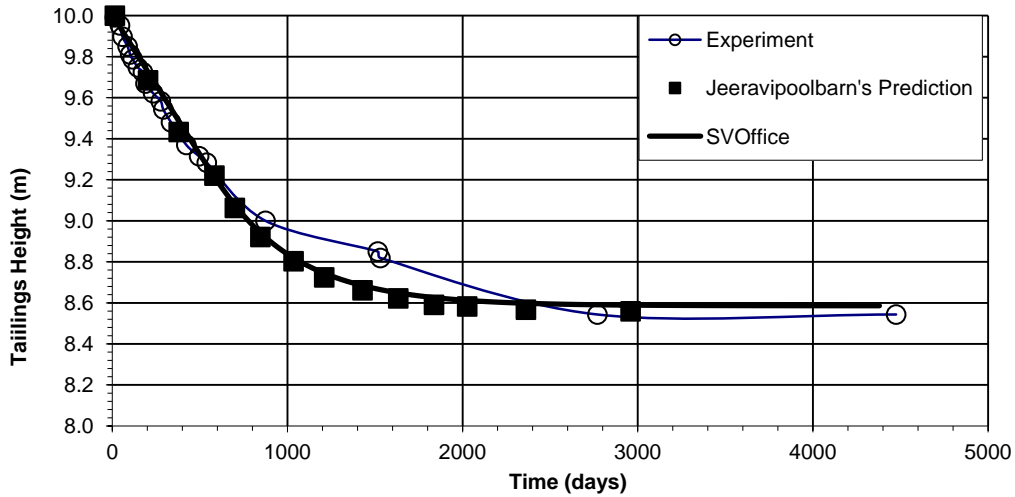
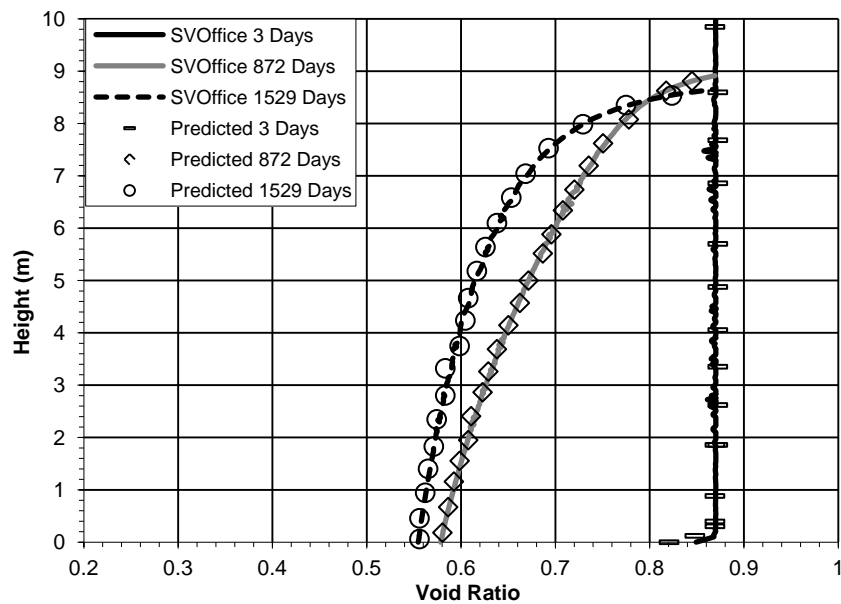


Figure 14 Oil Sands Column 3 Results

Table 4: Summary of Oil Sands Column 3 Model Parameters

| Initial Conditions: | |
|--|--|
| Model Run Time: | 4380 Days |
| Maximum Time Increment: | 10 Days |
| Body Load Time: | 5 Days |
| Initial Height: | 10 m |
| Initial Void Ratio: | 0.87 |
| Specific Gravity: | 2.28 |
| Initial Water Level: | 10 m |
| Initial Stress Expression: | $sx0 = uw0 + (\ln((vr0-1.08)/(-0.77))/(-1.3))^{(1/(-0.29))}$, $sy0 = sx0$, $sz0 = sx0$ |
| Initial Flux Condition: | Head Expression = 10 m |
| Flux Boundary Conditions: | |
| Bottom Boundary: | Zero Flux |
| Top Boundary: | Head Expression = 10 m |
| Deformation Boundary Conditions: | |
| Bottom Boundary: | Fixed |
| Top Boundary: | Free |
| Material Parameters: | |
| Effective Stress – Void Ratio: | |
| Weibull Function $e = 1.08 - 0.77 \exp(-1.3\sigma^{-0.29}) (kPa)$ | |
| Hydraulic Conductivity – Void Ratio: | $k = 2.76 \times 10^{-5} 3e^{3.824} (m/day)$ |
| Poisson's Ratio: | 0.49 |
| Initial Stress Limit: | 1.00 |
| Unit Weight Option: | Based On Initial Void Ratio |

**Figure 15: Jeeravipoolbarn Column 3 Void Profile Comparison**

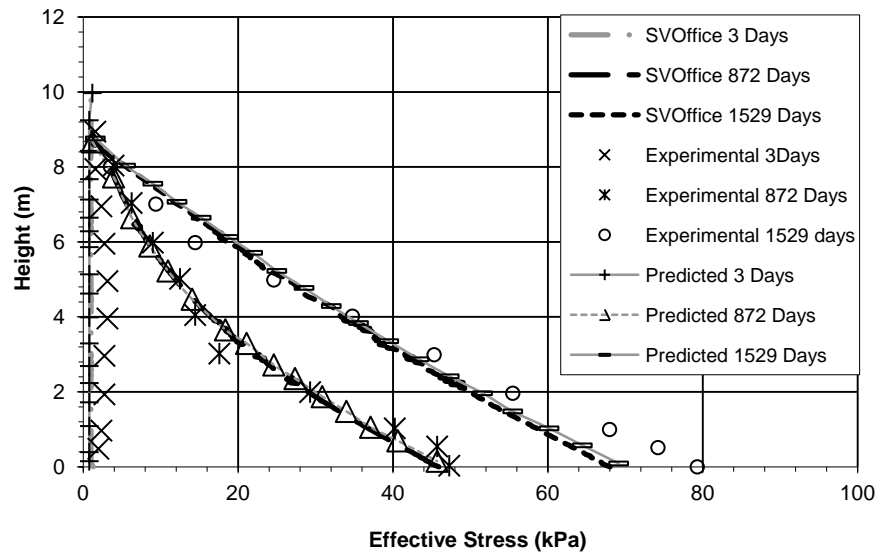


Figure 16: Jeeravipoolbarn Column 3 Excess Stress Comparison

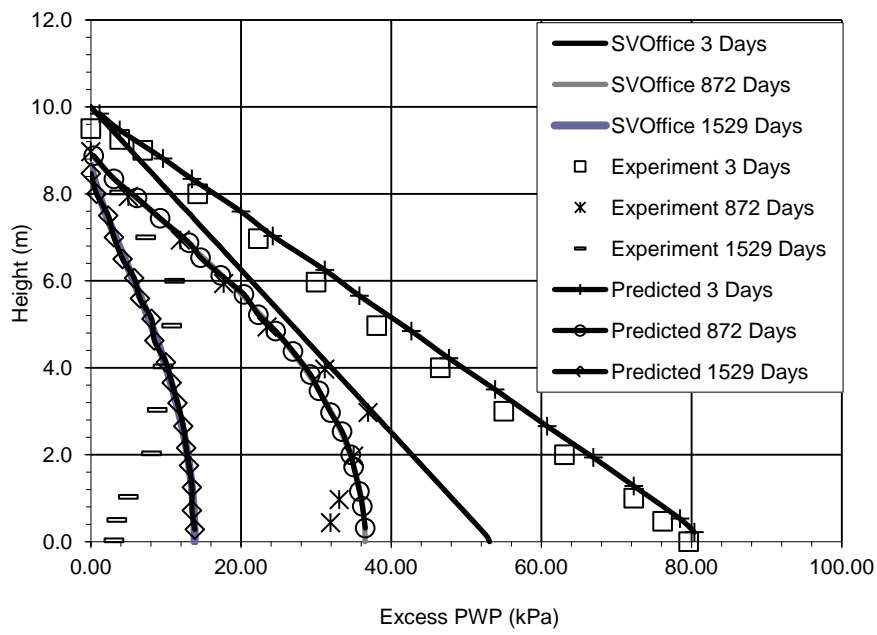


Figure 17: Oil Sands Column 3 Excess Porewater Pressure Profiles found using SVOOffice and compared to Jeeravipoolvarn's predictions and experimental results

2.5 STANDPIPE TESTS ON OIL SANDS TAILINGS PART B - MULTI-DIMENSIONAL VERIFICATION

Reference: Jeeravipoolbarn et al. (2009)

Project: LS_SaturatedConsolidation
 Model: Oil_Sands_Column_1_1D, Oil_Sands_Column_1_1D_Power, Oil_Sands_Column_1_2D, Oil_Sands_Column_1_3D

Main Factors Considered:

Correlation to Literature of 1D Consolidation Model
 Large Strain 2D and 3D Consolidation of a Circular Column
 Comparison of the Power and Weibull Effective Stress – Void Ratio Functions

2.5.1 Model Description

Jeeravipoolbarn et al. created this benchmark in 2008 when the experimental results of a long term consolidation test on oil sands tailings became available. This example is part of the same study as the Oil_Sands_Column_3 model presented in Standpipe Tests on Oil Sands Tailings Part A.

The 1D results of SVOFFICE were compared to the experimental and predicted results in this verification. 2D and 3D models are compared to the 1D results to examine any dimensional effects.

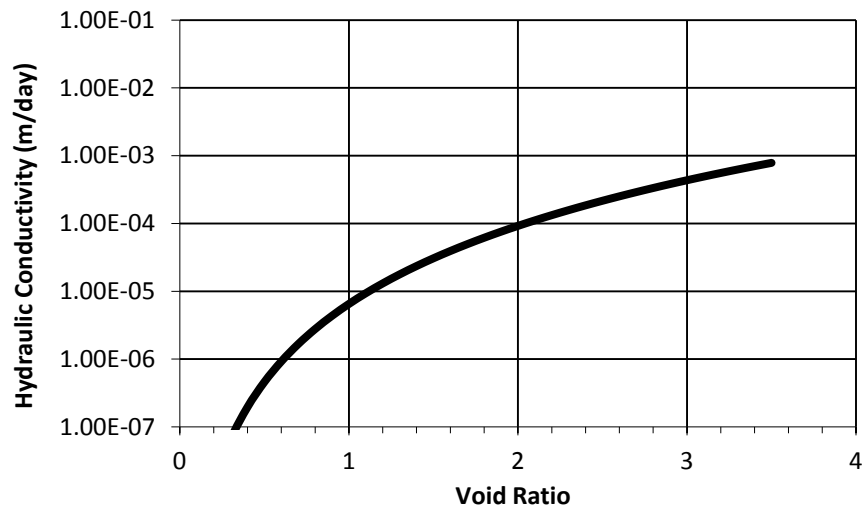


Figure 18: Weibull Compressibility Function

2.5.1.1 Material Parameters

The material used consists of oil sands tailings taken from Syncrude's Mildred Lake Tailings Impoundment in 1982. It has a specific gravity of 2.28 and an initial void ratio of 5.17.

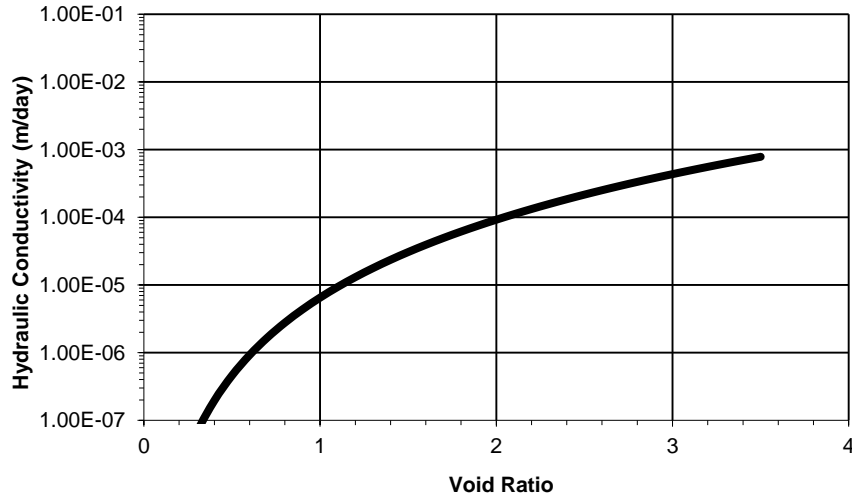


Figure 19: Oil Sands Column 1 Void Ratio-Hydraulic Conductivity Curve

Jeeravipoolbarn et al. uses a Weibull function to relate effective stress and void ratio, whereas the SVOFFICE software has implemented a number of different functions, including Weibull. To compare the differences between the different functions both the Weibull and the Power Functions were tested. A suitable power series was found in Jeeravipoolbarn, 2010. The differences between the functions are shown in Figure 18. The Weibull function is provided in equation [12] and the Power function in equation [13]. Equation [14] shows the permeability – void ratio relationship.

$$e = 5.50 - 4.97 \exp(-1.03\sigma'^{-0.67}) \text{ (kPa)} \quad [10]$$

$$e = 3.391(\sigma')^{-0.308} \text{ (kPa)} \quad [11]$$

$$k = 6.51 \times 10^{-6} e^{3.824} \text{ (m/day)} \quad [12]$$

The initial stress limit was set to be 0.254 kPa, as this is the minimum effective stress that should be observed. A Poisson's ratio of 0.4 was assumed, since none was specified in the literature. In the 2-D and 3-D model, the Coefficient of Lateral Earth Pressure (K_o) was based upon the Poisson's ratio.

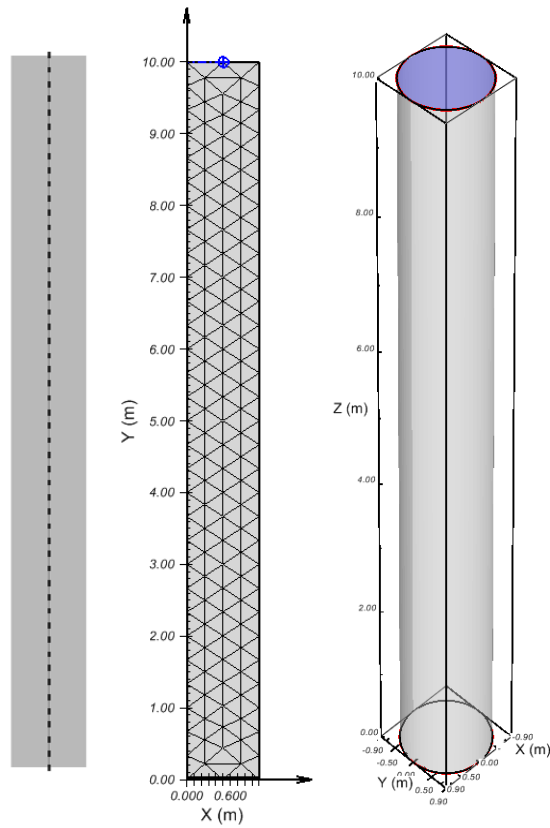


Figure 20 Oil Sands Column 1 Model Geometry in 1D, 2D and 3D. Note: only 25% of nodes are shown for the 1D analysis for the sake of clarity

2.5.1.2 Geometry/Boundary Conditions

The model consists of a circular column, with a height of 10 m (Figure 20). It is assumed that the tailings are initially homogeneous and deposited instantaneously. The deformation boundary conditions consist of a lower boundary that is fixed in place, and an upper boundary that is free to deform. In the multi-dimensional models, the lateral boundaries are fixed in the horizontal, but are free to deform vertically. The flux conditions consist of a constant head of 10 m at the top boundary and a zero flux boundary at the bottom. This forces the water to flow from bottom out through the top boundary, while simulating a constant water table above the soil region.

Table 5: Summary of Oil Sands Column 1 Model Parameters

| Initial Conditions: | |
|---|--|
| Model Run Time: | 10000 Days |
| Maximum Time Increment: | 1 Day |
| Body Load Time: | 0.5 Days |
| Initial Height: | 10 m |
| Initial Void Ratio: | 5.17 |
| Specific Gravity: | 2.28 |
| Initial Water Level: | 10 m |
| Initial Stress Expression (Weibull Function Model): | $sx_0 = uw_0 + (\ln((vr_0 - 5.50)/(-4.97))/(-1.03))^{(1/(-0.67))}$, $sy_0 = sx_0$, $sz_0 = sx_0$ |
| Initial Stress Expression (Power Function Model): | $sx_0 = uw_0 + (vr_0/3.391)^{(1/(-0.308))}$, $sy_0 = sx_0$, $sz_0 = sx_0$ |
| Initial Flux Condition: | Head Expression = 10 m |
| Flux Boundary Conditions: | |
| Bottom Boundary: | Zero Flux |
| Top Boundary: | Head Expression = 10 m |
| Side Boundaries: | Zero Flux |
| Deformation Boundary Conditions: | |
| Bottom Boundary: | Fixed |
| Top Boundary: | Free |
| Side Boundaries: | Fixed Horizontally |
| Material Parameters: | |
| Effective Stress – Void Ratio: | Weibull Function |
| | $e = 5.50 - 4.97 \exp(-1.03\sigma'^{-0.67})$ (kPa) |
| | Power Function |
| Hydraulic Conductivity – Void Ratio: | $e = 1.69(\sigma')^{-0.12}$ (kPa) |
| | $k = 6.51 \times 10^{-6} e^{3.824}$ (m / day) |
| | Poisson's Ratio: |
| Initial Stress Limit: | 0.40 |
| Unit Weight Option: | Based On Initial Void Ratio |

2.5.2 Results

Figure 21 shows a comparison of the interface heights predicted and those found experimentally. It can be seen that SVOOffice was able to nearly duplicate the results predicted, although these results are not consistent with the experimental results. Furthermore, it can be seen that the 1D, 2D and 3D Weibull results are identical. This was expected, as the side boundary conditions of a column test would not impact the degree of consolidation significantly. Also it can be seen that the Power function predicts slightly more consolidation than the Weibull function.

Figure 22, Figure 23, and Figure 24 compare the height profiles of the effective stress, excess pore-water pressure, and void ratio between Jeeravipoolbarn et al (2009) and the results obtained using the power function in 1D. It can be seen that the results are nearly identical. SVOOffice does predict slightly higher effective stress values, yet these values are still very low in comparison to the total stress and pore water pressure.

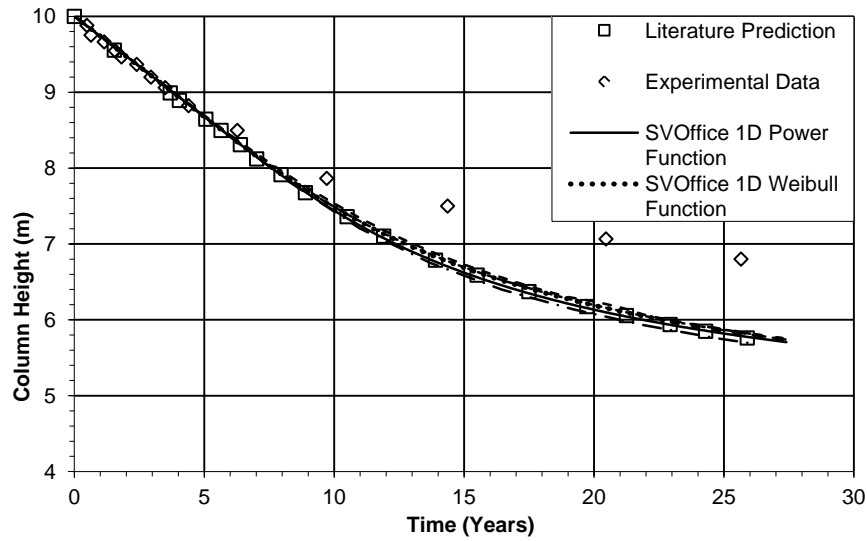


Figure 21 Oil Sands Column 1 Model Comparison

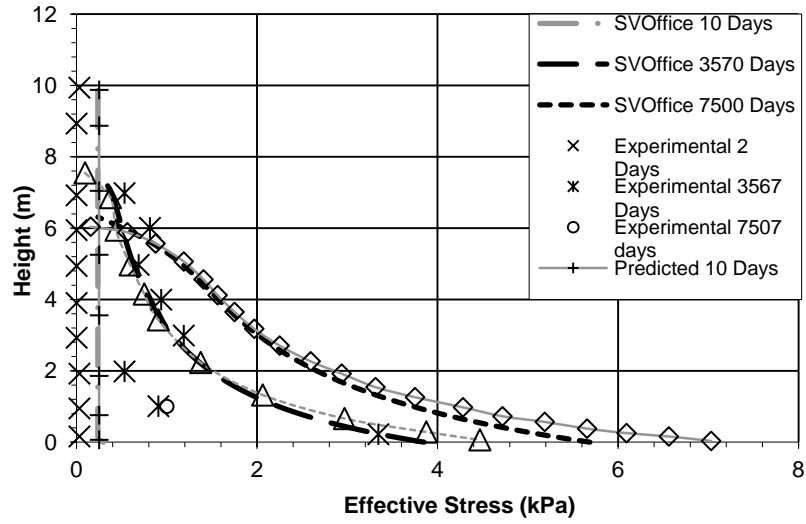


Figure 22: SVOOffice, Experimental and Literature Prediction Effective Stress Profiles at Various Times

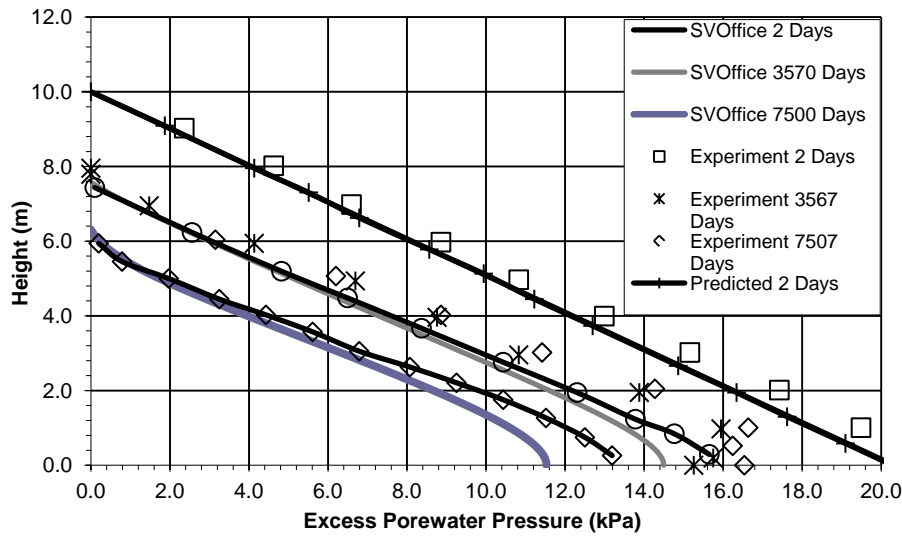


Figure 23: SVOOffice, Experimental and Literature Prediction Excess Porewater Pressure Profiles at Various Time Times

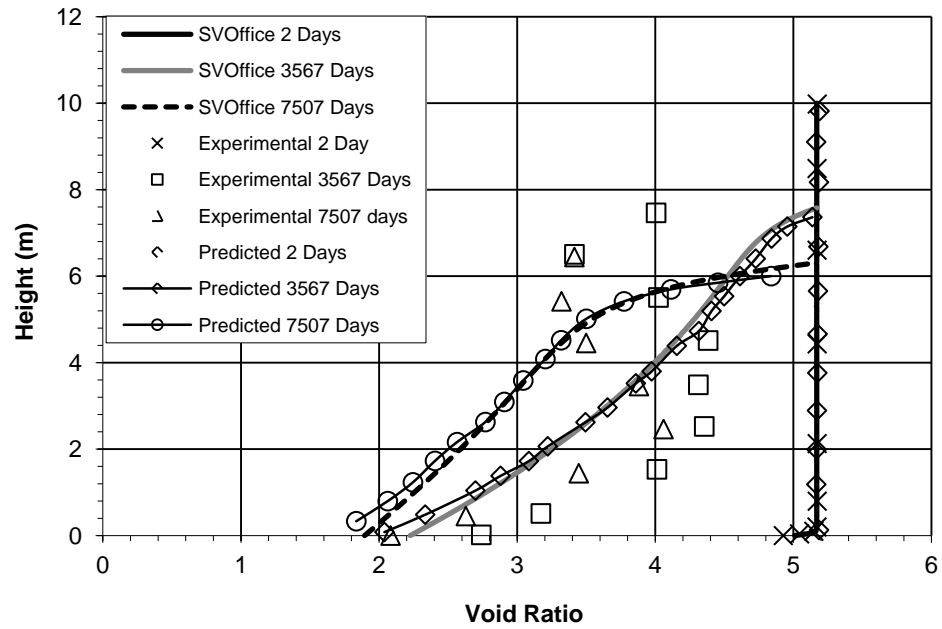


Figure 24: SVOOffice, Experimental and Literature Prediction Void Ratio Profiles at Various Times

2.6 TOWNSEND SCENARIO A

Reference: Townsend and McVay, (1990)

Project: LS_SaturatedConsolidation

Model: Townsend_A_PRp1, Townsend_A_PRp2, Townsend_A_PRp3, Townsend_A_PRp4, Townsend_A_PRp5

Main Factors Considered:

1D Consolidation of a homogeneous column of tailings

Effects of Poisson's Ratio on final settlement, as well as one year profiles of void ratio and excess pore-water pressure

Analysis of a material with a large Initial Void Ratio

2.6.1 Model Description

Townsend's Scenario A is intended to represent waste ponds that have recently received thickened clays. These clays are allowed to consolidate under self-weight conditions. The system remains saturated with flow from the system only through the surface boundary. Since a Poisson's ratio hasn't been defined for this system, a sensitivity analysis of Poisson's Ratio is part of this verification. This is a relatively challenging system to solve, as the initial void ratio is quite high (14.8). This means that large deformations are seen over extremely small effective stress ranges.

2.6.1.1 Material Parameters

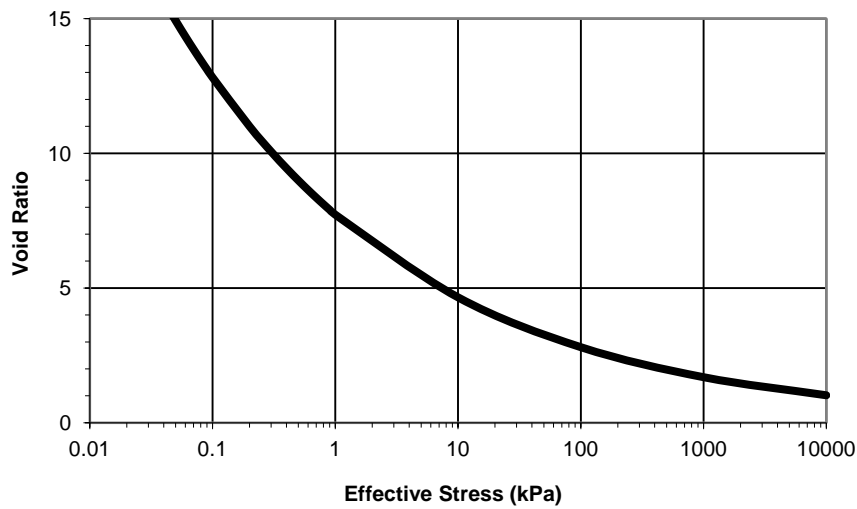


Figure 25 Townsend A Void Ratio Effective Stress Relationship

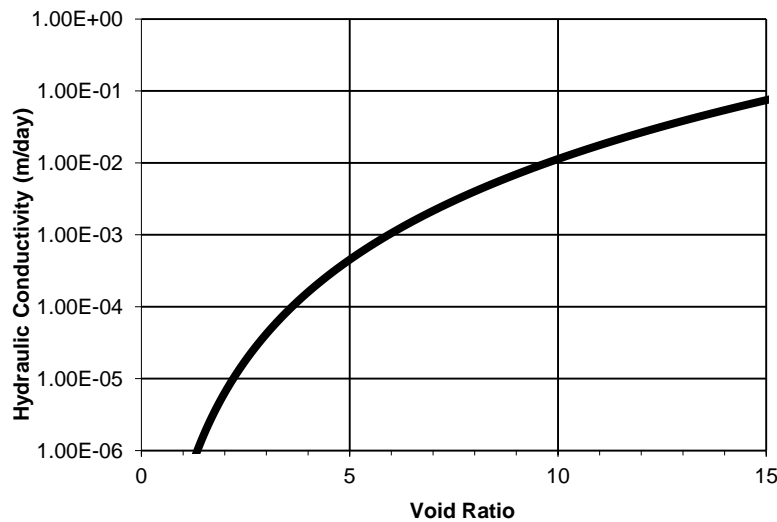


Figure 26 Townsend A Hydraulic Conductivity - Void Ratio Relationship

The tailings slurry consists of a clay mixture commonly found in the phosphate industry. The clay has a specific gravity of 2.82 and an initial void ratio of 14.8 (solids content = 16%). The material parameters are provided using a power equation relating effective stress to void ratio [14] and another relating void ratio to hydraulic conductivity [15]. These formulas are provided below and are graphed above in Figure 25 and Figure 26.

2.6.1.2 Geometry/Boundary Conditions

The model consists of 9.6m of homogeneous tailings placed instantaneously at an initial void ratio (e_o) of 14.8 and allowed to consolidate. The column is allowed to drain freely through the top surface. The bottom boundary has a zero flux boundary condition. Deformation is fixed on the bottom plane. Initial conditions are defined by the water table, which is maintained at 10.6m for the entire trial.

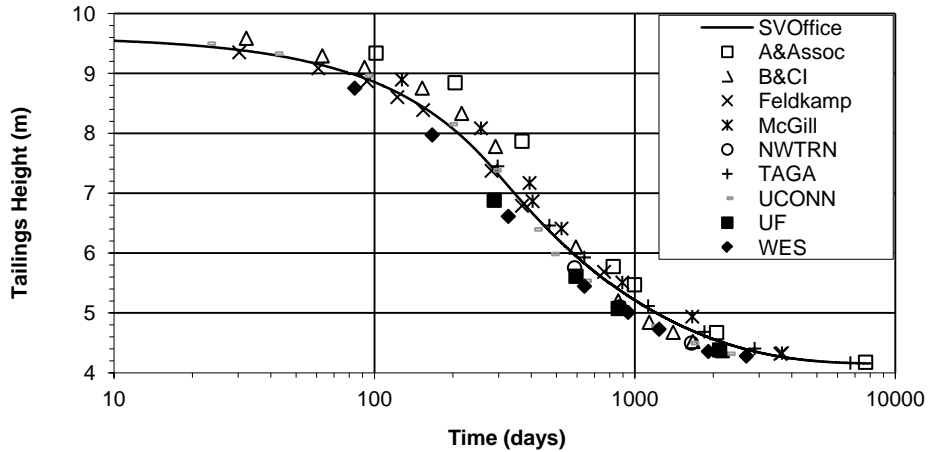
$$e = 7.72(\sigma')^{-0.22} \text{ (kPa)} \quad [13]$$

$$k = 0.2532E - 6 * e^{4.65} \text{ (m / day)} \quad [14]$$

Table 6: Summary of Townsend A Model Parameters

| Initial Conditions: | |
|--------------------------------------|---|
| Model Run Time: | 8000 Days |
| Maximum Time Increment: | 0.5 Days |
| Body Load Time: | 5 Days |
| Initial Height: | 9.6 m |
| Initial Void Ratio: | 14.8 |
| Specific Gravity: | 2.82 |
| Initial Water Level: | 10.6 m |
| Initial Stress Expression: | $sy_0=uw_0+(vr_0/7.72)^{1/(-0.22)}$, $sx_0=sy_0, sz_0=sy_0$ |
| Initial Flux Condition: | Head Expression = 10.6 m |
| Flux Boundary Conditions: | |
| Bottom Boundary: | Zero Flux |
| Top Boundary: | Head Expression = 10.6 m |
| Deformation Boundary Conditions: | |
| Bottom Boundary: | Fixed |
| Top Boundary: | Free |
| Material Parameters: | |
| Effective Stress – Void Ratio: | Power Function |
| | $e = 7.72(\sigma')^{-0.22} (kPa)$ |
| Hydraulic Conductivity – Void Ratio: | $k = 0.2532 \times 10^{-6} e^{4.65} (m / day)$ |
| Poisson's Ratio: | 0.49 |
| Initial Stress Limit: | 0.0519 |
| Unit Weight Option: | Based On Initial Void Ratio |

2.6.2 Results

**Figure 27: Townsend Model A Tailings Height with Time**

It can be seen in Figure 27, Figure 28, and Figure 29 that this model shows an extremely good fit to the literature data provided. The literature predicts an average final tailings height of 13.66 feet (4.16 m). SVOffice predicts a final height of 13.64 feet. Consolidation was 90% complete at 1650 days and 99% complete at 4500 days.

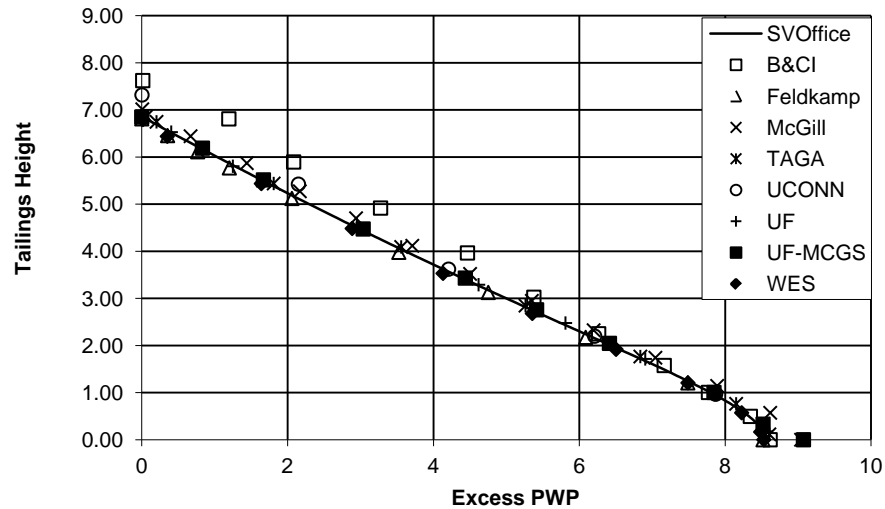


Figure 28: Townsend Model A 1-Year Excess PWP Profile

The one-year values were found to be sensitive to the body load time. A body load time less than or equal to 5 days produced the results shown here. The literature predicted average 1-Year Height, Base Void Ratio and Base Pore-water Pressures of 23.6 feet (7.20 m), 6.58 and 182 psf (8.7 kPa) respectively. SVOOffice produced 1-Year results of 22.6 feet (6.88 m), 6.45 and 178.6 psf (8.55 kPa). As is shown in Figure 28 and Figure 29, there is some variation in the parameters at this early stage of the consolidation process, yet the SVOOffice results match the dominant trends observed.

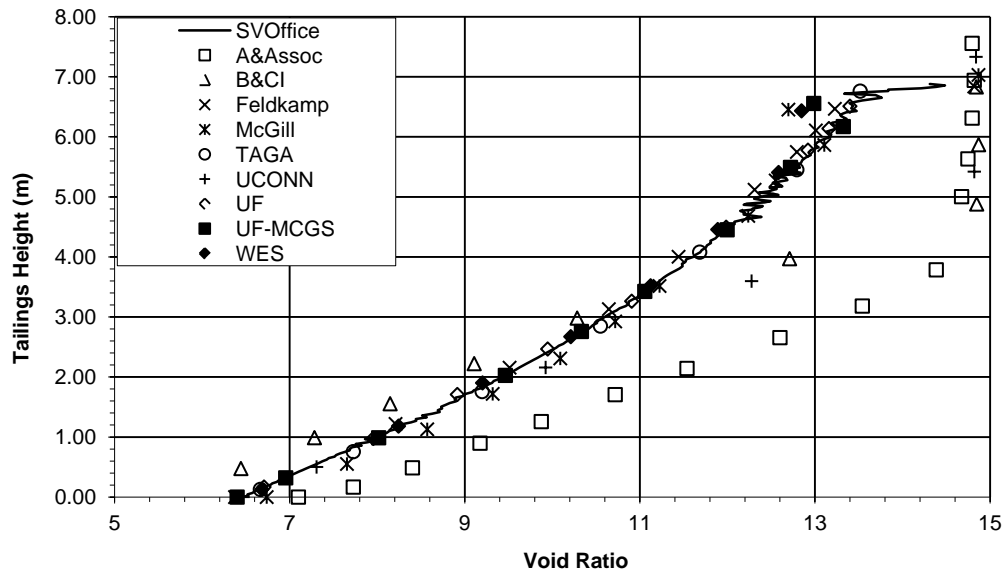


Figure 29 Townsend Model A 1-Year Void Ratio Profile

Figure 30, Figure 31, and Figure 32 show the results of a sensitivity analysis performed on the Poisson's Ratio parameter. It can be seen from Figure 30 that Poisson's ratio does have a significant impact on the final tailings height with variations of up to approximately 1.0 m. Higher Poisson's Ratios lead to larger amounts of final consolidation. Less noticeable, but still significant amounts of variation can be observed in the 1 Year Excess Pore-water Pressure and Void Ratio profiles in Figure 31 and Figure 32. It can be seen that the largest variations occur in the bottom 2 meters of the column. This is likely due to the slightly different degree of consolidation observed, with the higher Poisson's Ratio leading to faster consolidation. The noise that is observed in the void ratio near the surface in Figure 32 is likely due to the large changes in void ratios caused by tiny changes in effective stress. This is most pronounced in the cases where there is a lower Poisson's ratio, where the deposit is less consolidated and thus looser.

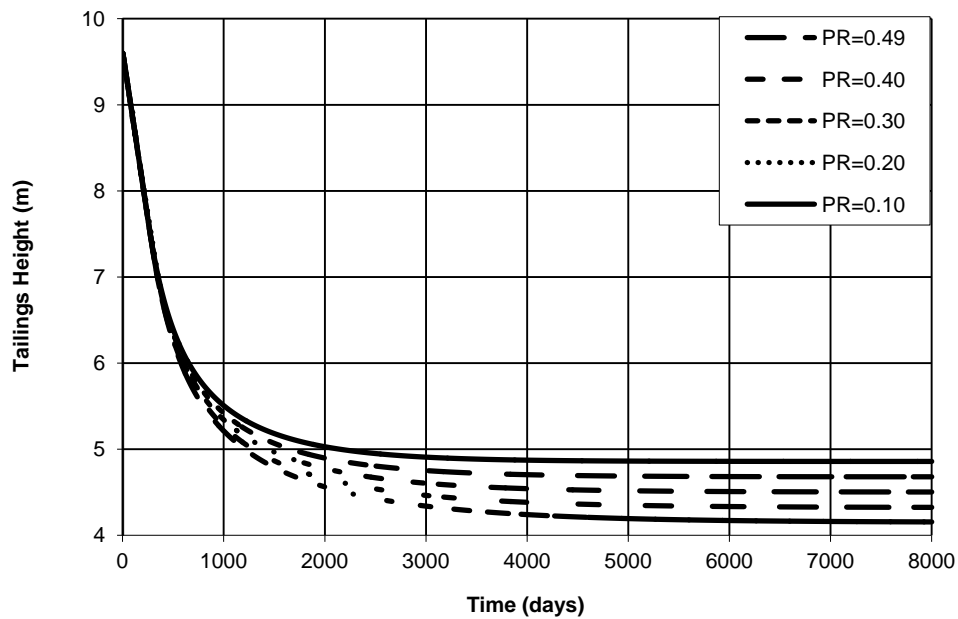


Figure 30 Sensitivity Analysis of Poisson's Ratio on Tailings Height

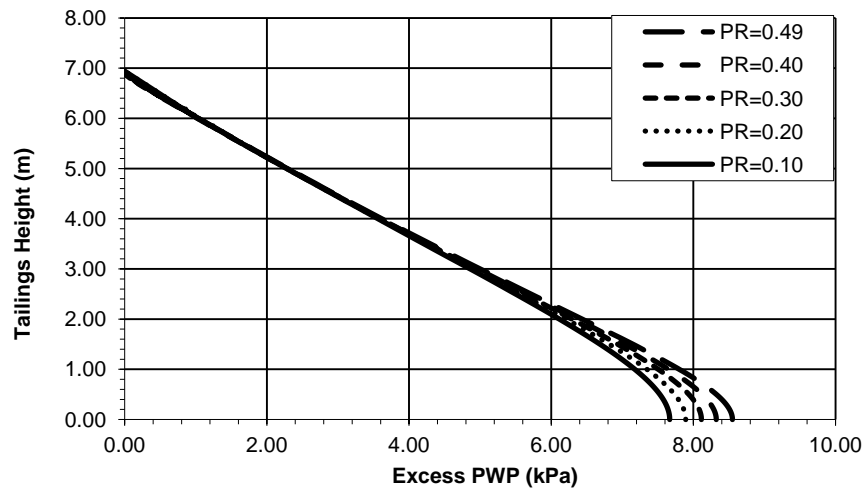


Figure 31 Sensitivity Analysis of Poisson's Ratio on the 1-Year Excess PWP Profile

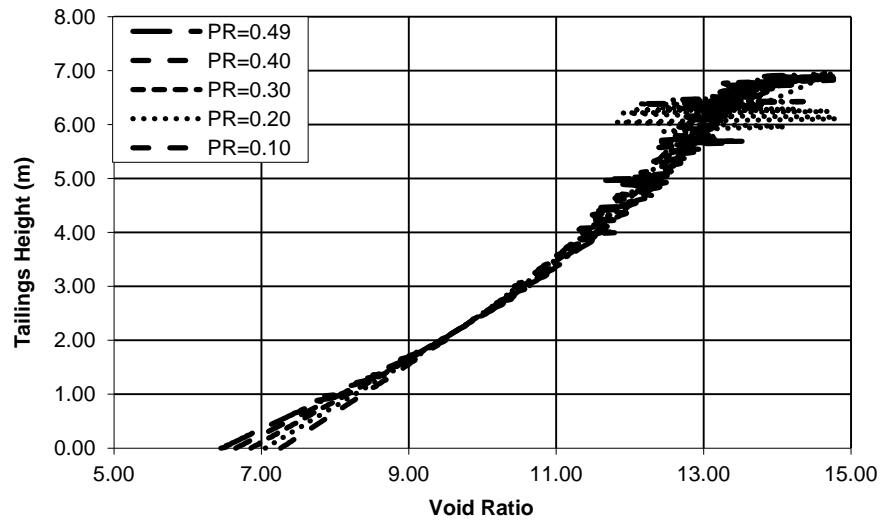


Figure 32 Sensitivity Analysis of Poisson's Ratio on the 1-Year Void Ratio Profile

In order to recreate this benchmark, it was necessary to assume a Poisson's ratio of 0.49. As a Poisson's ratio was not specified in the literature there is no data available on the actual Poisson's ratio of the tailings studied.

2.7 TOWNSEND MODEL B

Taken from Townsend and McVay, 1987

Project: Consolidation Benchmarks
 Model: Townsend_B.svm

Main Factors Considered:

- Comparison of a staged filling scenario against literature results
- Very high initial void ratio examined in the upper layer

Table 7: Summary of Townsend B Model Parameters

| Initial Conditions: | |
|--------------------------------------|---|
| Model Run Time: | 1200 Days |
| Maximum Time Increment: | 0.5 Days |
| Body Load Time: | 2 Days |
| Initial Height: | 0 m |
| Initial Void Ratio: | 14.8, 22.8 |
| Specific Gravity: | 2.82 |
| Initial Water Table Height | 8.2 meters |
| Initial Stress Expression: | $sy_0 = uw_0 + (vr_0/7.72)^{(1/(-0.22))}$, $sx_0 = sy_0, sz_0 = sy_0$ |
| Initial Flux Condition: | Head Expression = 8.2 m |
| Flux Boundary Conditions: | |
| Bottom Boundary: | Zero Flux |
| Top Boundary: | Head Expression = 8.2 m |
| Side Boundaries: | Zero Flux |
| Deformation Boundary Conditions: | |
| Bottom Boundary: | Fixed |
| Top Boundary: | Free |
| Side Boundaries: | Fixed |
| Material Parameters: | |
| Effective Stress – Void Ratio: | Extended Power Function $e = 7.72(\sigma')^{-0.22} (kPa)$ |
| Hydraulic Conductivity – Void Ratio: | $k = 0.2534 \times 10^{-6} e^{4.65} (m/day)$ |
| Poisson's Ratio: | 0.495 |
| Initial Stress Limit: | 0.0519 |
| Unit Weight Option: | Based On Initial Void Ratio |

2.7.1 Model Description

Scenario B predicts the degree of consolidation in a 7.2m pond filled in two 6 month stages (with a 6 month latency period between) and at different initial voids ratios. This simulates mature tailings ponds that have been filled intermittently with thickened slurries.

2.7.1.1 Material Parameters

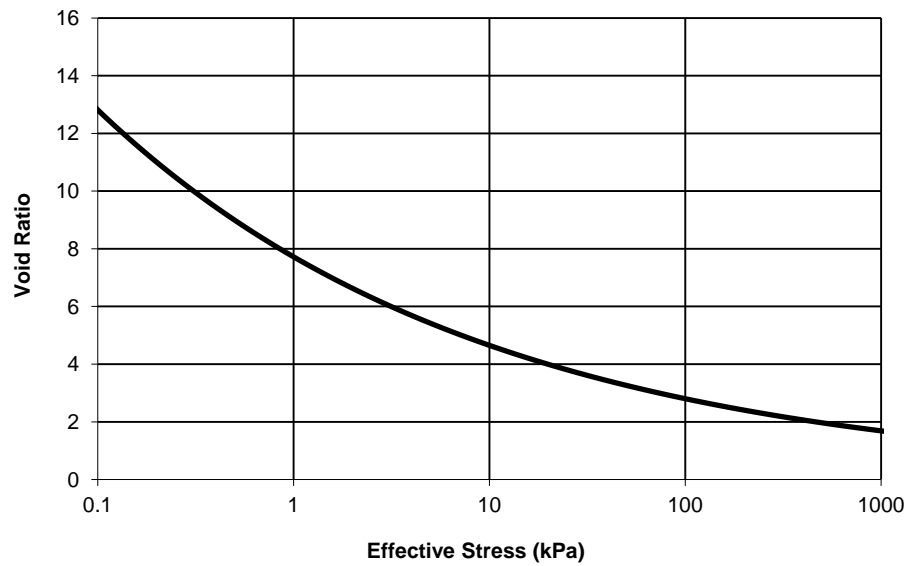


Figure 33: Void Ratio Effective Stress Curve

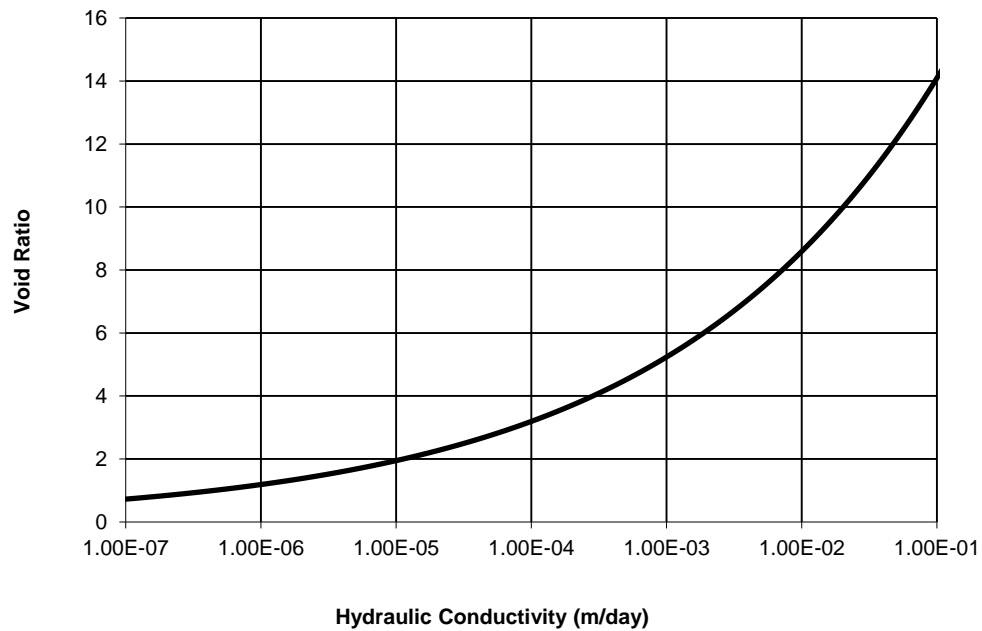


Figure 34: Sand and Clay Conductivity - Void Ratio Relationship

The tailings slurry consists of a clay mixture commonly found in the phosphate industry. The material parameters are provided using a power equation relating effective stress to void ratio and another relating void ratio to hydraulic conductivity. These formulas are provided below for the clay and depicted in Figures 34 and 35 respectively.

$$e = 7.72(\sigma')^{-0.22} \text{ (kPa)} \quad (20)$$

$$k = 0.2532E - 6 * e^{4.65} \text{ (m / day)} \quad (21)$$

2.7.1.2 Geometry and Boundary Conditions

The model consists of two 3.6 m lifts of clay tailings placed over a period of 6 months, with a 6 month latency period between lifts. The initial lift is placed at a uniform void ratio (e_0) of 14.8 and allowed to consolidate for a period of one year. The second lift is placed at an initial void ratio of 22.8. The column is allowed to drain only through the surface requiring a no flow boundary at the bottom of the column. Deformation is completely fixed (x, y and z directions) on the bottom plane and fixed horizontally (x and y directions) along the vertical boundaries. Initial conditions are defined by the water table, which is maintained at 10.6 m for the entire trial. Figure 33 shows a diagram of the model as well as the filling curve.

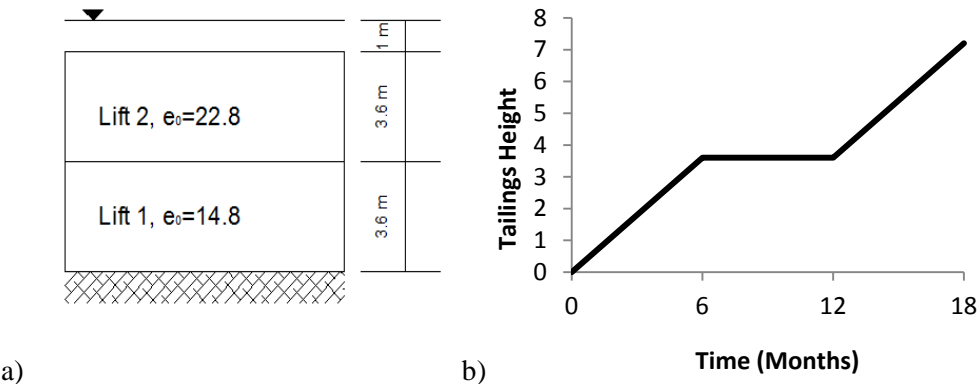


Figure 35 a) Townsend's Scenario B Diagram and b) Filling Curve (after Townsend & McVay, 1990)

2.7.2 Results and Discussions

Figure 36 to 38 compares the results found by Townsend et al. and those obtained in SVOffice. It can be seen that the results are virtually identical, and therefore it can be concluded that SVOffice did duplicate the results found in Townsend et al.

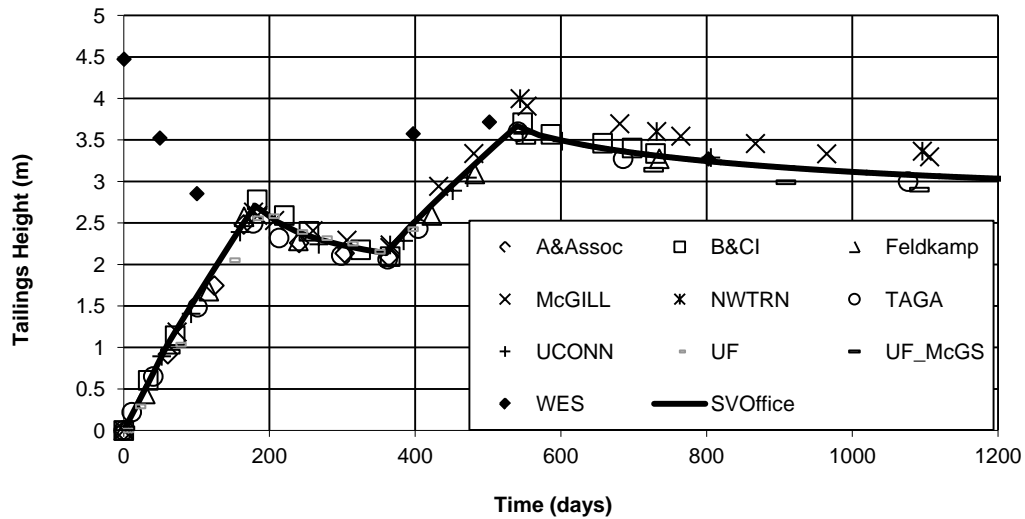


Figure 36: Townsend B Tailings Height with Respect to Time

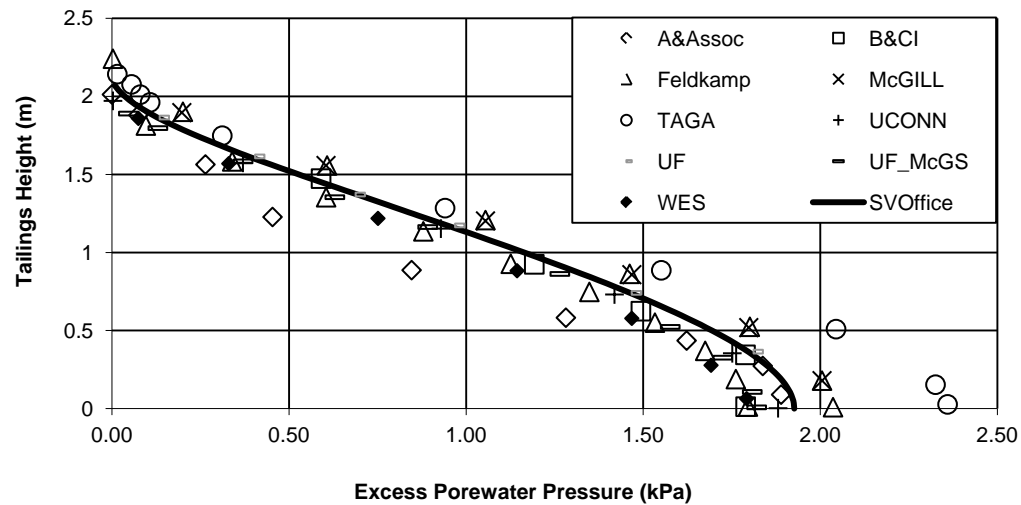


Figure 37: Townsend B One Year Excess Porewater Pressure Profile

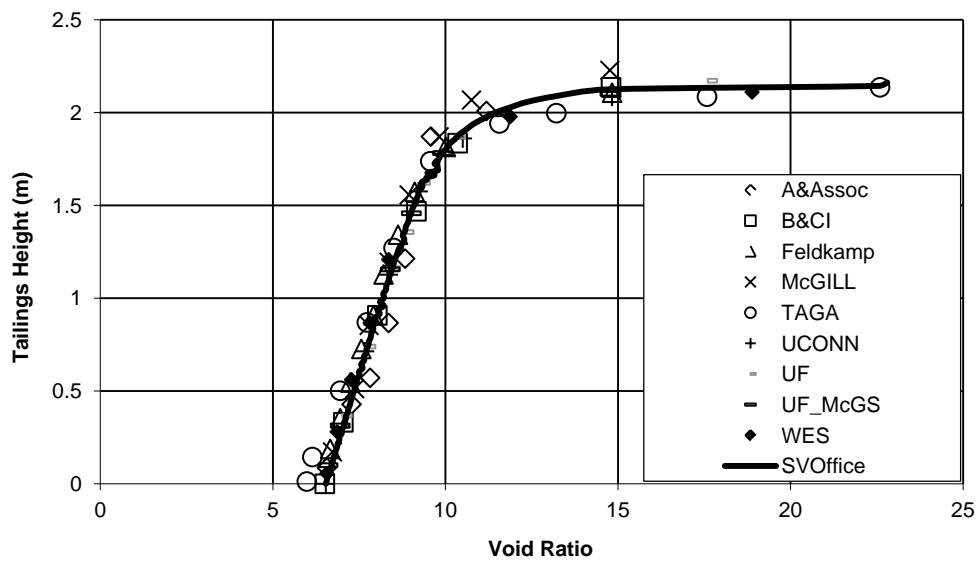


Figure 38: Townsend B One Year Void ratio Profiles

2.8 TOWNSEND SCENARIO C

Reference: Townsend and McVay, (1990)

Project: LS_SaturatedConsolidation
 Model: Townsend_C

Main Factors Considered:

1D Large Strain Consolidation under a fixed load

2.8.1 Model Description

Scenario C predicts consolidation in a homogeneous waste pond with a surcharge load applied at the surface. This simulates young tailings ponds with a sand cap constructed on top of the tailings.

2.8.1.1 Material Parameters

Table 8: Summary of Townsend C Model Parameters

| Initial Conditions: | |
|--------------------------------------|---|
| Model Run Time: | 6000 Days |
| Maximum Time Increment: | 0.5 Days |
| Body Load Time: | 5 Days |
| Initial Height: | 7.2 m |
| Initial Void Ratio: | 14.8 |
| Specific Gravity: | 2.82 |
| Initial Water Level: | 8.2 m |
| Initial Stress Expression: | $sy_0=uw_0+(vr_0/7.72)^{1/(-0.22)}$, $sx_0=sy_0, sz_0=sy_0$ |
| Initial Flux Condition: | Head Expression = 8.2 m |
| Flux Boundary Conditions: | |
| Bottom Boundary: | Zero Flux |
| Top Boundary: | Head Expression = 8.2 m |
| Deformation Boundary Conditions: | |
| Bottom Boundary: | Fixed |
| Top Boundary: | Load = -9.65 kPa |
| Material Parameters: | |
| Effective Stress – Void Ratio: | Power Function $e = 7.72(\sigma')^{-0.22} (kPa)$ |
| Hydraulic Conductivity – Void Ratio: | $k = 0.2534 \times 10^{-6} e^{4.65} (m/day)$ |
| Poisson's Ratio: | 0.495 |
| Initial Stress Limit: | 0.0519 |
| Unit Weight Option: | Based On Initial Void Ratio |

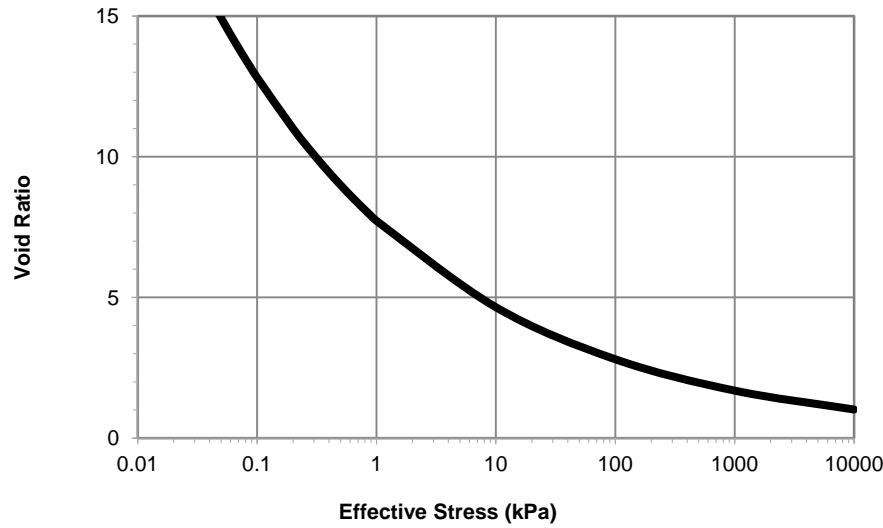


Figure 39 Townsend C Void Ratio Effective Stress Curve

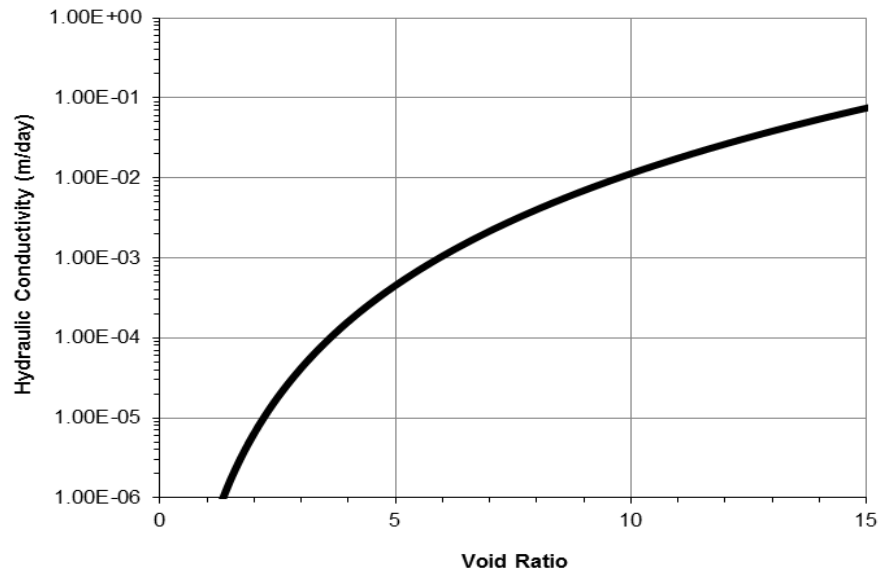


Figure 40 Townsend C Hydraulic Conductivity - Void Ratio Relationship

The tailings slurry consists of a clay mixture commonly found in the phosphate industry. The material parameters are provided using a power equation relating effective stress to void ratio [16] and another relating void ratio to hydraulic conductivity [17]. These formulas are provided below and graphed above in Figure 39 and Figure 40.

The clay has a specific gravity of 2.82 and an initial void ratio of 14.8 (solids content = 16%). A Poisson's ratio isn't specified in the original paper, but a value of 0.495 was chosen based on the results of Townsend A.

$$e = 7.72(\sigma')^{-0.22} \text{ (kPa)} \quad [15]$$

$$k = 0.2532E - 6 * e^{4.65} \text{ (m / day)} \quad [16]$$

2.8.1.2 Geometry/Boundary Conditions

The model consists of a 7.2 m deep layer of clay tailings with a surcharge load of 967.5 kg/m² or 9.675kPa. The initial lift is placed at a uniform void ratio (e_0) of 14.8 and allowed to consolidate for a period of 6000 days. The column is allowed to drain freely, so there is no need for flux boundary conditions. However, deformation is completely fixed (x, y and z directions) on the bottom plane and fixed horizontally (x and y directions) along the vertical boundaries. Initial conditions are defined by the water table, which is maintained at 8.2m for the entire trial.

2.8.2 Results

Figure 41, Figure 42, and Figure 43 show the settlement curve, as well as the 1-year Excess Pore-water pressure and void ratio curves respectively. It was found that the deposit consolidated to a height of 2.5 meters or 35% of the initial height.

Figure 43 shows the void ratio profile with depth after one year of consolidation. It is worth noting that the superficial layers have consolidated more than the underlying layers, due to the applied load, creating a low permeability crust layer near the surface. This is an important aspect of consolidation analyses because the crust will impede flow from the system, meaning that the system will take longer to consolidate.

It should be noted that the information included on Figure 41, Figure 42, and Figure 43 is taken from the results of the Symposium on Consolidation and Disposal of Phosphatic and Other Waste Clays (<http://www1.fipr.state.fl.us/fipr/fipr1.nsf/129fc2ac92d337ca85256c5b00481502/767e8ed1f541e51c85256b2e00771cea!OpenDocument>). This is due to the incorrect data presented by Townsend and McVay (1990) in their graphs (Figures 8, 9 and 10 of Townsend & McVay, 1990) showing less consolidation (final height of 55% of initial height) than what is discussed within the summary table (Table 5 of Townsend & McVay, 1990) and body of the literature (final height of 35% of initial height).

The data Townsend and McVay presented in the symposium results, as well as discussed in the text of the 1990 paper matched up extremely well with the values that were retrieved from SVOFFICE. A comparison of these values is presented in Table 8.

Table 9: Summary of Confirmatory Parameters for Townsend C

| | Final Height (m) | 1 Year Height (m) | 1 Year Void Ratio at Column Bottom | 1 Year Excess Pore-water Pressure at Bottom (kPa) |
|-----------------|------------------|-------------------|------------------------------------|---|
| Townsend et al. | 2.5 | 4.75 | 6.44 | 15.5 |
| SVOFFICE | 2.47 | 4.69 | 6.46 | 15.5 |

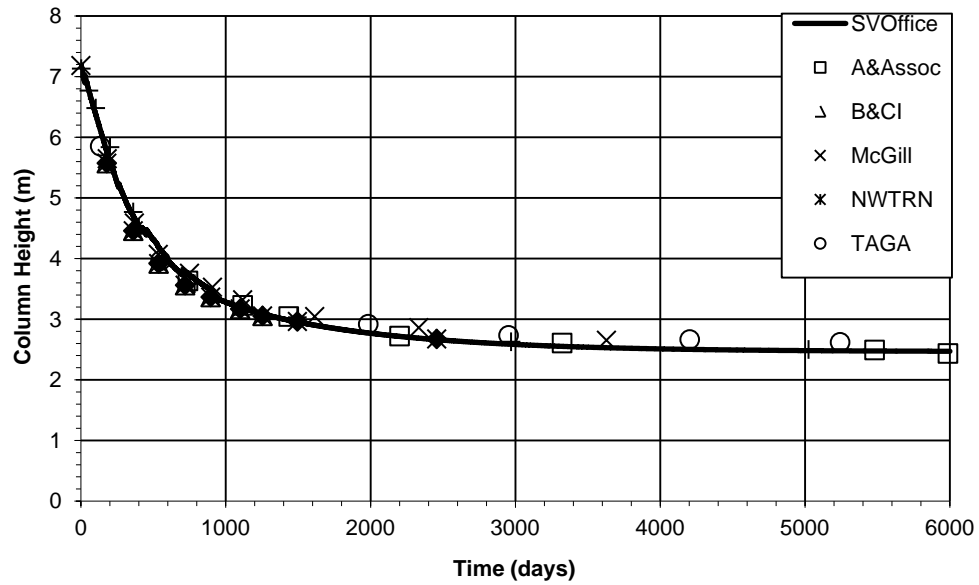


Figure 41 Townsend C Settlement of Tailings over Time

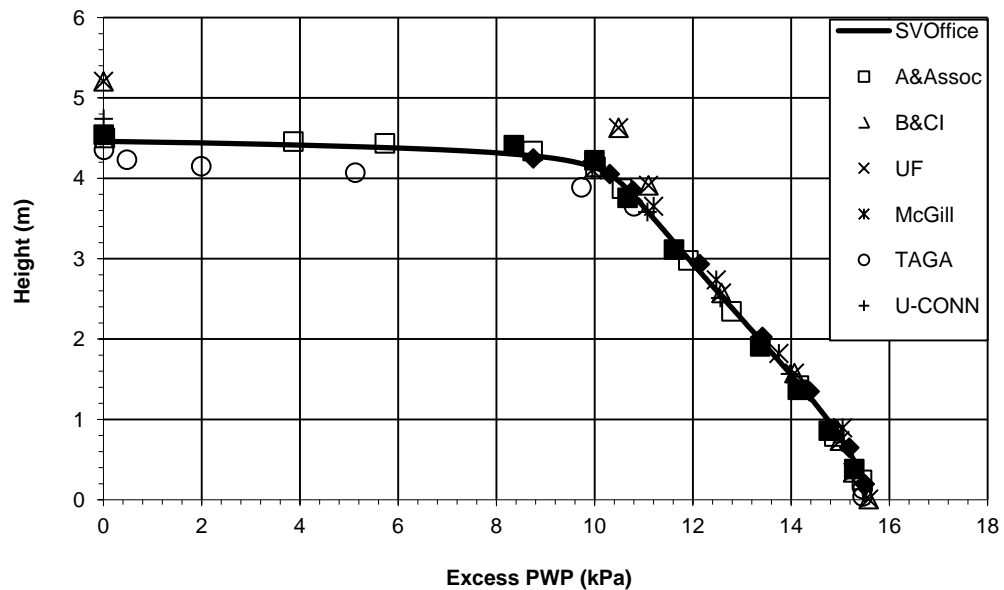


Figure 42: Townsend C 1-Year Excess Pore-water Pressure Profile

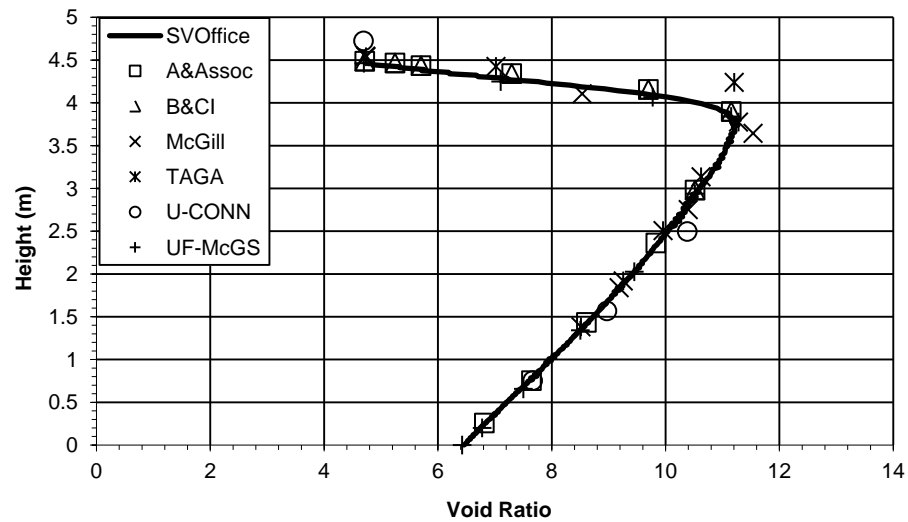


Figure 43 Townsend C 1-Year Void Ratio Profile

2.9 TOWNSEND SCENARIO D

Reference: Townsend and McVay, (1990)

Project: LS_SaturatedConsolidation
 Model: Townsend_D

Main Factors Considered:

1D Consolidation
 Effect of the addition of a capping system
 Multi-material systems
 Heterogeneous initial void ratio profiles

2.9.1 Model Description

Scenario D predicts consolidation in a stable waste pond with an initial void ratio profile varying with depth and a surcharge load applied by a sandy-clay cap. This simulates mature tailings ponds that have been filled intermittently with thickened slurries and reclaimed using a capping system.

Townsend and McVay state that the models used for their study were not able to solve this problem without further assumptions. This is due to coding and computational limits in place at the time. The relevant assumptions as stated by Townsend and McVay are as follows:

- B&CI recalculated the geometry and initial solids content so that only a single material was used. It was assumed that the sand clay cap did not consolidate significantly
- Piecewise functions are used which solve for the consolidation of the sand/clay cap separately (NWTRN and McGill)
- Permeability and pressure gradients at the interface between the two materials are not considered (NWTRN and McGill)
- TAGA assumed that the permeabilities were inversely proportional to their porosities at the same effective stress.

To create a similar model, the system was modeled in SVOOffice with the sand/clay cap in place, however, instead of applying a mass to it, a surcharge load of equal weight was applied to the top surface.

2.9.1.1 Material Parameters

The tailings slurry consists of a clay mixture commonly found in the phosphate industry. The material parameters are provided using a power equation relating effective stress to void ratio and another relating void ratio to hydraulic conductivity. These formulas are provided below for the clay [18],[19] and the Sand Cap [20], [21]. The void ratio distribution within the deposit is shown in Figure 35. The sand/clay cap has a specific gravity of 2.82 and an initial void ratio of 2.1 (solids content = 16%). A Poisson's ratio isn't specified in the original paper, but a value of 0.495 was chosen based on Townsend A.

$$e = 7.72(\sigma')^{-0.22} \text{ (kPa)} \quad [17]$$

$$k = 0.2532E - 6 * e^{4.65} \text{ (m/day)} \quad [18]$$

$$e = 15.67(\sigma')^{-0.24} \text{ (kPa)} \quad [19]$$

$$k = 0.1291E - 6 * e^{4.15} \text{ (m/day)} \quad [20]$$

2.9.1.2 Geometry/Boundary Conditions

The model consists of four 1.8 m lifts of clay tailings covered with a 1.2 m 6:1 sandy clay cap. The bottom lift is placed at a uniform void ratio (e_0) of 6.3, while subsequent 1.8 m lifts with void ratios of 7.0, 10.6 and 14.8 were added. The column is allowed to drain freely from the surface. Deformation is completely fixed at the base, while a surcharge equivalent to that of the sand/clay cap (4195 kPa) is applied to the surface. Initial conditions are defined by the water table, which is maintained at 9.4m for the entire trial. Figure 44 shows a diagram depicting the model.

Table 10: Summary of Townsend D Model Parameters

| Initial Conditions: | |
|---|---|
| Model Run Time: | 8000 Days |
| Maximum Time Increment: | 0.5 Days |
| Body Load Time: | 5 Days |
| Initial Height: | 8.4 m |
| Initial Void Ratio: | Varies |
| Specific Gravity: | 2.82 |
| Initial Water Level: | 9.4 m |
| Initial Stress Expression: | $sy0 = \text{if } y > 7.2 \text{ then } uw0 + (vr0/15.67)^{(1/(-0.24))}$ $\text{else } uw0 + (vr0/7.72)^{(1/(-0.22))}, sx0=sy0, sz0=sy0$ |
| Initial Flux Condition: | Head Expression = 9.4 m |
| Flux Boundary Conditions: | |
| Bottom Boundary: | Zero Flux |
| Top Boundary: | Head Expression = 9.4 m |
| Deformation Boundary Conditions: | |
| Bottom Boundary: | Fixed |
| Top Boundary: | Free |
| Material Parameters: | |
| Clay Effective Stress – Void Ratio: | Power Function $e = 7.72(\sigma')^{-0.22} (kPa)$ |
| Clay Hydraulic Conductivity – Void Ratio: | $k = 0.2534 \times 10^{-6} e^{4.65} (m/day)$ |
| Sand Effective Stress – Void Ratio: | Power Function $e = 15.67(\sigma')^{-0.24} (kPa)$ |
| Sand Hydraulic Conductivity – Void Ratio: | $k = 0.1291E - 6 * e^{4.15} (m/day)$ |
| Poisson's Ratio: | 0.495 |
| Initial Stress Limit: | 0.0519 |
| Unit Weight Option: | Based On Initial Void Ratio |

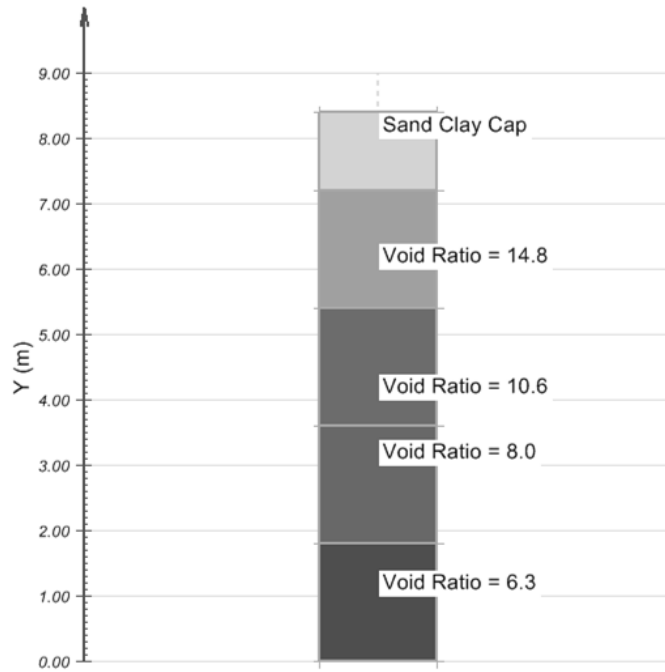


Figure 44 Townsend's Scenario D (Townsend & McVay, 1990)

2.9.2 Results

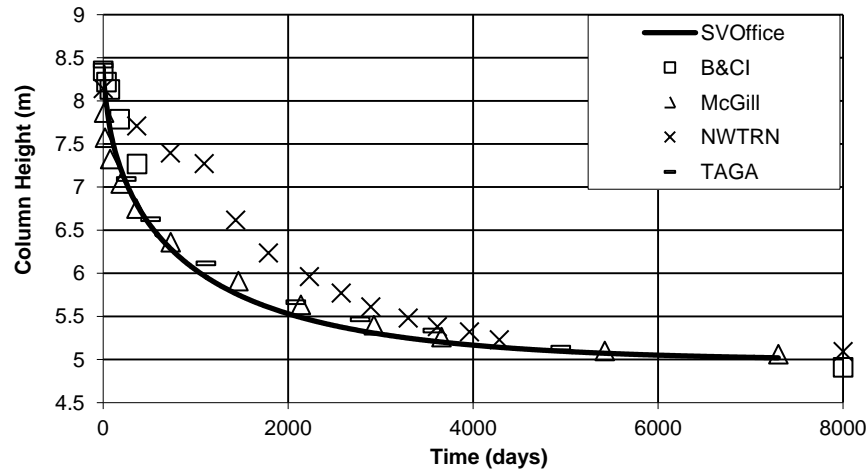


Figure 45 Townsend D Column Settlement over Time

Figure 45 shows that SVOOffice predicts approximately the same amount of settlement as the other estimates. Also seen is the fact that the rate of consolidation is slightly faster than the literature values (with the exception of the NWTRN model). The one year excess porewater pressure and void ratio profiles are provided below in Figure 46 and Figure 47. It can be seen that the one year data from SVOOffice is similar to the literature values. The void

ratio profile in Figure 47 shows the formation of a crust, similar to that seen in the Townsend C scenario. This develops due to the application of the external load.

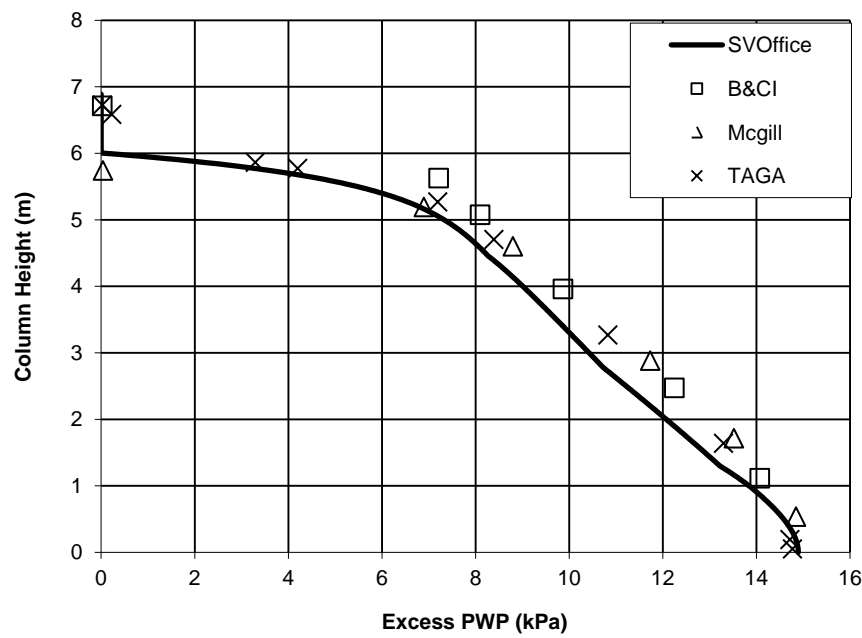


Figure 46 Townsend D 1-Year Excess PWP Profile

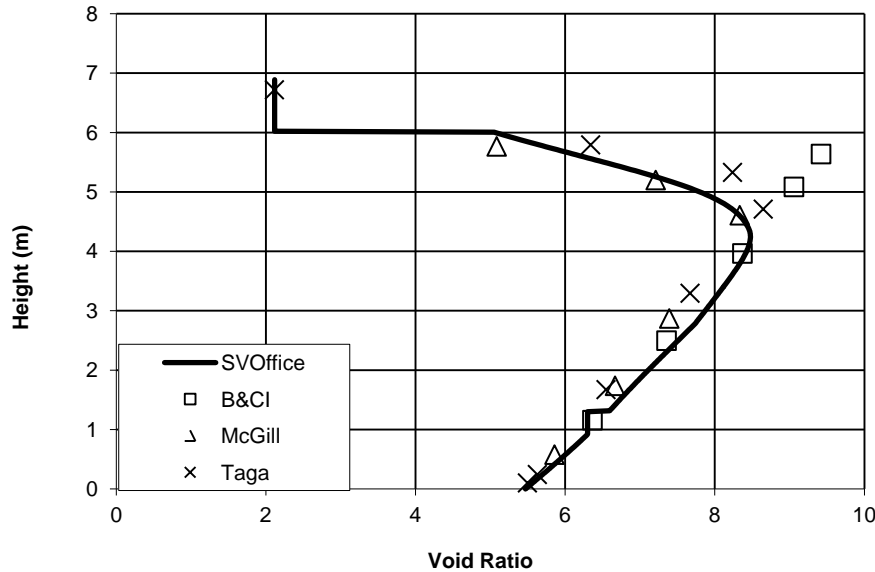


Figure 47 Townsend D 1-Year Void Ratio Profile

2.10 CALDWELL CASE 1 STAGED FILLING ANALYSIS OF SULFIDE TAILINGS

Taken from Caldwell et al, 1984

Project: Caldwell Case 1

Model: Caldwell_1S.svm

Main Factors Considered:

Coupled Deformation/Flux Analysis

Staged Filling Analysis in 1-D

Application of SVOFFICE to tailings impoundment undergoing long term filling

Comparison to Literature Results

Table 11: Summary of Caldwell Case 1 Model Parameters

| Initial Conditions: | |
|--------------------------------------|---|
| Model Run Time: | 20 Years |
| Maximum Time Increment: | 0.01 Years |
| Body Load Time: | 0.1 Years |
| Initial Height: | 0 m |
| Initial Void Ratio: | 1.20 |
| Specific Gravity: | 2.72 |
| Initial Water Level: | 47.15 m |
| Initial Stress Expression: | $sy0=uw0+(vr0/1.29)^{1/(-0.0771)}$, $sx0=sy0$, $sz0=sy0$ |
| Initial Flux Condition: | Head Expression = 47.15 m |
| Flux Boundary Conditions: | |
| Bottom Boundary: | Zero Flux |
| Top Boundary: | Head Expression = 47.15 m |
| Side Boundaries: | Zero Flux |
| Deformation Boundary Conditions: | |
| Bottom Boundary: | Fixed |
| Top Boundary: | Free |
| Side Boundaries: | Fixed |
| Material Parameters: | |
| Effective Stress – Void Ratio: | Power Function |
| | $e = 1.29(\sigma')^{-0.771} (kPa)$ |
| Hydraulic Conductivity – Void Ratio: | $k = 1.6572e^{6.7026} (m/day)$ |
| Poisson's Ratio: | 0.30 |
| Initial Stress Limit: | 9.43 kPa |
| Unit Weight Option: | Based On Initial Void Ratio |

2.10.1 Model Description

The purpose of this model is to demonstrate the ability to create realistic models whereby tailings impoundments are filled gradually over long periods of time. This is a more realistic simulation as opposed to instantaneous filling. SVOFFICE uses a phased approach whereby regions are added on a regular basis. This means that filling occurs in a number of steps. In the professional version of SVOFFICE there is no limit to the number of steps and therefore, the filling sequence can be as detailed as is required. An annual increase, applied mid-year, is generally considered an acceptable practice for long term impoundments.

2.10.1.1 Geometry and Boundary Conditions

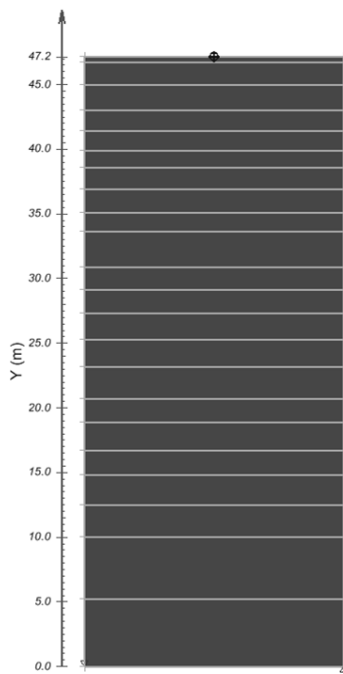


Figure 48: Pile Consolidation Geometry

The model consists of a 47.15 m column of sulfide tailings. The column is filled in irregular increments based upon the filling chart provided in Caldwell et al, 1984. The model geometry is shown in Figure 48. Each individual region is a layer that is phased in at a certain point in time. Regions were phased in at the midway point between the time when the column reached the maximum height within the region and the end time of the previous phase. This might lead to slight variations from the original filling scheme, but the overall trend should be accurate. Furthermore, consolidation processes should be more accurate than if height increases were applied at the very beginning or end of each phase.

Deformation is entirely fixed along the bottom boundary. No deformation boundary conditions are applied to the top surface. The flux boundaries are set to zero along the bottom, while the water level on top of the pool is held constant at 47.15 m throughout filling. While Caldwell et al. states that the tailings were deposited under water, testing has shown that there are only minimal differences in pond height between a saturated column where the water table is kept constant with the surface and a case where a constant water level above the interface is maintained.

2.10.1.2 Material Parameters

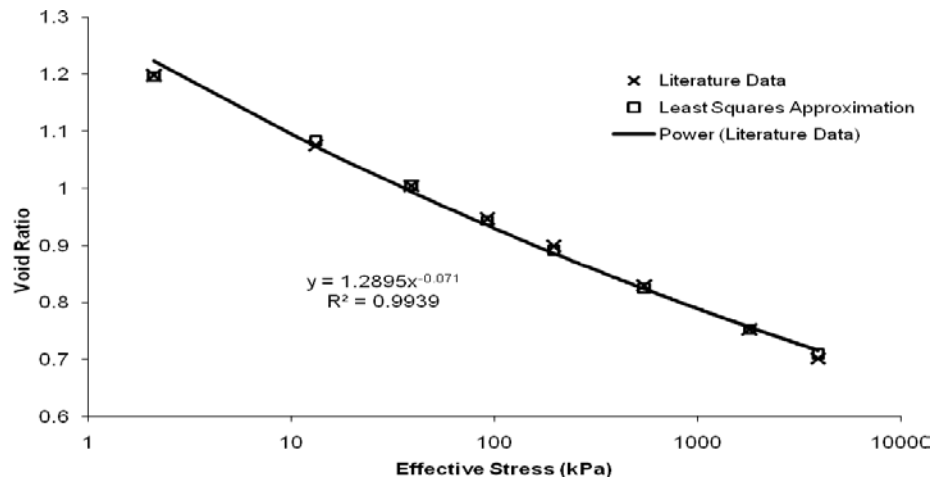


Figure 49: Trend-line of Caldwell et al.'s Effective Stress Curve

Caldwell et al. provided the effective stress – void ratio – hydraulic conductivity relations used in their calculations. Equations were fit to these results and are provided below (Refer to Figure 49 and Figure 50). The tailings were found to have a specific gravity of 4.2 and an initial void ratio of 1.2.

$$e = 1.29(\sigma')^{-0.771} \text{ (kPa)} \quad (30)$$

$$k = 1.6572e^{6.7026} \text{ (m/day)} \quad (31)$$

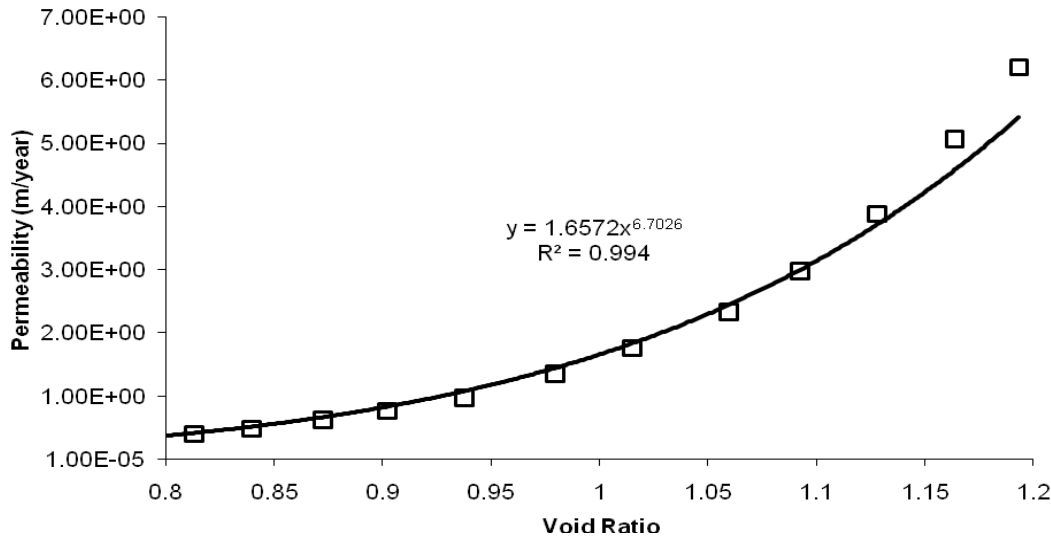


Figure 50: Trend-line of Caldwell et al.'s Void Ratio Permeability Curve

Poisson's ratio was not provided in the report. Therefore, a sensitivity analysis was performed to determine the effect of varying Poisson's ratio on the final interface height (Refer to Figure 51). It was found that Poisson's ratio

did have a large impact on the final interface height, but that an average value of 0.30 provided the literature value. This value appears reasonable and was therefore adopted. The same value was used for Caldwell et al Case Study 2, as the Poisson ratio assumption is thought to be a matter of calculation technique rather than one of soil parameters.

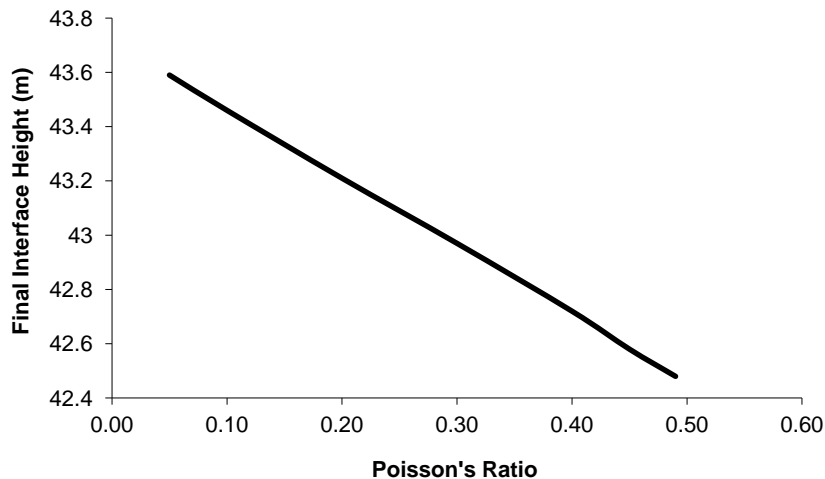


Figure 51: Effect of Poisson's Ratio on Final Interface Height

2.10.2 Results and Discussions

It can be seen from Figure 52 that the SVOFFICE results are extremely close to the results obtained from Caldwell et al. The largest variations occur early in the trial, with the SVOFFICE results showing slightly less consolidation than those recorded in the literature.

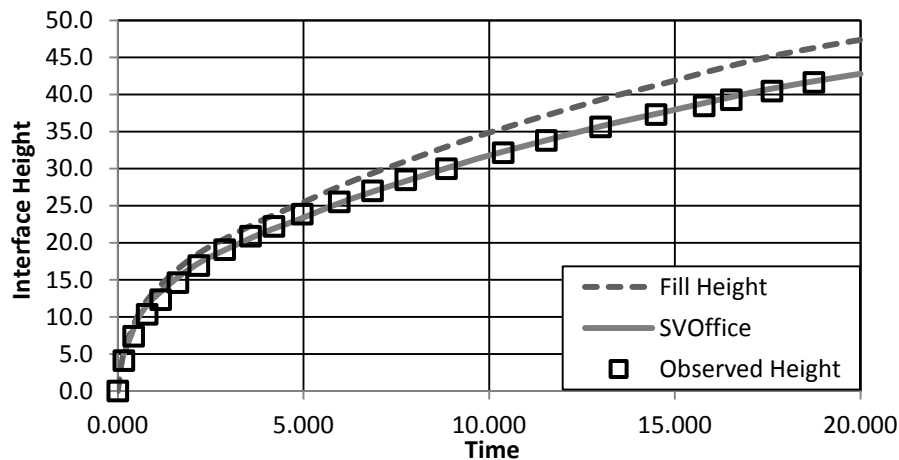


Figure 52: Predicted Heights and Filling Curve

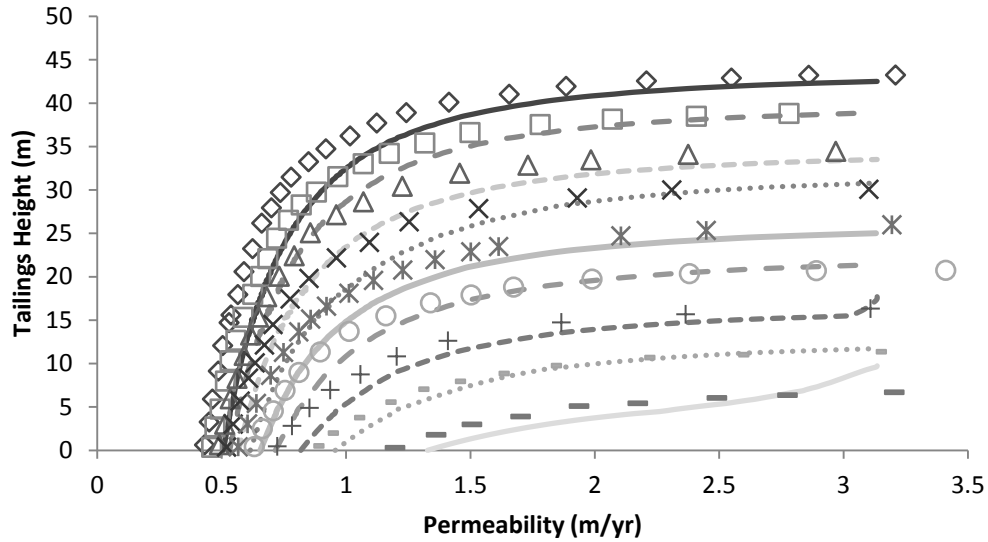


Figure 53: Permeability Curves at Various Tailings Heights*

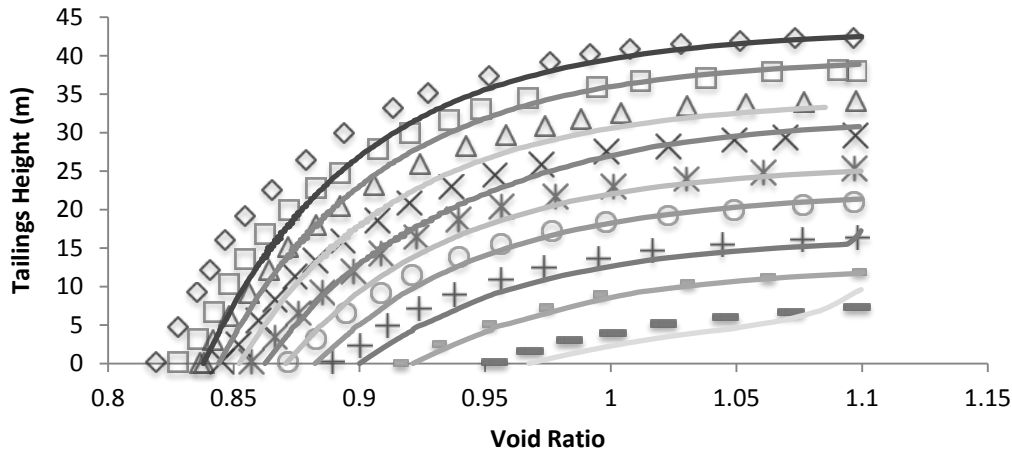


Figure 54: Void Ratio Curves at Various Tailings Heights (Literature values are plotted as points while SVOffice values are plotted as lines. The time of the profile can be found by looking at the largest tailings height of a curve and interpolating the time from Figure 53)

Figures 53 and 54 show the void ratio and permeability profiles of the tailings at various times. It can be seen that there are some variations in the profiles, but that the values are generally in line with the values expected. The variations are likely caused by the staged nature of the SVOffice profile. It is likely that more correct results would be obtained if more stages were added to the analysis.

2.11 CALDWELL CASE 2 - STAGED FILLING ANALYSIS

Taken from Caldwell et al, 1984

Project: Consolidation Benchmarks
 Model: Caldwell_2.svm

Main Factors Considered:
 Coupled Deformation/Flux Analysis
 Staged Filling Analysis in 1-D
 Application of SVOOffice to tailings impoundment undergoing long term filling
 Comparison to Literature Results
 Use of Imperial Units

Table 12: Summary of Caldwell Case 1 Model Parameters

| Initial Conditions: | |
|--------------------------------------|--|
| Model Run Time: | 27 Years |
| Maximum Time Increment: | 0.01 Years |
| Body Load Time: | 0.1 |
| Initial Height: | 0 m |
| Initial Void Ratio: | 2.4 |
| Specific Gravity: | 2.83 |
| Initial Water Level: | 119.3 ft |
| Initial Stress Expression: | $sy0=uw0 + (vr0/3.069)^{(1/(-0.098))}$, $sx0=sy0, sz0=sy0$ |
| Initial Flux Condition: | Head Expression = 119.3 ft |
| Flux Boundary Conditions: | |
| Bottom Boundary: | Zero Flux |
| Top Boundary: | Head Expression = 119.3 ft |
| Side Boundaries: | Zero Flux |
| Deformation Boundary Conditions: | |
| Bottom Boundary: | Fixed |
| Top Boundary: | Free |
| Side Boundaries: | Fixed |
| Material Parameters: | |
| Effective Stress – Void Ratio: | Power Function $e = 3.0692(\sigma')^{-0.098} (kPa)$ |
| Hydraulic Conductivity – Void Ratio: | $k = 4.4369e^{-4.513} (m/day)$ |
| Poisson's Ratio: | 0.30 |
| Initial Stress Limit: | 12.39 psf |
| Unit Weight Option: | Based On Initial Void Ratio |

2.11.1 Model Description

This model is very similar to the one created in Caldwell et al. Case Study 1 Sulfides. It was performed to verify the validity of the assumption of a Poisson's ratio of 0.3 and to further test the staged filling feature of SVOOffice.

2.11.1.1 Geometry and Boundary Conditions

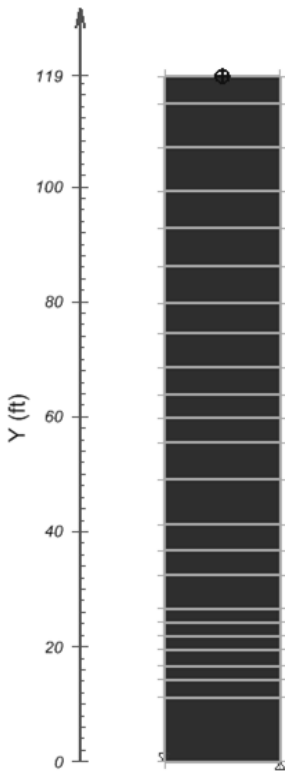


Figure 55: Pile Consolidation Geometry

The model consists of a 119 ft column of sulfide tailings. The column is filled in irregular increments based upon the filling chart provided in Caldwell et al, 1984. The model geometry is shown in Figure 55. Each individual region is a layer that is phased in at a certain point in time according to the filling curve provided in Figure 58.

Deformation is entirely fixed along the bottom boundary. No deformation boundary conditions are applied to the top surface. The flux boundaries are set to zero along the bottom, while the water level on top of the pool is held constant at 119 ft throughout filling. While Caldwell et al. states that the tailings were deposited under water, testing has shown that there are only minimal differences in pond height between a saturated column where the water table is kept constant with the surface and a case where a constant water level above the interface is maintained.

2.11.1.2 Material Parameters

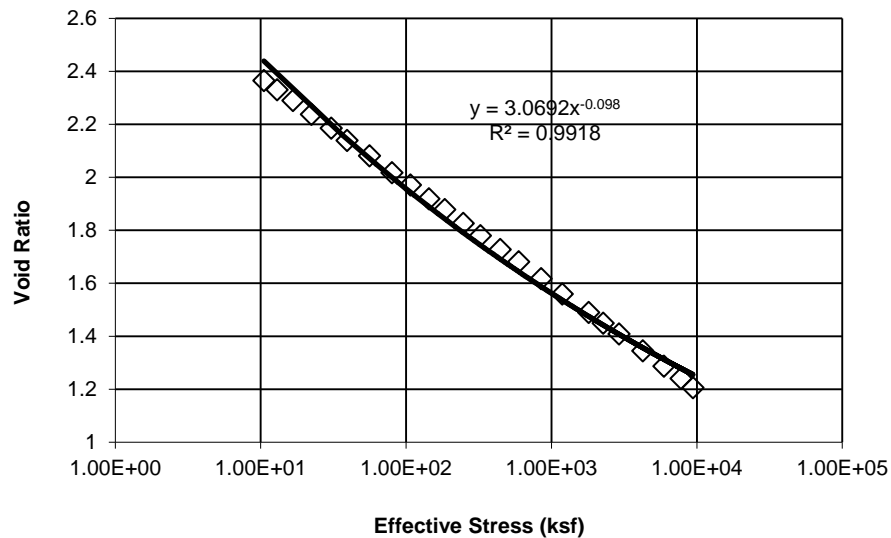


Figure 56: Trend-line Fitted to Caldwell et al. Effective Stress Curve

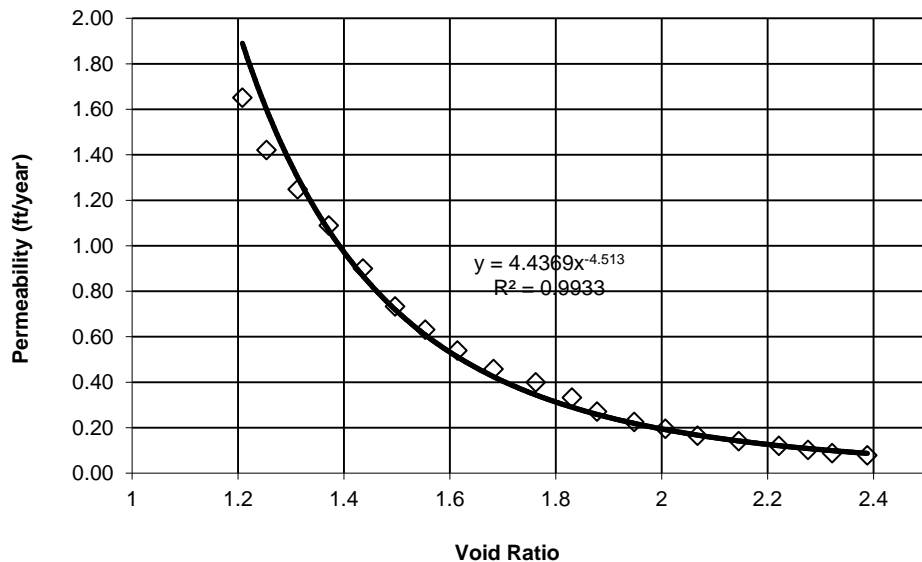


Figure 57: Trend-line Fitted to Caldwell et al. Permeability Curve

Caldwell et al. provided the effective stress – void ratio – hydraulic conductivity relations used in their calculations. Equations were fit to these results and are provided above in Figures 56 and 57. The tailings were found to have a specific gravity of 2.83 and an initial void ratio of 2.4.

$$e = 3.0692(\sigma')^{-0.098} \text{ (kPa)} \quad (32)$$

$$k = 4.4369e^{-4.513} \text{ (m/day)} \quad (33)$$

Poisson's ratio was not provided in the report. Based upon the results from Caldwell Case Study 1 Sulfides, a value of 0.30 was chosen.

2.11.2 Results and Discussions

It can be seen from Figure 58 that the SVOOffice results are extremely close to the results obtained in Caldwell et al. The largest variations occur early in the trial, with the SVOOffice results showing slightly less consolidation than those recorded in the literature.

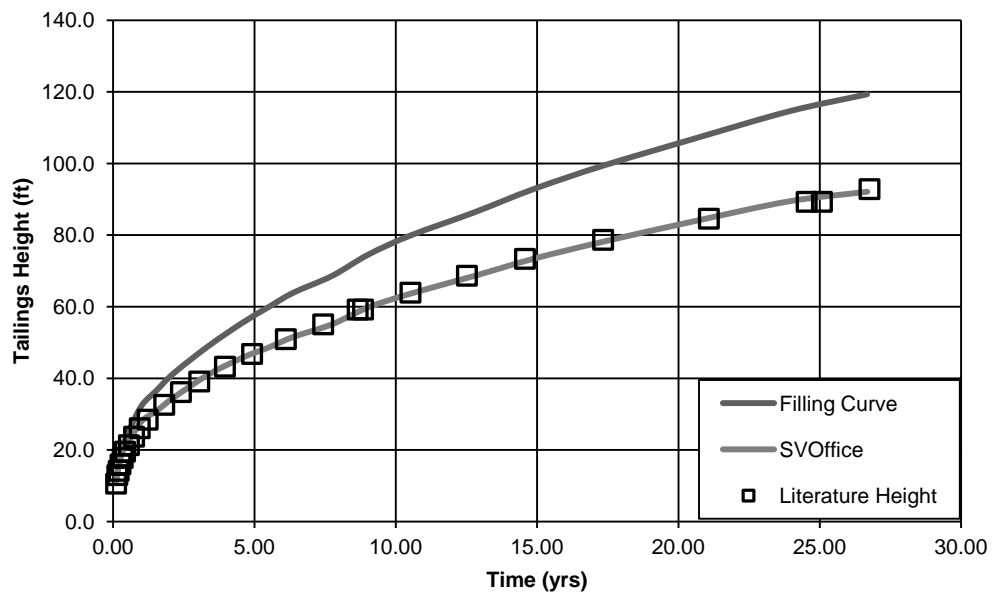


Figure 58: Predicted Heights and Filling Curve

3 REFERENCES

Bartholomeeuseen, G., Sills, G.C., Znidarcic, D., Van Kesteren, W., Merckelbach, L.M., Pyke, R., et al. (2002). Sidere: numerical prediction of large-strain consolidation. *Geotechnique* 52, No. 9, 639-648.

Jeeravipoolvarn, S. 2010. Geotechnical Behavior of In-Line Thickened Oil Sands Tailings. Ph.D. thesis, Department of Civil and Environmental Engineering, University of Alberta, Edmonton, AB.

Jeeravipoolvarn, S., Scott, J.D., and Chalaturnyk, R.J. 2009. 10 m standpipe tests on oil sands tailings: long term experimental results and prediction. *Canadian Geotechnical Journal*, 46:875-888.

Townsend, F. C., & McVay, M. C. (1990). SOAs LARGE STRAIN CONSOLIDATION. *Journal of Geotechnical Engineering*, 116 (2).

Yao, D.T.C., and Znidarcic, D. (1997). CONDESO User's Manual. University of Colorado, Boulder, CO.

This page has been left blank intentionally.

Appendix B Large Strain Consolidation Testing Methods

B.1 Oedometer Step-Loading Test

In the standard oedometer test, step-loading is performed by applying incremental loads to a thin specimen. The consolidation process is monitored during each step of loading and a resultant void ratio-effective stress relationship is used to back calculate the consolidation parameters.

Analyses techniques for the oedometer test includes the Terzaghi curve fitting method, the square root of time fitting method, the logarithm of time fitting method, and the linear finite strain method.

The primary disadvantage of the traditional oedometer test is the time required to achieve consolidation which may vary from weeks to months. This time may be significantly longer for very soft specimens.

B.2 Constant Rate of Deformation (CRD) Test

This test was developed by Hamilton and Crawford (1959*) to provide a more efficient laboratory method that better reflects deformation rates observed in the field. The original formulation of the method resulted in void ratio-effective stress relationships that were sensitive to the rate of deformation applied. There was insufficient data collected during the initial testing to carry out a complete consolidation analysis; however, subsequent analysis methods have been proposed (Znidarcic et al. 1984)

Advancements in back-calculation methods using non-linear finite strain theory have increased the notoriety of this test procedure; results are obtained faster than the step-loading tests and results have been field-validated (Znidarcic, Shiffman, Pane, Croce, Ko, & Olsen, 1984).

B.3 Controlled Gradient Test

In this procedure, the loading rate is adjusted so that the pore pressure at the undrained boundary of the test cell remains constant throughout the test. The set-up is complicated by the need for a feedback mechanism to monitor pressure and adjust the loading accordingly. The assumptions in the analyses require that there is negligible excess pore pressure developed at the undrained boundary so that the void ratio remains essentially constant. (Znidarcic et al., 1984)

B.4 Constant Rate of Loading Test

The constant rate of loading test was introduced by Aboshi et al (1979*). The analysis procedure requires that the hydraulic conductivity and the coefficient of consolidation are constant throughout the test. Furthermore, the validity of the analyses technique requires that void ratio is essentially constant in the specimen throughout testing and can therefore limit the rate of loading. (Znidarcic et al., 1984)

B.5 Continuous Loading Test

This method is similar in concept to the CRD, controlled gradient and constant rate of loading test. The procedure requires that the ratio of the applied load to excess pore water pressure is held constant and this necessitates a complex feedback system. Hydraulic conductivity is assumed to be constant throughout consolidation. During testing, the magnitude and rate of loading, excess pore water pressure development, and specimen compression must be carefully monitored and adjusted using a data acquisition system. (Znidarcic et al., 1984)

B.6 Seepage-Induced Consolidation Test

The aforementioned consolidation test methods require the assumption of constant hydraulic conductivity and generally do not involve the direct measurement of Material Parameters. The following procedure proposed by Znidarcic et al (1986) involves direct measurement of material parameters and is hence more amenable to the study of consolidation involving large strains.

In this direct-measurement procedure, a constant-head hydraulic gradient across the specimen induces seepage flow thus developing an effective stress gradient. The difference in effective stress across the specimen induces consolidation. During consolidation, the specimen develops zones of different void ratios; hence, this method yields material characteristics under a range of void ratio conditions in only one test. Pore-water pressures are measured directly at locations within the specimen and the void ratio-effective stress relationship can be determined. The seepage gradient is determined and the flow through the cell is measured so hydraulic conductivity can be easily calculated using Darcy's Law. From these direct measurements, the void ratio-hydraulic conductivity relationship can be established and thus the consolidation parameters determined.

Znidarcic et al (1986) recognized that the measurement of void ratio requires specimen manipulation (slicing) could result in specimen rebound, thus overestimating void ratio. Nonetheless, the seepage test procedure allows for direct measurement of void ratio and hydraulic conductivity within the specimen. The effective stress at individual locations can then be back calculated.